Brain state and changes of mind: Probing the neural bases of multi-stable perceptual dynamics

Kloosterman, N.A.

Publication date
2015

Document Version
Final published version

BRAIN STATE AND CHANGES OF MIND

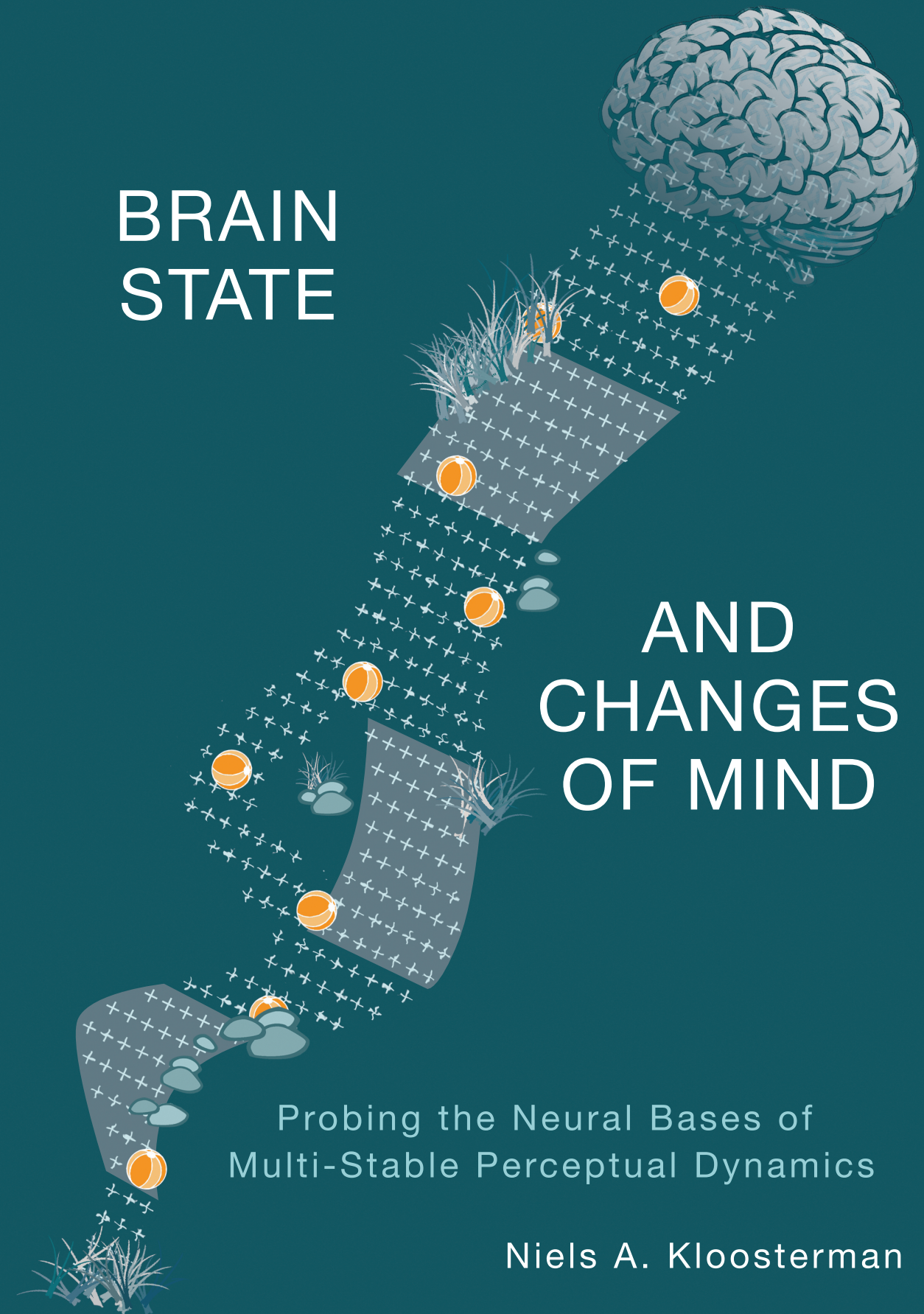

Probing the Neural Bases of Multi-Stable Perceptual Dynamics

Niels A. Kloosterman

BRAIN STATE AND CHANGES OF MIND

Niels Arend Kloosterman

Printed by GOB, Houten, The Netherlands

ISBN: 978-90-824111-0-2

Cover design: Niels Kloosterman & Hanneke van Ewijk

BRAIN STATE AND CHANGES OF MIND

Probing the neural bases of multi-stable perceptual dynamics

ACADEMISCH PROEFSCHRIFT

ter verkrijging van de graad van doctor

aan de Universiteit van Amsterdam

op gezag van de Rector Magnificus

prof. dr. D.C. van den Boom

ten overstaan van een door het college voor promoties ingestelde

commissie, in het openbaar te verdedigen in de

Agnietenkapel op

dinsdag 22 september 2015, te 14:00 uur

door Niels Arend Kloosterman geboren te Franeker

Promotor:	prof. dr. V. A. F. Lamme
Copromotor:	dr. T. H. Donner
Overige leden:	prof. dr. B. U. Forstmann
	prof. dr. S. Nieuwenhuis
	prof. dr. K. R. Ridderinkhof
	prof. dr. P. R. Roelfsema
	prof. dr. P. Sterzer
	dr. K. Linkenkaer-Hansen

Faculteit der Maatschappij- en Gedragswetenschappen

Voor Oona Siiri

CONTENTS

1 Introduction 8

2 Top-Down Modulation in Human Visual Cortex Predicts the Stability of a Perceptual Illusion 22

3 Modulation of Beta-Band Activity in Human Visual Cortex by Covert Perceptual Decisions 54

4 Short-term Stabilization in Bistable Visual Perception 72

5 Pupil Size Tracks Perceptual Content and Surprise 88

6 Pupil-linked Modulation of Decision-related Signals in Human Primary Visual Cortex 118

7 Summary and Discussion 144

8 Nederlandse samenvatting 158

A Appendix 166

References

List of publications

Dankwoord

Chapter 1

Introduction

Consciousness, then, does not appear to itself chopped up in bits… A "river" or a "stream" are the metaphors by which it is most naturally described. In talking of it hereafter, let us call it the stream of thought, of consciousness, or of subjective life.

- William James (1890)

The internal state of our cerebral cortex changes continuously. Cortical state changes alter the mode in which cortical circuits operate, and they are evident in the temporal structure of neural population activity (Steriade, 2000; Harris and Thiele, 2011; Lee and Dan, 2012; Zagha and McCormick, 2014). The major sources of these state changes are the neuromodulatory systems ascending from the brainstem, such as the diffuse release of acetylcholine from the basal forebrain over the cerebral cortex (Lee and Dan, 2012).

Traditionally, changes in cortical state have been exclusively associated with slow fluctuations in the level of wakefulness (Steriade, 2000; Harris and Thiele, 2011; Haider et al., 2012). But recent work is beginning to reveal that similar changes in cortical state are continuously taking place even during full wakefulness (Harris and Thiele, 2011; Reimer et al., 2014; Zagha and McCormick, 2014) and that neuromodulatory systems may also be transiently activated during specific and rapid cognitive processes such as perceptual inference, attention, and decision-making (Aston-Jones and Cohen, 2005; Gilbert and Sigman, 2007; Parikh et al., 2007; Harris and Thiele, 2011). These transient neuromodulatory events and resulting changes in cortical state may have important, but so far largely unknown, effects on subsequent information processing in the cortex and, hence, subsequent perception, cognition, and behavior.

To illustrate, consider the picture in Figure 1. If you have never seen this image before, you likely see nothing particular, even if you study it for some time. But after convincing yourself there is nothing there, please turn this page to see what is in fact depicted (Figure 2). As it turns out, you were looking at a degraded photograph of a well-known domesticized herbivore. Very likely, knowing the solution has triggered a sudden change in the state of the visual processing machinery in your cerebral cortex at the moment you looked back at Figure 1. This cortical state change resulted in a profound (and, in this case, lasting) change in the way the same image is processed and represented in your brain. In other words, the perceptual switch, evoked by the solution, triggered a change in cortical state that makes your new *perceptual* state permanent.

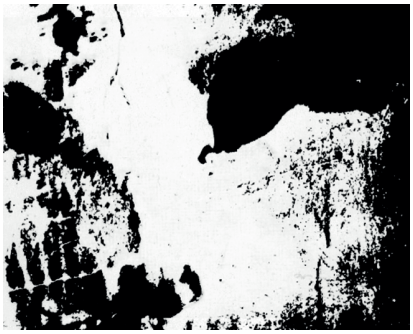

Figure 1 | Changes in brain state affect perception

Can you see which animal is shown in this picture? At first sight, most people see nothing particular. But discovering the animal triggers a cortical state change, which drastically and permanently changes your perception of the image. See Figure 2 for the solution.

What are the cognitive factors that drive such rapid changes in cortical state? Can we measure them in the human brain? And what are their effects on subsequent perception?

To date, the neurophysiological properties of fast changes in cortical state and their consequences for perception are unknown. In this thesis, I will explore the factors that drive these fast state changes in human visual cortex, how these state changes relate to phasic neuromodulatory events, and how they affect perception. To this end, I will use different neuroimaging measures (MEG and fMRI) to uncover complementary features of the neural population activity in visual cortex (in terms of its temporal and spatial structure), which help differentiate cortical state changes from representations of the sensory input. Further, I will use so-called bistable perceptual phenomena as a psychophysical tool throughout all my experiments. What is remarkable about these phenomena is that perception continuously switches back and forth between distinct subjective interpretations of a constant stimulus for as long as people look at the stimulus (Leopold and Logothetis, 1999; Kim and Blake, 2005). I will explore a novel idea about the possible role of global cortical state changes in perception – namely, that changes in global brain state are triggered by the perceptual switches, and, in turn,

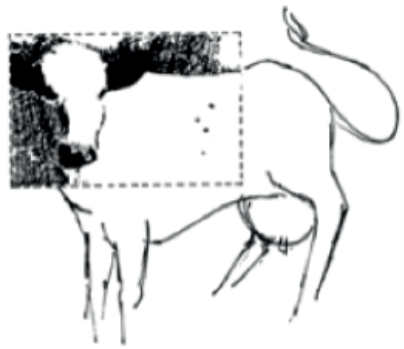

Figure 2 | Solution to the image shown in Figure 1

The dotted inset shows the outline of the picture shown in Figure 1. If you now turn back to Figure 1, your perception of this image has probably changed dramatically.

have a profound influence on the subsequent perceptual dynamics by *stabilizing* a newly selected perceptual interpretation for some period of time. A few previous reports have alluded to similar ideas (Leopold et al., 2002; Einhauser et al., 2008) but the general notion of an active mechanism that changes cortical state, and thereby transiently stabilizes perception, differs substantially from current standard accounts of the mechanisms of bistable perception (reviewed below in the section *Current models of the visual cortical interactions underlying bistable perception*) (Aston-Jones and Cohen, 2005).

Below, I will first motivate the focus on visual perception and specifically bistable perceptual phenomena as an experimental tool to study these state changes. Then I will present a class of computational models of the factors that cause the switches in bistable perception. After pointing out existing evidence for rapid state changes during both bistable perceptual phenomena and other perceptual tasks, I will consider modulatory brainstem systems as a possible underlying mechanism. The chapter concludes with an outline of this thesis.

Using visual cortex as a model system for understanding cortical processing

Using tasks in the visual domain makes it possible to build on the knowledge of one of the best-understood functions of the human brain: the processing of visual information. This process starts with the propagation of visual information from the eye, via the optic nerve and the thalamus to a specialized region in the back of the brain known as the visual cortex (Figure 3). The visual cortex consists of a complex hierarchy of many sub-regions that are specialized for different types of visual information (Grill-Spector and Malach, 2004). Neurons in so-called “early” visual regions, such as the primary visual cortex (V1), respond primarily to specific stimulus features, for example specific line orientations in the picture in Figure 1. From V1, this information is fed forward to regions higher up in the hierarchy (V2 and above), which respond to increasingly more complex stimulus features, such as shapes. The visual cortex is retinotopically organized, so that every location in the visual field is represented at a specific location within every sub-region (Wandell et al., 2007).

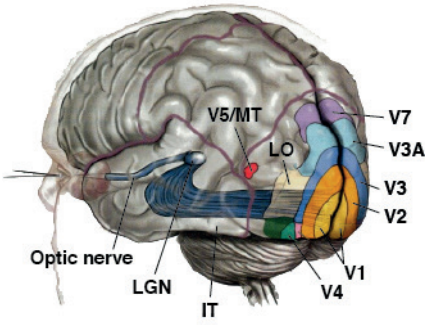

Figure 3 | Organization of the visual system

Light enters the retina and is relayed through the optic nerve via the LGN to the primary visual cortex (V1). From V1, the information is subsequently transferred to higher-order visual areas, that process increasingly complex information.

Bistable perception as a tool to study the functional origins and consequences of cortical state changes

The solution to Figure 1 has changed your perception of this image forever, as you cannot go back to "unseeing" the animal. Thus, this type of stimulus yields only a single perceptual switch, precluding experimental analysis of the corresponding change in brain state. In bistable perceptual phenomena, in contrast, abrupt switches in perception occur continuously despite an unchanging stimulus, as if the brain constantly changes its mind. Thus, these phenomena allow for the generation of countless cortical state changes, making them an excellent tool for studying the state changes. Famous visual bistable phenomena that can readily be experienced are the Necker cube (Figure 4A) (Necker, 1832) and Rubin's vase-face figure (Figure 4B) (Rubin, 1958). Strikingly, bistable illusions can even render a salient stimulus completely invisible. For example, in binocular rivalry (BR), dissimilar stimuli presented separately to the two eyes compete for perceptual dominance (Figure 4C) (Blake and Logothetis, 2002; Alais and Blake, 2005). Finally, during motion-induced blindness (MIB), a small but clear "target" stimulus completely disappears from perception for some time when surrounded by a moving pattern, only to reappear seconds later (Figure 4D) (Bonneh et al., 2001). Please note that throughout this thesis, I use the term "state change" to refer to a change in the dynamics of cortical activity and not the change in subjective perception of the observer (for instance the perceptual switches from target visible to invisible states in MIB that trigger the cortical state changes).

Besides yielding a large number of state changes in little time, there are more reasons why bistable phenomena are a useful experimental tool for studying the origins and consequences of rapid cortical state changes. Most importantly, bistable phenomena

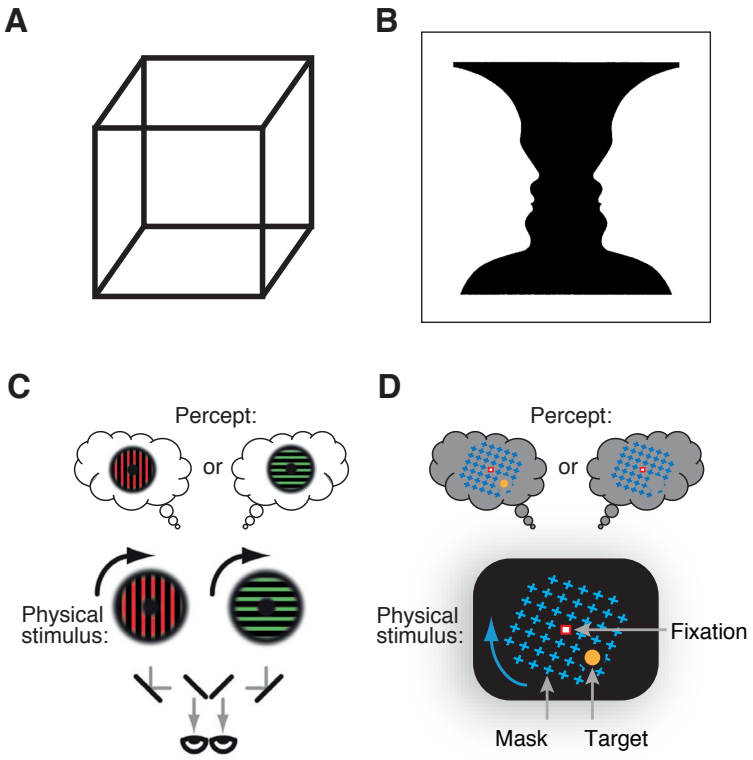

Figure 4 | Bistable visual phenomena.

A. Necker cube. With extended viewing, perception switches between looking at the cube from below and from above. **B**. Rubin's vase/face figure. Perception switches between seeing a white vase against a black background and two black faces against a white background. **C**. Binocular rivalry (BR). Bottom, schematic of the binocular rivalry stimuli. Two dissimilar stimuli presented to the two eyes. Top, alternating perception. The inputs to the two eyes compete for perceptual dominance. **D**. Motion-induced blindness Bottom: Schematic of the physical MIB stimulus. A salient target (yellow) is surrounded by a moving pattern (blue), appearing as a rotating grid. Top, alternating perception of the target due to MIB. The target intermittently and completely disappears from perception, to re-appear after some time.

enable us to study the bidirectional link between cognitive factors (in this case, perceptual dynamics) and cortical state changes: they allow us not only to investigate whether the switches in perception trigger cortical state changes, but also what impact the state changes, in turn, could have on perception, for instance by stabilizing perception for some time. Bistable percepts differ in terms of their stability, defined as the duration of a percept from the moment of switching. These durations are highly variable, even within an observer, and show stochastic independence, so that the duration of the current percept

cannot be predicted from the duration of the preceding percept (Leopold and Logothetis, 1999). Due to this large variability, percept duration can be used as a trial-by-trial index of the stability of percepts to investigate the role of state changes in shaping the dynamics of conscious perception. The first chapters of this thesis focus on the hypothesis that state changes can stabilize perceptual interpretations.

The later chapters focus on how the perceptual dynamics trigger the state changes. Bistable stimuli are well suited to investigate this relationship, because they allow us to isolate the endogenous (internally generated) changes in brain state from stimulus-related activity, which stays constant over time due to the spontaneous nature of the perceptual switches. In contrast, in other visual tasks, for example detection tasks (Ress et al., 2000; Moradi et al., 2007), observers are required to detect small changes in the visual stimulus. In these tasks, a change in brain state around a perceptual decision is always accompanied by a change in the stimulus, precluding a firm conclusion about its cause. MIB has the additional advantage over other bistable phenomena that the bistable target stimulus is limited to a very specific location in the visual field, instead of the complete stimulus. This feature can be exploited to decouple the neural representation of the small target stimulus (which is confined to a specific location in each sub-region of visual cortex) from retinotopically global modulations of neural activity, such as changes in brain state (Donner et al., 2008, 2013). Hence, I focus on MIB for studying the state changes in this thesis.

Finally, bistable percept dynamics resemble the dynamics of many higher-order cognitive acts, such as thought and exploratory decision formation. Although the process of switching itself seems random, *distributions* of bistable percept durations are highly predictable and consistent and have a similar shape as distributions of thought and decision formation durations. These distributions are characterized by a sharp rise at shorter durations and a long tail towards longer durations and are often modeled as a gamma distribution (Figure 5). Further, one observer typically produces similarly shaped distributions across different bistable illusions, suggesting a common mechanism underlying higher-level cognition and bistable perceptual dynamics. Similarly shaped distributions are observed in free-viewing fixation times in infants and naïve adults (Harris et al., 1988), fixation durations in cognitive tasks (Suppes et al., 1983), and look durations in young infants viewing a stimulus (Rubin, 1958). Finally, the rate of perceptual switching is correlated with intelligence (Crain, 1961), personality variables (Meredith, 1967), and

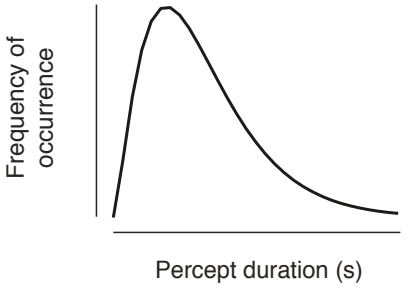

Figure 5 | Typical bistable percept distribution

Bistable percept distributions are typically skewed, with a sharp rise at shorter durations and a long tail towards longer durations. They are often modeled as a gamma distribution.

mood disorders (Hunt and Guilford, 1933; Pettigrew and Miller, 1998; Leopold and Logothetis, 1999), suggesting that bistable perceptual dynamics can be used as a marker of cognitive processing. Taken together, these findings suggest that bistable perception can be used as a simple model to identify general principles governing the dynamics of cognition (Leopold and Logothetis, 1999).

Current models of the visual cortical interactions underlying bistable perception

What causes the dynamics of bistable perception? A class of current standard computational models of the neural interactions in visual cortex during bistable perception provides an insight (Figure 6). This model consists of two populations of neurons driven by distinct stimulus components, for example, the two types of gratings in the binocular rivalry stimulus (Figure 3C), or the target and mask in the MIB stimulus (Figure 3D). These populations are subject to several forces that affect their level of activity. First, there is slow decay in activity due to sensory adaptation. This adaptation effect results from the decreased firing of neurons after prolonged stimulation by a stimulus (Alais and Blake, 1999). Second, the populations compete with each other by mutual inhibition, in which increased activity in one population suppresses activity in the other (van Loon et al., 2013). Finally, the populations are subject to random fluctuations of neural activity ("noise") (Moreno-Bote et al., 2007). The interaction between adaptation, mutual inhibition and noise gives rise to spontaneous transitions between dominance of one of the two populations (Moreno-Bote et al., 2007), which are thought to underlie the perceptual switches (Noest et al., 2007) (Figure 6).

Various studies have isolated modulations of neural activity that presumably play a causal role in prompting the illusory perceptual switches. These modulations have

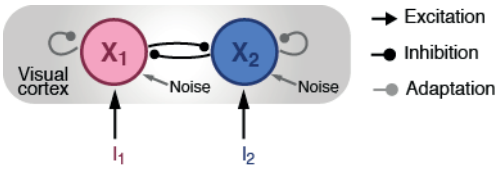

Figure 6 | Architecture of a standard class of bistability models

Two neural populations (X_1 and X_2) are driven by distinct inputs (I_1, I_2). The populations compete via mutual inhibition, and both populations are subject to slow adaptation dynamics and random fluctuations of neural activity ("noise"). The interplay of excitation, inhibition, adaptation and noise underlies the dominance of the populations and consequently dominance in perception.

been interpreted as causal because they precede the transition and are absent when the perceptual switches are evoked by physical stimulus changes (Lumer et al., 1998; Sterzer and Kleinschmidt, 2007; Britz et al., 2008; Donner et al., 2008, 2013) Notably, in the case of MIB, these modulations are confined to sub-regions in visual cortex that represent either the target (visual region V4) or the mask stimulus (intra-parietal sulcus) (Figure 7). Similar competition dynamics have been observed during binocular rivalry (Logothetis et al., 1996).

Evidence for global state changes in visual cortex during perceptual switches and choices

An increasing number of studies report fast and global modulations of activity in the cerebral cortex that seem to belong to a completely new and unexpected class of signals. Specifically, during MIB, a fast, widespread modulation of fMRI-activity occurs around the "decision" that the target has disappeared, which is tied to a behavioral report (e.g. a button press) (Donner et al., 2008; Hsieh and Tse, 2009; Donner et al., 2013). Similar modulation occurs during a replay condition, in which the perceptual switches are not illusory, but evoked by physical target offsets and onsets on the screen. This finding indicates that the modulation is not related to the cause of the spontaneous disappearance, because then it would only have occurred during MIB, but not replay. These modulations are neither represented in classical models of bistable perception and also not in the older measurements of single-unit activity during bistable tasks (Logothetis and Schall, 1989, 1990).

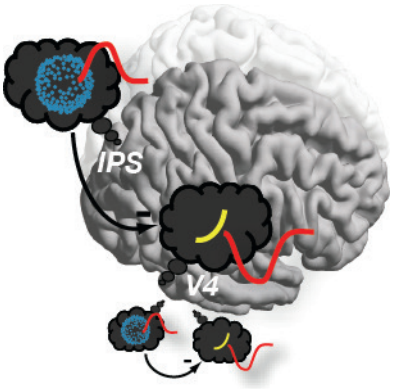

Figure 7 | Stimulus-specific neural populations in extrastriate visual cortex compete for dominance during MIB

Schematic representation of the results from two fMRI studies of MIB (Donner et al., 2008, 2013). In extrastriate ventral area V4, the response to the target stimulus decreases just before the subjective target disappearance. By contrast, in motion-sensitive dorsal areas of the intraparietal sulcus (IPS), the response to the mask increases. Both of these effects are only evident during the MIB illusion, not the replay of the illusion, pointing to a causal role of these competitive cortical dynamics in inducing the illusion. A similar competition between mask and target representations seems to take place at a local scale within area V4. In V1, there is no modulation specific for the target or mask around target disappearance, only a delayed and retinotopically global decrease in the fMRI signal, presumably reflecting a switch-related state change (see main text for details). (Donner et al., 2008, 2013).

The characteristics of the modulation of fMRI-activity in MIB suggest that the modulation reflects a rapid change in brain state during perceptual switches (Donner et al., 2008). Following the target-specific suppression of fMRI-activity (Figure 7), a modulation occurs throughout early visual cortex, the sign of which reflects the type of switch that subjects reported: negative for disappearance, positive for re-appearance. Thus, the modulation is not indifferent to the *type* of switch, as would be expected from attention. Second, the modulation occurs even in regions of visual cortex that are not stimulated by the target and mask stimuli, indicating that the modulation is not due to a change in the strength of the stimulus representation in visual cortex. Third, during replay, the modulation seems more closely time-locked to the report of the switch than to the corresponding stimulus change, pointing to a top-down origin of the signal. Finally, the modulation depends on task-relevance of the switches, because it does not occur during passive viewing of perceptual switches. Taken together, these findings are consistent with a post-decisional state change in visual cortex. In line with these fMRI-modulations (which are an indirect measure of neural activity), results from local field potential studies in monkey visual cortex and thalamus (Gail et al., 2004; Wilke et al., 2006; Wilke et al., 2009) show similar modulations in the lower frequency bands, suggesting a possible electrophysiological underpinning of these modulations.

These global modulations might be a general phenomenon. Signals suggesting rapid changes in brain state have also been observed during other bistable illusions (de-Wit et al., 2012) and in many other types of perceptual tasks. Several studies reported modulations of population activity in human and monkey early visual cortex, which were largely decoupled from representations of the stimulus in the cerebral cortex, but coupled to behaviorally relevant events (Jack et al., 2006; Wilke et al., 2006; Donner et al., 2008; Hsieh and Tse, 2009; Sirotin and Das, 2009; Cardoso et al., 2012; de-Wit et al., 2012; Swallow et al., 2012; Donner et al., 2013; Choe et al., 2014). Taken together, these signals call for a systematic characterization. In this thesis, I will detail the neurophysiological signals around bistable switches and assess whether they are linked to the stability of bistable perception.

The role of neuromodulatory brainstem mechanisms

What are the sources of the rapid changes in cortical state during cognitive acts? Neuromodulatory brainstem systems are in an ideal position to play such a role, because they exhibit transient activity during perceptual decisions, such as detecting faint stimulus changes or bistable switches (Aston-Jones and Cohen, 2005; Parikh et al., 2007; Einhauser et al., 2008; Hupe et al., 2009; de Gee et al., 2014). Specifically, two neuromodulatory systems are key candidates for state changes in visual cortex during perceptual decisions: the locus coeruleus-noradrenaline (LC-NA) system and the basal forebrain-acetylcholine (BF-Ach) system. Both systems project broadly to the entire cortex, including visual cortex. Both systems also exhibit transient bursts of activity during perceptual decisions. For example, during a visual cue detection task, the medial prefrontal cortex of rats showed transient increases in cholinergic activity in response to detected, but not missed cues (Parikh et al., 2007). Likewise, during an oddball discrimination task, LC neurons in monkeys were phasically and selectively activated by target, but not non-target cues (Aston-Jones et al., 1994). Both these findings indicate that neuromodulatory systems are capable of responding selectively, depending on the content of perceptual decisions. In humans, similar responses have been observed around perceptual decisions in pupil dilation, a putative marker of neuromodulator release under constant lighting conditions (Einhauser et al., 2008; Hupe et al., 2009; de Gee et al., 2014). In the second part of this thesis, I use pupillometry to investigate the relationship between neuromodulatory brainstem systems controlling pupil diameter and rapid changes in brain state.

Outline of this thesis

The first part of the thesis focuses on the hypothesis that cortical state changes shape the time course of bistable perception by stabilizing percepts. Using MEG, **Chapter 2** provides a detailed characterization of the neurophysiological signatures of rapid state changes, as well as a test of this hypothesis. The chapter reports a transient, retinotopically widespread modulation of beta (12-30 Hz) frequency power over visual cortex that is closely linked to subjects' behavioral report of target disappearance in MIB and its replay. This beta-modulation is a top-down signal, decoupled from both the physical stimulus properties and the motor response, but contingent on the behavioral relevance of the perceptual change. Critically, the modulation amplitude predicts the duration of the subsequent target disappearance. The results suggest that the transformation of the perceptual change into a report triggers a top-down mechanism that stabilizes the newly selected perceptual interpretation.

Using a different MEG system and a new group of subjects, **Chapter 3** shows that the beta power modulation over visual cortex not only occurs when subjects promptly report the perceptual switches by button press, but also when they covertly count the switches. This finding convincingly decouples the global modulation from the beta modulation over parietal cortex that is related to the motor response used to report switches. This finding adds important further support to the notion that the top-down modulation is related to the decision-making process, but it is not necessarily tied to an immediate motor response to indicate the decision.

A hallmark of bistable perceptual dynamics is the lack of very short-lasting percepts, which is reflected in the skewed percept duration distributions (Figure 5). **Chapter 4** employs psychophysics to show that this lack of brief percepts is not due to an inability of observers to report fast switches via button press. Thus, observers experience a genuine lack of short percepts, indicating that perception indeed briefly stabilizes after a perceptual switch.

The second part of this thesis focuses on the role of phasic neuromodulatory events in rapid state changes. The global modulation of fMRI- and MEG-activity during MIB reflects the contents of perception, with opposite signs for disappearance and re-appearance. If neuromodulatory systems play an active role in the state changes, then their activity should also reflect the contents of perception. **Chapter 5** employs pupillometry,

a peripheral measure of neuromodulator release, to investigate this hypothesis. This chapter shows that switch-related pupil dilation on individual switches indeed encodes perceptual content, with larger amplitude for target disappearance than re-appearance. Independent of this effect, pupil dilation during stimulus-evoked perceptual switches also scales with the level of surprise about the timing of switches.

Using whole-brain fMRI, **Chapter 6** specifies the exact spatial extent of the global modulation and examines the relationship between the amplitude of the modulation and pupil dilation at the time of the perceptual switches. The chapter reports the previously observed percept-encoding modulation of fMRI activity around perceptual switches. Strikingly, this decision-related suppression of activity in a non-stimulated part of V1 around target disappearance is stronger when the concomitant pupil dilation is larger. A similar pattern of activity occurs in anterior cingulate cortex, a region with strong projections to neuromodulatory systems located in the brainstem.

Taken together, these results support an active role of phasic neuromodulation in fast changes in cortical state during elementary perceptual decisions. In **Chapter 7,** I summarize the empirical findings and consider possible sources of the modulation, focusing on neuromodulation. To accommodate these findings, I then incorporate a post-decisional modulatory population into the standard bistability model introduced above. Finally, I discuss the implications of the findings presented in this thesis for other, more abstract types of decision making and psychopathological conditions, such as schizophrenia.

Chapter 2

Top-Down Modulation in Human Visual Cortex Predicts the Stability of a Perceptual Illusion

This chapter is based on:

Kloosterman, N. A., Meindertsma, T., Hillebrand, A., van Dijk, B. W., Lamme, V. A., & Donner, T. H. (2015). Top-Down Modulation in Human Visual Cortex Predicts the Stability of a Perceptual Illusion. *Journal of neurophysiology, 113*(4), 1063-1076.

ABSTRACT

Conscious perception sometimes fluctuates strongly, even when the sensory input is constant. For example, in motion-induced blindness (MIB), a salient visual target surrounded by a moving pattern suddenly disappears from perception, only to reappear after some variable time. While such changes of perception result from fluctuations of neural activity, mounting evidence suggests that the perceptual changes, in turn, may also cause modulations of activity in several brain areas, including visual cortex. Here, we asked whether these latter modulations might affect the subsequent dynamics of perception. We used magneto-encephalography (MEG) to measure modulations in cortical population activity during MIB. We observed a transient, retinotopically widespread modulation of beta (12-30 Hz) frequency power over visual cortex that was closely linked to the time of subjects' behavioral report of the target disappearance. This beta-modulation was a top-down signal, decoupled from both the physical stimulus properties and the motor response, but contingent on the behavioral relevance of the perceptual change. Critically, the modulation amplitude predicted the duration of the subsequent target disappearance. We propose that the transformation of the perceptual change into a report triggers a top-down mechanism that stabilizes the newly selected perceptual interpretation.

Keywords: beta-oscillations, bistable perception, brain dynamics, brain state, perceptual decision-making

INTRODUCTION

When the sensory input to the brain is ambiguous, perception often changes spontaneously, followed by periods of stable perception, a phenomenon called multistable perception (Leopold and Logothetis, 1999; Blake and Logothetis, 2002; Deco and Romo, 2008; Sterzer et al., 2009)Leopold DA and NK Logothetis (1999). For example, in an illusion dubbed "motion-induced blindness" (MIB), a salient visual target surrounded by a rotating mask suddenly disappears from perception for some time (Figure 1 A) (Bonneh et al., 2001; Bonneh and Donner, 2011). A hallmark of these MIB disappearances (as well as of other multistable illusions) is that the duration of each percept varies widely and unpredictably from one perceptual change to the next (Figure 1 B). Intriguingly, the statistics of these perceptual dynamics correlate to the dynamics of thought and exploratory decision-making (Leopold and Logothetis, 1999; Carter and Pettigrew, 2003).

Studies of the neural basis of multistable perception have reported transient modulations of activity during the perceptual switches, in visual cortex (Leopold and Logothetis, 1996; Polonsky et al., 2000; Tong and Engel, 2001; Haynes and Rees, 2005; Lee et al., 2007; Donner et al., 2008) as well as parietal and frontal association cortex (Lumer et al., 1998; Sterzer and Kleinschmidt, 2007; Zaretskaya et al., 2010; Britz et al., 2011; Knapen et al., 2011). Some of the switch-related modulations of cortical activity appear to precede the switches and are absent when switches are evoked by the physical stimulus, in line with a causal role in prompting the switch (Lumer et al., 1998; Sterzer and Kleinschmidt, 2007; Donner et al., 2008; Britz et al., 2011). Others, however, occur later in time and irrespective of whether the perceptual switches emerge spontaneously or are evoked by a stimulus change (Donner et al., 2008; Knapen et al., 2011; Frassle et al., 2014). Specifically, functional magnetic resonance imaging (fMRI) studies of MIB have identified a retinotopically widespread modulation in early visual cortex, which is decoupled from the cortical target representation (Donner et al., 2008; Hsieh and Tse, 2009; Donner et al., 2013). This modulation is contingent on the behavioral report of target disappearance and absent during passive viewing (Donner et al., 2008).

Here, we used whole-head MEG recordings (Hamalainen et al., 1993) during MIB to (i) characterize the electrophysiological signatures of the report-related transient modulations in visual cortex identified with fMRI, and (ii) to test whether they might shape the subsequent perceptual dynamics. Subjects' reports of perceptual switches

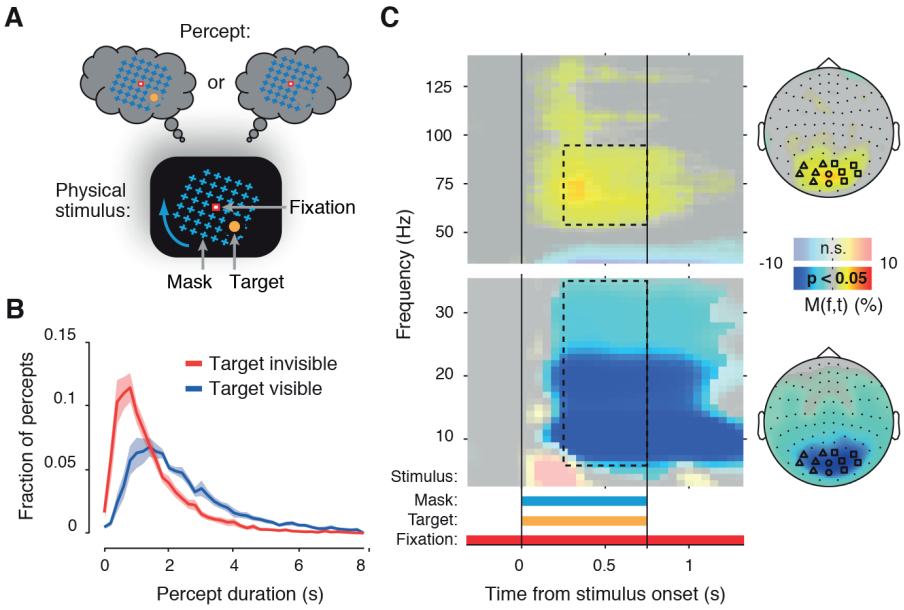

Figure 1 | MIB stimulus, perceptual dynamics, and cortical stimulus response

A. Schematic of the MIB illusion. Bottom: Stimulus configuration. The small, but salient target (yellow disc) was surrounded by a large moving mask (rotating blue grid). The target was presented in different visual field quadrants for different subjects, at an eccentricity of 3°. Top, alternating perception of the target. **B**. Group average frequency distributions of target invisible and target visible durations during MEG (N = 11 subjects). Shaded areas, s.e.m. **C**. Cortical response to the MIB stimulus during Stimulus-on-off. Scalp maps, topography of 8-35 Hz and 60-90 Hz modulations (0.25-0.75 s after stimulus onset; see dashed outlines on time frequency representations). Transparency level indicates clusters of significant modulation ($p < 0.05$, two-sided permutation test across subjects, cluster-corrected, N = 10 subjects). Highlighted symbols, MEG sensors showing the biggest stimulus response. These sensors are used for the subsequent analyses of overall power modulations (triangles and squares, sensors used for lateralization analyses; Figure 3).

were accompanied by a transient modulation of beta-band (12-30 Hz) activity over visual cortex, which was decoupled from both the stimulus properties and motor response, but strongly linked to the behavioral relevance of target disappearance. The amplitude of this modulation predicted (in the case of MIB) the duration of the subsequent illusory target disappearance. We propose that behaviorally relevant changes of perception trigger an active top-down mechanism that stabilizes the internal state of visual cortex as well as perceptual suppression.

MATERIALS AND METHODS

We report data from two MEG experiments: A main experiment and a control experiment including high-resolution eye tracking to test for a dependence of the effects reported in this paper on microsaccades.

Main experiment

Subjects

MEG data were acquired at the VU University Medical Center, Amsterdam from eleven healthy subjects with normal or corrected-to-normal vision (4 female, age range: 23 - 37 years). The experiment was approved by the local ethics committee and each subject gave written informed consent. Each subject participated in several MEG sessions on different days of about 2 h duration each.

Stimulus

The target was a salient yellow disc (full contrast, diameter: 0.12 or 0.2° of visual angle) surrounded by a moving mask (square, equally spaced grid of 9 by 9 blue crosses, 17° width/length), both superimposed on a black background and centered on a fixation mark (red outline, white inside, 0.8° width and length) (Figure 1 A). The target was located on one of the four visual field diagonals at an eccentricity of 3°. Target size and location (visual field quadrant) were individually selected for each subject prior to MEG, to yield a percentage of target invisible time of at least 20%. The mask rotated around the fixation square (speed: 120°/s). The target was separated from the mask by a black “protection zone” subtending about 2° around the target (Bonneh et al., 2001).

Stimuli were presented using the Presentation Software (NeuroBehavioral Systems, Albany, CA, USA) and projected via two mirrors onto the ceiling of the MEG scanner room by an LCD projector (BarcoData 8200 LC, Barco Projection Systems, Kuurne, Belgium) with a pixel resolution of 800 x 600 and 60 Hz refresh rate. Subjects were supine and viewed the stimuli projected onto the ceiling of the MEG room (field of view of 18 x 23°).

Behavioral tasks and design

All subjects participated in various tasks designed to (i) determine the factors driving transient modulations of cortical activity around reports of perceptual switches and (ii) identify the impact of these transient modulations on subsequent neural activity and perception.

Stimulus-on-off condition

On each trial, the complete MIB stimulus (target, mask, and fixation mark) was presented for 0.75 s, preceded and succeeded by fixation of an otherwise black screen. This stimulus duration was too short to induce MIB target disappearance, but sufficiently long to measure the stimulus-induced modulation of cortical population activity (Figure 1 C). Subjects' task was to maintain stable fixation and passively view the stimulus.

MIB condition

The MIB stimulus was continuously presented for several runs of 2 min duration each. The subjects' task was to maintain stable fixation and report the spontaneous disappearance and re-appearance of the target, by pressing or releasing a response button with their index finger (left or right, counterbalanced across subjects). The mapping between perceptual switch and motor response was flipped between the two recording days (Figure 4 A): button press for indicating target disappearance (release for re-appearance) on day 1, and button release for disappearance (press for re-appearance) on day 2.

Replay conditions

In the three different Replay conditions, the target was physically removed from the screen in the same temporal sequence as it had previously disappeared during one of several previous MIB runs completed by the corresponding subject. The physical offsets and onsets of the target were always instantaneous, mimicking the typically abrupt quality of the perceptual switches in MIB for the small target used here. The general purpose of the Replay conditions was to test whether report-related, transient modulations in cortical activity during MIB may have prompted the spontaneous perceptual switch (then they should be specific to MIB), or were driven by the perceptual switch (then they may also occur during Replay-active). Based on previous fMRI results (Donner et al., 2008),

we expected a retinotopically widespread modulation in visual cortex around behavioral report of target disappearance and re-appearance, in both MIB and Replay.

Replay-active: This condition was identical to MIB in all respects except for the changes in the physical presence of the target.

Replay-no-mask: This condition was identical to Replay-active, except that the target was presented without mask. The purpose of this condition was to test whether potential report-related modulations during MIB and Replay-active may have reflected a contextual effect in the sensory processing of the mask stimulus: It is conceivable that the sensory processing of the mask differed between the (perceived or physical) presence and the (perceived or physical) absence of the target. The Replay-no-mask condition allowed us to differentiate between (i) contextual modulations of the sensory processing of the mask and (ii) report-related, non-sensory modulations that were decoupled from the physical MIB stimulus: Modulations should disappear during *Replay-no-mask* in the former case, but persist in the latter case.

Replay-passive: This condition was identical to Replay-active, except that subjects did not report the target on- and offsets, and that target present and absent durations were drawn from Gaussian distributions (mean: 2.2 s for target on, 2 s for target off, ± 0.184 s s.d.). The purpose of this condition was to test whether activity modulations during MIB and Replay-active depended on the need for behavioral report of the target disappearance and re-appearance events. We ensured that subjects attended to the stimuli by excluding all trials in which subjects broke fixation or made eye blinks.

General design

All eleven subjects participated in the main experiment consisting of the MIB, Replay-active, and Replay-no-mask conditions. Across two recording sessions (days 1 and 2), subjects performed 32 MIB runs, 24 Replay-active runs and 8 Replay-no-mask runs. In each session, the experimental conditions were presented in blocks of four 2-minute runs, each preceded and succeeded by a 30 s blank fixation period. Conditions were presented in pseudo-random order. The first four runs of each session were MIB. In the remaining runs, MIB, Replay-active, Replay-no-mask conditions were randomly selected, under the constraint that the total number of runs per session would be 16, 12, and 4, for MIB, Replay-active, and Replay-no-mask, respectively. Ten subjects participated in two

further scanning sessions, during which they performed the Stimulus-on-off (300-600 trials) and Replay-passive conditions (12-20 runs).

MEG data acquisition

Whole-head MEG data were acquired at 1250 Hz in a magnetically shielded room on a 306-channel whole-head neuromagnetometer (Elekta Neuromag Oy, Helsinki, Finland), for several recording blocks. During each recording block, subjects performed four of the 2-minute runs of the different experimental conditions described above. Each of the 102 sensor units consisted of two orthogonal planar gradiometers and one magnetometer. An anti-aliasing filter and high-pass filter of 410 Hz and 0.1 Hz were applied online, respectively. The electrooculogram (EOG) (measured from the upper right eye canthi) and electrocardiogram (ECG) were simultaneously recorded. Prior to MEG recordings, the positions of four head localization coils and the outline of the subjects' scalp (500 points) were digitized with a 3D digitizer. During each 10 min recording block, the relative position of the coils to the MEG sensors was continuously monitored. For all blocks, head motion was below 5 mm (Eucledian distance).

Preprocessing of MEG data

The MEG data were analyzed using MaxFilter (version 5.10.2) software, Fieldtrip (Oostenveld et al., 2011) and custom-made MATLAB (The Mathworks, Natick, MA, USA) software. The following preprocessing steps were performed: signal space separation, trial extraction, muscle and eye artifact rejection, and resampling to 500 Hz. All sensors were used for signal space separation. Only planar gradiometers were included in muscle artifact rejection and further analyses of the experimental effects of interest. MEG signals measured by these planar gradiometers peak primarily above the source (Hamalainen et al., 1993).

Noise removal

Background noise in the MEG data was removed using the temporal extension of Signal Space Separation (tSSS) technique within the MaxFilter software (Elekta Neuromag Oy, version 2.10) (Taulu et al., 2004). To this end, we used a time window of 8 s, and correlation limit of 0.9.

Trial extraction

For the Stimulus-on-off condition, we extracted trials of fixed durations, ranging from 0.5 s before to 1.75 s after stimulus onset (i.e., 1 s after stimulus offset).

For the MIB and Replay conditions involving subjects' reports, we extracted trials of variable duration, centered on subjects' button presses or releases, from the 2 min runs of continuous stimulation. Thus, in the case of MIB, the term "trial" refers to an epoch of constant stimulation and is solely defined based on subjects' subjective reports of target disappearance and re-appearance. The following constraints were used to avoid mixing data segments from different percepts when averaging across trials: (i) The maximum trial duration ranged from -1.5 s to 1.5 s relative to report; (ii) when another report occurred within this interval, the trial was terminated 0.5 s from this report; (iii) when two reports succeeded one another within 0.5 s, no trial was defined; (iv) for the analysis of Replay-active and Replay-no-mask, we included only those reports that were preceded by a physical change of the target stimulus within 0.2 to 1 s, thus discarding reports following illusory target disappearances.

In an alternative analysis of all Replay conditions, trials were defined in the same way as described above, but now aligned to physical target on- and offsets, eliminating the need to discard illusory target disappearances.

Trial rejection and line noise removal

Trials containing eye blinks, saccades, or muscle artifacts were rejected from further analysis using standard automatic methods. The signal time courses were band-pass filtered in the specific frequency range that contained most of the artifact. These ranges were as follows: 1 to 15 Hz (EOG channel only) for blinks and 110 to 140 Hz (MEG gradiometers only) for muscle activity. Filtering was followed by z-transformation. Trials exceeding a predefined threshold z-score were removed completely from analysis. We used the following thresholds: blinks: $z = 4$ (all subjects); muscle: $z = 7.5$ for nine subjects and $z = 10$ for two subjects.

Line noise was removed by subtracting the 50, 100, 150 and 200 Hz Fourier components from the raw MEG time course of each trial.

Analysis of MEG power modulations

Spectral analysis of MEG power

We used sliding window Fourier transform (Mitra and Pesaran, 1999) (window length: 400 ms, step size: 50 ms) to calculate time-frequency representations of the MEG power (spectrograms) for the two gradiometers of each sensor and each single trial. We used a single Hanning taper for the frequency range 3 - 35 Hz (frequency resolution: 2.5 Hz, bin size: 1 Hz) and the multi-taper technique for the frequency range 36 - 140 Hz (spectral smoothing: 8 Hz, bin size: 2 Hz, five tapers). After time-frequency analysis, the two orthogonal planar gradiometers of each sensor were combined by taking the sum of their power values.

Stimulus-induced power modulations

For Stimulus-on-off, spectrograms were averaged aligned to MIB stimulus onsets. For MIB and Replay conditions, spectrograms were averaged aligned to perceptual reports of target disappearances/re-appearances (MIB and Replay), or aligned to the corresponding target off-/onsets (Replay).

Switch-related power modulations

Power modulations (denoted as M(f,t) in the figures) were characterized as the percentage of power change at a given time and frequency bin, relative to a "baseline" power value for that frequency bin. For Stimulus-on-off, the baseline was computed as the mean power across the pre-stimulus blank fixation interval (from -0.25 s to 0 s relative to stimulus onset). For MIB and Replay, the baseline was computed by averaging the power values across all time points within each trial (maximum time range -1.5 to 1.5 s around the event), and then across all trials from a given recording session, pooling across disappearance and re-appearance trials. We computed separate baselines for each experimental condition (i.e., MIB, Replay-active, etc.), and each recording session. Consequently, the M(f,t) values around perceptual reports represent the modulation of MEG power relative to the mean power across all artifact-free epochs from all runs of a given condition (MIB, Replay-active, etc.).

We focused our analysis of MEG power modulations around MIB reports on those cortical regions that also processed the physical MIB stimulus (i.e. visual cortex).

Therefore, before performing the statistical tests described in this and the following section, we averaged all power modulations across the twelve occipital sensors exhibiting the biggest stimulus-induced (high and low-frequency) response during Stimulus-on-off (marked in Figure 1 C).

Statistical tests of power modulations

We used a two-tailed permutation test (1000 permutations) (Efron and Tibshirani, 1998) to test the significance of the overall power modulations of this sensor group, and of the difference in power modulation between the sensors contralateral and ipsilateral to the target location (i.e., power lateralization). We tested the overall power modulation and power lateralization for (i) significant deviations from zero, (ii) significant differences between disappearance and re-appearance, and (iii) for differences between MIB and Replay-active. For all these tests, we used a cluster-based procedure (Oostenveld et al., 2011) to correct for multiple comparisons. For time-frequency representations of power modulations (Figures 1, 2, 7), this was done across all time-frequency bins. Because the focus of the current study was on transient modulations of cortical activity around the perceptual switches, we averaged power modulations across the time window -0.3 to 0.3 s around report ("transient" time window indicated by black bar in Figure 2 A) for all subsequent analyses before statistical tests (Figures 3-7). For statistical tests of the spectra of transient power modulations around report (Figures 3, 4, 5, 7), we performed the permutation test with cluster-based multiple comparison correction across frequency bins. Because our focus was on the MIB illusion (with the Replay conditions as controls), we defined our frequency band for further analyses based on the significant cluster around disappearance reports during MIB (12-30 Hz, see Figures 2A and 3A).

Correlation analysis

We intended to test if the overall power modulation in the beta-band (12-30 Hz) that we observed during the transient time window around subjects' reports (-0.3 to 0.3 s from report) predicted the duration (i.e., stability) of the perceptual suppression. To this end, we collapsed the single-trial power modulation values across the transient time window around report and the beta-band. This yielded one scalar modulation value per trial. These scalar modulation values were then concatenated into a new (across-trial) time series, which was submitted to piece-wise linear de-trending, to remove slow intrinsic

dynamics from the cortical power that are unrelated to perceptual or cognitive processing (Leopold et al., 2003; Donner et al., 2009). Based on the amplitude of the de-trended single-trial modulation values, we then grouped trials (within subjects) into 10 (or other numbers for control, see below) percentile bins (see Linkenkaer-Hansen et al. (2004) for an analogous procedure).

Each trial was then associated with a transient beta-band modulation and with the duration of the preceding percept (target visible) and succeeding percept (target invisible). After normalizing individual percept durations by each subject's median percept duration (separately for both percepts), we collapsed the normalized percept durations per bin (based on transient beta-modulation within subjects; see above), and finally computed the mean and normalized duration per bin across subjects. The normalization compensated for substantial inter-individual variability in the perceptual durations, thereby isolating the trial-to-trial variability of percept durations. However, the results reported in this paper were qualitatively identical without this normalization (data not shown). We then correlated the bin rank number to normalized percept duration.

We used a permutation (shuffling) procedure (1000 permutations) to test the significance of the correlations (Efron and Tibshirani, 1998). Mapping the individual power modulation values into a common range of percentile bins before averaging them across subjects compensated for the inter-individual variability in the power modulation values, which is due to many factors other than neural activity (e.g., individual differences in head geometry and brain anatomy). To assess the robustness of the observed correlations, we repeated these analyses for several different bin numbers (15, 30, and 60 bins).

A stabilizing effect of the transient beta-band modulation on the duration of perceptual suppression would predict (i) a significant and strong correlation with the duration of the succeeding (target invisible) percept during MIB, (ii) no correlation with the duration of the preceding (target visible) percept during MIB, and (iii) no correlation with the duration of the succeeding (target invisible) percept during Replay, where the percept durations are largely determined by the physical target on- and offsets. Thus, we predicted significant differences in the correlation coefficients for (i) versus (ii) and for (i) versus (iii). To test for these two predicted *differences* in correlation, we again used a permutation procedure (1000 permutations). Here, we permuted the labels (e.g., "preceding" versus "succeeding") of pairs of bin rank number and corresponding percept durations.

Microsaccade control experiment

Subjects

MEG data and high resolution (infra-red) eye data were simultaneously acquired at the Universitätsklinikum, Hamburg-Eppendorf, from 22 healthy subjects with normal or corrected-to-normal vision. The experiment was approved by the local ethics committee, and each subject gave written informed consent. One subject failed to complete the full experiment and one subject had poor eye tracking data quality. Both subjects were excluded. Thus, twenty subjects (11 female, age range 20 - 54 years) were included in the analysis.

Stimulus and behavioral task

The target was a full contrast Gabor patch (diameter: 2°, two cycles) surrounded by a rotating mask (17°x17° grid of white crosses) both superimposed on a gray background and centered on a fixation mark (red outline, white inside, 0.8° width and length) in the middle of the screen. The target was located in either the lower left or lower right visual field quadrant (eccentricity: 5°, counterbalanced between subjects). The mask rotated at a speed of 160°/s. and was separated from the target by a protection zone of 2°. We used a Gabor target on a gray background in this experiment to eliminate any changes in perceived brightness during MIB, for analyses of changes in pupil diameter that will be the focus of a separate report.

Stimuli were presented using the Presentation Software (NeuroBehavioral Systems, Albany, CA, USA). Stimuli were back-projected on a transparent screen using a Sanyo PLC-XP51 projector with a resolution of 1024x768 pixels at 60 Hz.

Subjects were seated 58 centimeters from the screen in a whole-head magnetoencephalography (MEG) scanner setup in a dimly lit room. The stimulus was continuously presented for six runs of 3 min duration each. During that time, subjects kept their gaze on the fixation mark and reported the spontaneous target disappearance and re-appearance by pressing a response button with their right index finger and right middle finger, respectively. To select the 25 sensors overlying visual cortex that showed the biggest stimulus-induced response, subjects additionally performed the Stimulus-

on-off condition described above for the main experiment, but with the gray-scale MIB stimulus (see *Stimulus-on-off condition*).

Data acquisition

MEG data were acquired at 1200 Hz on a 275-channel whole-head neuromagnetometer (CTF 275, VSM/CTF Systems, Port Coquitlam, British Columbia, Canada). Subjects were placed in a seated position inside the scanner. The location of the subjects' head was measured real-time using three fiducial markers placed in the both ears and on the nasal bridge to control for excessive movement. The EOG and ECG were recorded to aid artifact rejection.

Concurrently with the MEG recordings, the position of the left eye's pupil was sampled at 1000 Hz with an average spatial resolution of 15 to 30 min arc, using an MEG-compatible EyeLink 1000 Long Range Mount system (SR Research, Osgoode, Ontario, Canada), placed on a table under the stimulus presentation screen. The eye tracker was calibrated before every block of four runs.

MEG and eye tracking data analysis

Preprocessing

Both the MEG and eye tracking data were analyzed using the Fieldtrip (Oostenveld et al., 2011) and custom-made MATLAB (The Mathworks, Natick, MA, USA) software. The following preprocessing steps of the MEG data were performed as described for the main experiment above: trial extraction, muscle and eye artifact rejection, and resampling to 500 Hz.

To align the eye and MEG data, the continuous eye data was first up-sampled to 1200 Hz to match the MEG sampling rate. Then, the triggers of perceptual reports in the MEG and eye data were used to align the two data sets. Periods of blinks in the eye data were detected using the EyeLink's standard algorithms with default settings. Blinks were removed by linear interpolation of values measured just before and after each identified blink (interpolation time window: from 0.1 s before until 0.1 s after blink). Trials in which the gaze was more than 100 pixels from the fixation cross for more than 10% of the trial's

duration were excluded from further analysis. Finally, the eye tracking data was down-sampled to 250 Hz.

Spectral analysis of MEG power

Spectral analysis of MEG power modulations was performed as described for the main experiment above. We used the 25 sensors over visual cortex showing the biggest increase in gamma power during the Stimulus-on-off condition for the analyses of power modulation during MIB (see scalp map insets in Figure 7).

Analysis of modulations of microsaccade rate

Microsaccades were detected using the algorithm developed by Engbert and Mergenthaler (2006). Preprocessed eye data were first smoothed with a window of 20 ms to optimize microsaccade extraction. The permitted amplitude range was 0.08 - 2 degrees of visual angle, with minimum duration of 16 ms; microsaccades outside these ranges were rejected. Microsaccades that occurred within 20 ms of one another were merged into one saccade. The algorithm yielded a binary time course of saccade occurences (i.e., 1's embedded in a stream of 0's) for each trial. These time courses were convolved with a Gaussian window (sigma 0.1 s) (Martinez-Conde et al., 2004; Bonneh et al., 2010) and averaged across trials, (separately for target disappearance and re-appearance) and subjects.

Correlation between MEG power and microsaccade rate change

One analysis tested whether changes in microsaccade rate around perceptual switches in MIB (Bonneh et al., 2010) cause modulations of MEG power over visual cortex. To this end, we correlated the microsaccade rate change around perceptual report to the MEG power modulation time courses M(f,t) on a trial-by-trial basis. We calculated the microsaccade rate change for each trial by subtracting the number of microsaccades during a time window showing the transient MEG power modulations (-0.35 to 0.25 s relative to report) from the number of saccades in the preceding window (-0.95 to -0.35 s relative to report). Because responses in visual cortex that are evoked in visual cortex must occur only after some delay, we shifted the first time window by 50 ms backward in time relative to the transient time window used to extract the transient MEG modulations analyzed in this study (-0.3 to 0.3 relative to report). The results reported here are robust

with respect to this choice and also occurred for other delays (including 0 ms, data not shown).

We then correlated this rate change with MEG power in target disappearance trials, separately for each time-frequency bin (interval -1 to 1 s around report in the 3-35 Hz frequency range). The resulting time-frequency representations of correlation values were then tested for significant clusters across subjects using the cluster-based permutation procedure described above (see *Statistical tests of power modulations*).

Assessing MEG power modulations in the absence of microsaccades

In a complementary analysis, we tested whether the transient beta-band modulation was also evident in the absence of *any* microsaccades during the critical time window (-0.35 to 0.25 relative to report), in which microsaccades could have evoked modulations in MEG power. Longer time windows would have yielded an insufficient number of microsaccade-free trials (zero for most subjects). Only subjects who had more than 15 microsaccade-free trials per condition were included in this analysis (N=11 for disappearance and N=6 for re-appearance). The results were qualitatively similar when an inclusion threshold of 5, 10, 20 or 25 trials was used (data not shown).

RESULTS

Eleven healthy subjects viewed the continuous presentation of the MIB stimulus (Figure 1 A) during 32 runs (2 min each), while MEG activity was recorded (see *Materials and Methods*). The durations of MIB target disappearances and re-appearances varied widely (Figure 1 B). In several control conditions, perceptual switches similar to MIB target disappearances and re-appearances were exogenously triggered by physically removing the target from the screen in the same temporal sequence as MIB disappearances in that same subject, thus “replaying” the subjective MIB illusion to the subject. We, therefore, collectively refer to these control conditions as Replay. We used three different Replay conditions to disentangle the relationships between physical stimulus components, perceptual switches, subjects’ behavioral reports, and the measured modulations of cortical activity (see below). During the Replay-active condition, subjects reported target disappearance and re-appearance as during MIB. The Replay-passive condition was identical to Replay-active, except that subjects did not report the target disappearances.

The Replay-no-mask condition was identical to Replay-active, except that the target was presented without the surrounding mask (see *Materials and Methods* and below for the motivation behind each condition).

We focused our analyses on MEG sensors overlying occipital cortex that were most strongly driven by the MIB-stimulus when presented for 0.75 s in separate runs (Figure 1 C). Consistent with previous studies (Fries, 2009; Donner and Siegel, 2011; Jensen and Mazaheri, 2011) sensors overlying visual cortex showed the strongest stimulus-induced enhancement of gamma-band (60-90 Hz) and suppression of low-frequency (8-35 Hz) power. We computed the overall power across 12 sensors with maximum stimulus-induced responses, as well as the lateralization (contralateral – ipsilateral) with respect to the variable (left or right) visual hemifield position of the target. The corresponding sensors are highlighted on the topographical maps in Figure 1 C.

Top-down modulation in visual cortex during report of perceptual change

We analyzed the switch-related modulations in these twelve visually responsive sensors during the continuous viewing of the stimulus in the MIB illusion and the three Replay conditions described above. This was done to test four predictions about the switch-related modulations, which were derived from previous studies (Wilke et al., 2006; Donner et al., 2008): There should be a widespread modulation over visual cortex that (i) exhibits opposite polarity for MIB target disappearance and re-appearance, (ii) occurs also during Replay-active, (iii) is contingent on the need for behavioral report of the perceptual changes (i.e., absent during Replay-passive), and (iv) is decoupled from the MIB stimulus components (target, mask). More specifically, regarding prediction (iv), we expected that the modulation would occur also in the absence of the mask (Replay-no-mask). The tests of these predictions are described in the following and shown in Figures 2 (all conditions) and 3 (focusing on MIB and Replay-active). A qualitative summary of the power modulations in all conditions is provided in Table 1.

As expected, we observed MEG power modulations over visual cortex with opposite polarity for MIB target disappearance (Figure 2 A) and re-appearance (Figure 2 F). Specifically, around target disappearance, power was transiently suppressed in the beta-band (12-30 Hz, Figure 2 A and Figure 3 A, left panel, red line). This transient suppression was followed by more sustained suppression, first in the < 8 Hz range (from

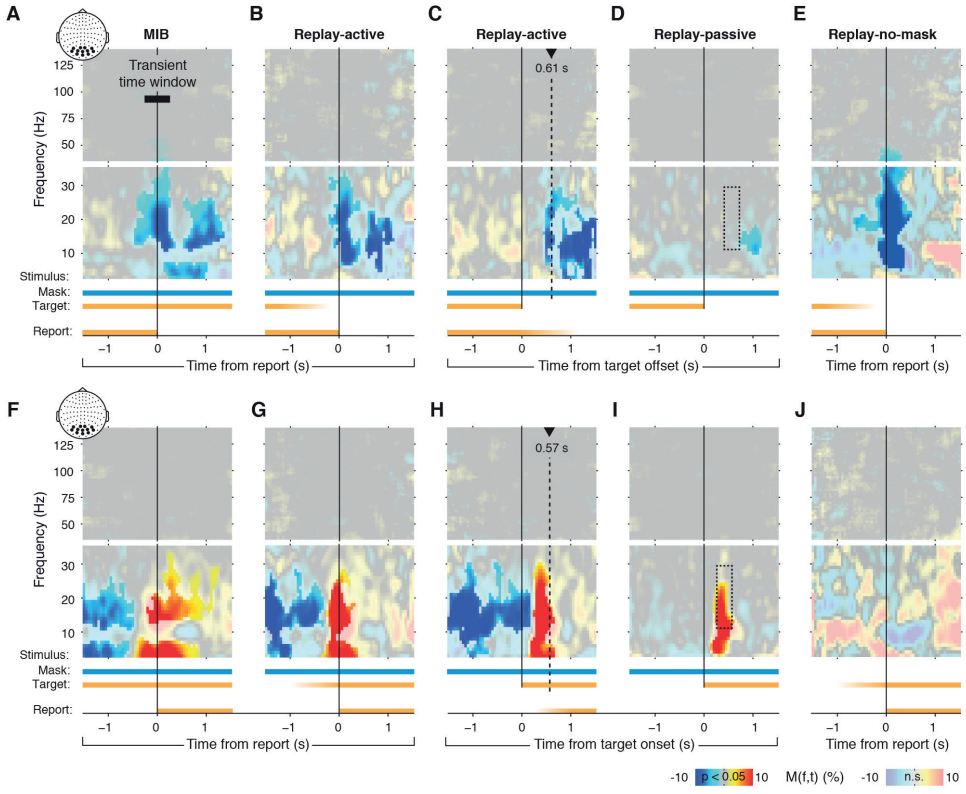

Figure 2 | Switch-related power modulations over visual cortex

MEG power modulations are shown as time-frequency representations, averaged across trials and subjects. Transparency level highlights clusters of significant modulation ($p < 0.05$, two-sided permutation test, cluster-corrected). In each panel, the first and middle rows correspond to high- and low-frequency ranges, respectively. Bottom row corresponds to time course of stimulus components and subjects' reports. Fading indicates variable timing of (instantaneous) stimulus changes with respect to the trigger. Different panels correspond to different experimental conditions and/or different trigger events. Inset scalp maps, sensor group used for this analysis. **A**. MIB, aligned to report. Black bar: transient time window used for subsequent analyses. **B**. Replay-active, aligned to report. **C**. Replay- active, aligned to stimulus change. Dotted vertical line, median reaction time. **D**. Replay-passive, aligned to stimulus change. **E**. Replay-no-mask, aligned to report; **F-J**: As A-E, but for target re-appearance. Dotted rectangle in **D, I**: time-frequency window for Table 1.

about 0.25 s after report) and then again in the beta-band (from about 0.5 s after report). The modulation profile was nearly inverted for re-appearance, with an enhancement of beta power around report (Figure 2 F and Figure 3 A, left panel, blue line). Notably, all these modulations around report excluded the gamma and alpha bands that are associated with bottom-up stimulus processing and attentional modulation in visual cortex (Fries, 2009;

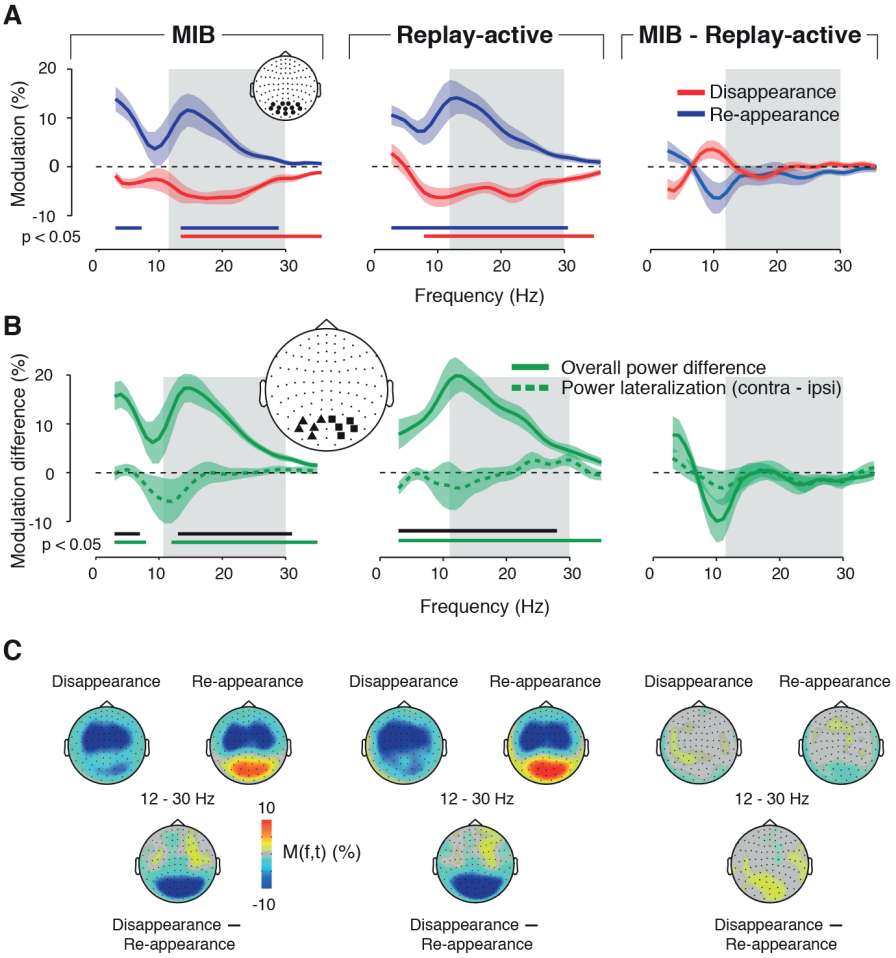

Figure 3 | Widespread beta-power transient over visual cortex encodes report

Top panels, spectra of mean low frequency (< 35 Hz) power modulation during transient time window (-0.3 to 0.3 s, see Figure 2 A) around report. Colored bars, clusters of significant modulation ($p < 0.05$, two-sided permutation test, cluster-corrected). **A**. MIB, Replay-active, and difference (MIB - Replay-active). Inset scalp map, sensor group used for this analysis. **B**. Solid line, re-appearance - disappearance difference for overall power modulation (i.e. difference between blue and red line in panel A). Dashed line, lateralization contralateral versus ipsilateral with respect to target hemifield. Triangles and squares in scalp map represent the sensors used for lateralization analyses. Green solid bar, clusters of significant overall modulation; black bar, clusters of significant difference between overall modulation and lateralization ($p < 0.05$, two-sided permutation test, cluster-corrected). There is no significant frequency cluster for the lateralization. **A, B**, shaded colored areas, s.e.m. (N = 11 subjects); shaded gray areas, range of beta-band modulation during MIB (12-30 Hz). **C**. Topographical maps of transient 12-30 Hz modulations and disappearance - re-appearance differences.

Donner and Siegel, 2011; Jensen and Mazaheri, 2011). Further, the modulations seemed widespread across the visual cortex (Figure 3 C, see section "Top-down modulation is decoupled from target stimulus and motor act" below).

Previous fMRI results indicate that – rather than prompting the perceptual switch – retinotopically global modulations in early visual cortex (in particular V1) are a consequence of the switch, occurring both in MIB and a replay of MIB, provided that these perceptual changes are actively reported (Donner et al., 2008). We, therefore, expected similar modulations during MIB and the Replay-active condition. Indeed, we found a similar beta-band modulation (with the same opposite polarity for disappearance and re-appearance) also in Replay-active (Figures 2 B and 2 G and 3 A, middle panel). Here, the modulation peaked closely around subjects' median reaction time relative to the physical target offsets or onsets in Replay-active (dashed vertical lines in Figure 2 C, H). There was no significant difference between transient power modulations during MIB and Replay-active across the beta-frequency range (Figure 3 A, right panel). The only difference between MIB and Replay-activity was a stronger modulation of alpha-band (8-12 Hz) power in Replay-active ($p = 0.026$, permutation test after collapsing across the 9-12 Hz range). This enhanced alpha modulation during Replay-active is consistent with attention capture by the transient change of the physical stimulus. The similarity in the spectral profile and amplitude of the power modulations during MIB and Replay-active is consistent with the beta-band modulation being a consequence, not the cause, of the perceptual switches during MIB.

Previous fMRI results showed that the global modulations in early visual cortex occurred only when the target disappearance and re-appearances were actively reported, while being absent during passive viewing (Donner et al., 2008). Similar observations were made for modulations of local field potential power in monkey cortex and thalamus (Wilke et al., 2009). Thus, we expected the beta-band modulation to be absent in the Replay-passive condition. Indeed, in line with this prediction, there was no transient beta-power suppression during disappearance (Figure 2 D). The dashed rectangle in Figure 2 D indicates the interval containing the significant transient modulation in Replay-active (compare with panels 2 C). During target re-appearance in Replay-passive, however, the power was enhanced across a wider range including the beta-band (Figure 2 H). Thus, the beta-suppression during target disappearance (but not the beta-enhancement during

target re-appearance) critically depended on the behavioral relevance of the perceptual change, possibly combined with the unpredictable timing of the changes.

Finally, we tested whether the beta-band modulation was independent of the presence of the mask. Indeed, in the Replay-no-mask condition the beta-suppression during target disappearance was robust (Figure 2 E), and at least as strong as in MIB and Replay-active (with mask), implying that it did not require the presence of the mask. By contrast, there was no significant power enhancement during target re-appearance (Figure 2 J). This might indicate that the power enhancement seen in the other conditions (Figure 2 F-I) might reflect a "contextual modulation" of the visual response to the mask by the re-appearance of the target (Zipser et al., 1996). Such a contextual modulation might occur, for example, because the target might interfere with the representation of the mask as a coherent surface.

There was a double dissociation between beta-power modulations during Replay-passive and Replay-no-mask (compare panels D-E vs. I-J in Figure 2, and columns 3 vs. 4 in Table 1). This indicates that the beta-suppression during target disappearance and the power-enhancement during target re-appearance are functionally distinct. The former, but not the latter, is consistent with a non-sensory modulation of population activity. This modulation does not reflect the cortical response to the MIB stimulus, but rather an endogenous signal originating within the brain. In the following, we therefore refer to this signal during target disappearance as a "top-down modulation".

Top-down modulation is decoupled from target stimulus and motor act

One well-characterized source of top-down modulation in visual cortex is spatial attention (Kastner and Ungerleider, 2000). Spatial attention to visual targets contained in one visual hemifield induces a selective lateralization of MEG power, relative to the target, in different frequency bands (Siegel et al., 2008; Wyart and Tallon-Baudry, 2008; Jensen and Mazaheri, 2011). During MIB, power modulations reflecting spatial attention might be selective for the target, the perception of which changes over time, as shown in an MIB study using one target per hemifield (Händel and Jensen, 2014). In contrast to the spatial attention prediction, we found that the beta-band modulation was not selective for target location during MIB (Figure 3 B, left panel) and Replay-active (Figure 3 B, middle panel). There was no evidence for lateralization in the beta-range, even for the most sensitive quantification

of the beta-band modulation (disappearance - re-appearance difference (dotted lines). Second, the overall power modulation (i.e., ipsilateral and contralateral sensors pooled; solid lines) was significantly stronger than the lateralization. Note that power suppression in the alpha-band (around 10 Hz), in contrast, exhibited a trend to significant lateralization, in particular during MIB, in line with the results of Händel and Jensen (2014). In sum, the beta-band modulation during perceptual changes is widespread across visual cortex, distinct from spatially selective attention signals that have been measured with similar techniques in other studies. Consequently, collapsing the beta-band modulation across subjects irrespectively of target location yielded a robust modulation (Figures 2, 3).

Given the strong link of the beta-band modulation to behavioral report, another possible source of the top-down modulation in visual cortex is the motor act (button presses / releases) used for report. Motor movements are commonly associated with a suppression of beta-band oscillations in the motor system (Pfurtscheller and Lopes da Silva, 1999; Donner et al., 2009). Indeed, we observed strong beta-power modulation over left and right motor cortices during report (Figures 3C and 4A). However, in line with previous studies (Pfurtscheller and Lopes da Silva, 1999; Donner et al., 2009), this motor beta-power modulation was stereotypically negative, irrespective of the type of report, in sharp contrast to the beta-modulation over visual cortex (Figures 3C). Further, the amplitude of the motor beta-suppression did not differ between disappearance and re-appearance reports (Figure 4), again in sharp contrast to the visual cortex beta modulation (Figure 3).

The dissociation between the visual beta-band modulation and motor act was also evident in a separate analysis of the two recording sessions, in which the mapping between perceptual switch and motor response was flipped (Figure 5). On day 1, subjects pressed the response button to indicate target disappearance and released the button to indicate target re-appearance; on day 2, this mapping was reversed (Figure 5 A). The beta-band modulation in visual cortex was qualitatively identical for both mappings, with a significant suppression of beta-power for disappearance and an enhancement for re-appearance (Figure 5 B, C).

In sum, the beta-band modulation in visual cortex was decoupled from the target, thus unlikely to reflect spatial attention, and it was also decoupled from activity in the motor cortex that was related to the behavioral report. A third possibility, which is

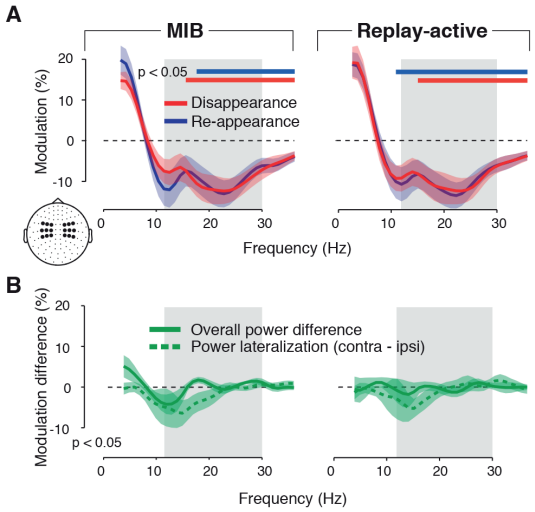

Figure 4 | Beta-power over motor cortex does not encode report

Same as Figure 3 A, B, but for sensors overlying motor cortex during MIB and Replay-active. **A**. Frequency spectra of MEG power modulation **B**. Re-appearance - disappearance difference for overall power modulation and lateralization contralateral versus ipsilateral with respect to hand used for report.

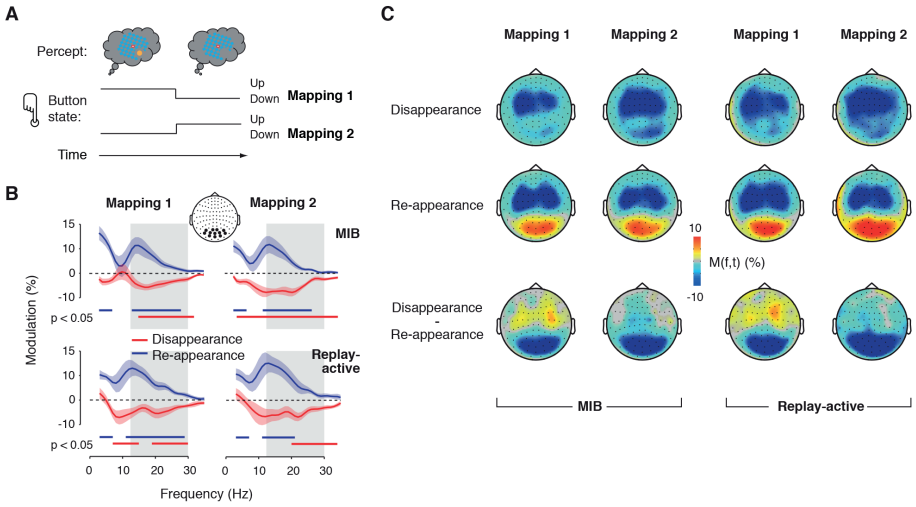

Figure 5 | Beta-power transient over visual cortex is unrelated to motor act

A. Opposite mappings of perceptual event to motor act on days 1 and 2. See main text for details. **B, C**. As Figure 3 A, C, but separately for both mappings (i.e., recording days).

consistent with all results presented here, is that the beta-power suppression during target disappearance, is driven by the central process that transforms the perceptual change into behavioral report: The beta-band suppression (i) is closely linked in time to the behavioral report; (ii) occurs irrespective of whether this perceptual change is spontaneous (MIB) or stimulus-evoked (Replay); (iii) is unaffected by large changes in the stimulus configuration (Replay-no-mask); (iv) but is strongly affected by eliminating the need for behavioral report (Replay-passive).

Top-down modulation predicts duration of perceptual illusion

We next tested for a possible functional role of the transient modulation in visual cortex: stabilization of the subsequent MIB illusion. To this end, we correlated the amplitude of the transient beta-suppression to the duration of the subsequent MIB target disappearance (i.e., using MIB duration as an index of perceptual stability; see *Materials and Methods*). Indeed, stronger beta-suppressions (i.e., populating the lower-rank bins) were followed by longer MIB durations (Figure 6 A, right panel). This correlation was highly significant across a range of different bin sizes as well as without normalizing individual MIB durations by the median per subject (data not shown).

There was no significant correlation to the preceding target visible duration (Figure 6 A, left panel), and a significant difference in the correlations for succeeding than preceding percept duration ($p = 0.03$, permutation test). Thus, as for the correlation to variability of cortical activity, the correlation to MIB duration was directed in time, specific for the succeeding target disappearance.

As shown in the previous sections, the beta-suppression (and its relation to trial-to-trial variability) was indistinguishable between MIB and Replay-active. The key difference between both conditions was the stability of perception: Target perception was bistable in MIB (i.e., percept durations governed by cortical interactions), but stable during Replay (i.e., percept durations governed by the physical on- and offsets of the target). Accordingly, as expected, there was no significant correlation during Replay-active (Figure 6 B), and the correlation was significantly smaller (i.e., less negative) than during MIB ($p = 0.002$, permutation test).

Finally, the association between beta-band activity and MIB disappearance duration was specific for the sensors overlying visual cortex. There was no significant correlation

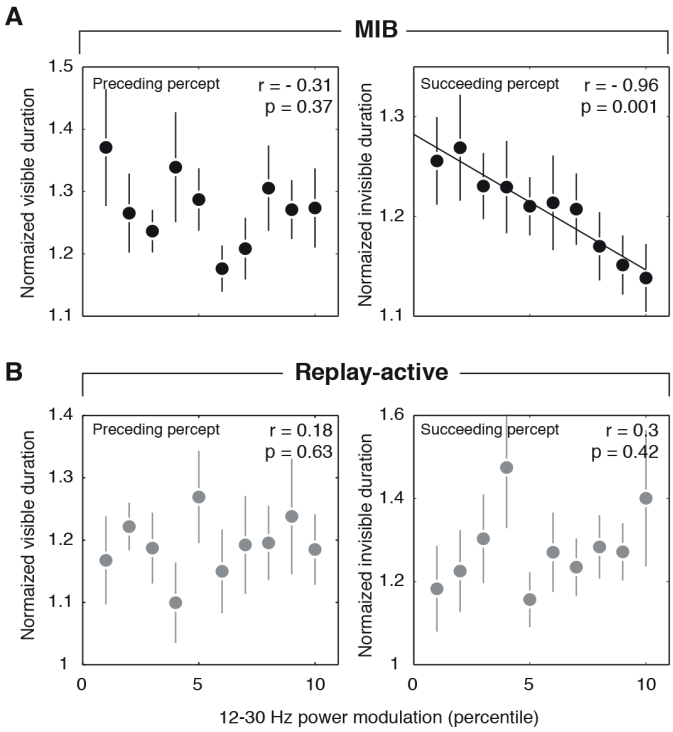

Figure 6 | Beta-power transient predicts stability of MIB illusion

Pearson correlation between beta-power suppression during disappearance report and the duration of the "preceding percept" (i.e., target visible, left column) or "succeeding percept" (i.e., target invisible, right column). Single-trial percept durations were normalized by each subject's median percept duration (see main text for details). **A**. MIB. **B**. Replay-active. Error bars, s.e.m. (N = 11 subjects).

between the beta-power suppression over motor cortex (which was even stronger than over visual cortex) during target disappearance and the subsequent MIB duration ($r = -0.34$, $p = 0.34$, permutation test; data not shown). In line with the findings reported above, this indicates that the beta-suppression during target disappearance reports reflects a top-down process confined to visual cortex and distinct from the process suppressing beta-band power over motor cortex.

Modulation is not due to microsaccades

One potential concern is that the power modulation in visual cortex may have been due to subtle changes in fixational eye movements during the perceptual switches (Hsieh and Tse, 2009; Bonneh et al., 2010). Specifically, target disappearance reports during

MIB and Replay are accompanied by a reduction in the rate of microsaccades (Bonneh et al., 2010). This reduction may have been associated with MEG power suppression in the beta range.

This concern seems unlikely for two reasons. First, our analysis excluded all trials containing blinks and saccades that were detectable with EOG. Second, smaller microsaccades during sustained visual stimulation induce broad-band (from low- to high-frequency) LFP power enhancements in visual cortex (Bosman et al., 2009) and associated eye movement artifacts in the extracranial EEG (Yuval-Greenberg et al., 2008). A modulation of microsaccades, therefore, predicts broadband power modulations, whereas the power modulation reported here was confined to the beta-band.

To conclusively rule out this concern, we performed an additional control experiment, in which we again measured MEG power modulations over visual cortex while simultaneously monitoring microsaccades with a high-resolution infrared eye tracker (see *Materials and Methods*). The microsaccade rate exhibited similar modulations as previously reported (Bonneh et al., 2010), decreasing before MIB target disappearance and increasing before re-appearance (Figure 7 A). However, during both target disappearance and re-appearance, no time-frequency cluster of the MEG power modulation was significantly correlated with this change in microsaccade rate (Figure 7 B).

Finally, we tested whether the transient beta-band modulation was also evident in the absence of *any* microsaccades. We selectively averaged MIB disappearance and re-appearance trials that contained no microsaccades (specifically in the time window from -0.35 to 0.25 s relative to report in which microsaccades could have evoked MEG power modulations) and found robust, statistically significant transient beta-band suppression for target disappearance (Figure 7 C, left) with a similar frequency profile as in the main experiment (Figure 7 D). Although beta-band modulation for re-appearance was again enhanced (Figure 7 C, right), it did not reach statistical significance, presumably due to the lower number of subjects that had a sufficient number of microsaccade-free trials to be included in this analysis (see *Materials and Methods*). These findings replicate the main neurophysiological signature reported in this paper in an independent group of subjects (on a different MEG system) and further rule out the concern that this signature may be due to microsaccades.

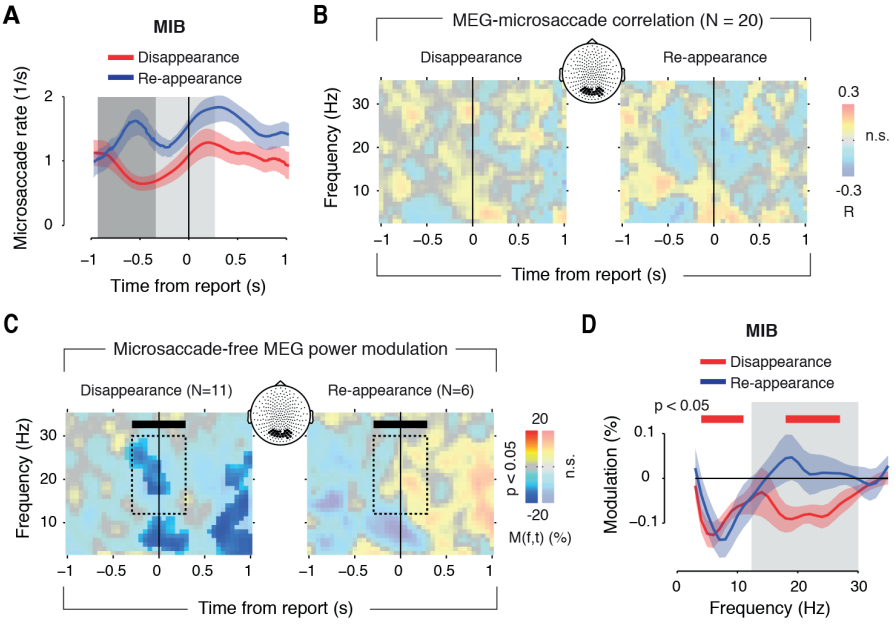

Figure 7 | Beta-band MEG power modulation during MIB is not due to microsaccades

A. Modulations of microsaccade rate for MIB target disappearance and re-appearance. Gray shaded areas represent the intervals used for computing the difference between the number of microsaccades before and around report (rate change). Error bars indicate s.e.m. across subjects. **B**. Time-frequency representation of the correlation between microsaccade rate change and MEG power modulation around MIB disappearance and re-appearance reports. Transparency level highlights clusters of significant modulation ($p < 0.05$, two-sided permutation test, cluster-corrected). Inset scalp map, sensor group used for this analysis. **C**. Time-frequency representation of MEG power modulation, selectively averaged across trials without microsaccades between -0.35 and 0.25 s relative to report (dotted outline). Transparency level highlights clusters of significant modulation ($p < 0.05$, two-sided permutation test, cluster-corrected). **D**. Frequency spectra of power modulation for disappearance and re-appearance in the transient time window for trials without microsaccades in this time window. Red solid bar, clusters of significant modulation ($p < 0.05$, two-sided permutation test, cluster-corrected)

DISCUSSION

We examined whether transient top-down modulations in visual cortex during perceptual changes in a multistable illusion may have an impact on the subsequent perceptual state. While some previous indirect evidence points to the existence of an active stabilization mechanism during continuous (Einhauser et al., 2008; Kloosterman et al., 2015a) or intermittent viewing (Leopold et al., 2002) of ambiguous stimuli, a neural signature of such a mechanism has not yet been observed. We reasoned that an active stabilization mechanism should be evident as a modulation of neural activity in visual cortex, which

predicts the stability of the subsequent cortical state and the perceptual interpretation of the ambiguous stimulus. Consistent with this idea, we found a transient modulation of beta-band activity in visual cortex right around reports of MIB target disappearances. The amplitude of this modulation predicts the duration of the subsequent perceptual suppression of the target. This modulation was (i) closely coupled to subjects' behavioral reports of the perceptual changes, (ii) independent of whether the perceptual change was initiated endogenously (MIB) or by an external stimulus change (Replay), but (iii) contingent on the changes' behavioral relevance and/or unpredictable timing, and (iv) decoupled from the components of the MIB stimulus (target and mask), as well as from (v) the motor cortical activity leading to the final button press reports.

Figure 8 illustrates our interpretation of the origin and functional impact of the transient beta-band suppression during disappearance reports. Our results suggest that this signal is of top-down origin, triggered by the process that transforms the perceptual change into a behavioral report (Figure 8 A). We here refer to this transformation as the perceptual decision, acknowledging that our task did not entail a choice between two options. Because the decision is independent of the cause of the perceptual change (intrinsic or stimulus-evoked), the beta-band suppression is evident during MIB and its replay. However, when there is no need for reporting the perceptual change (Replay-passive), no beta-suppression is observed.

Whatever the exact nature of this top-down signal, it seems to alter (stabilize) the internal state of visual cortex (Figure 8 B). The movement of a "percept variable" (green ball in Figure 8 B) (Moreno-Bote et al., 2007; Braun and Mattia, 2010) across an energy landscape with two valleys (basins of attraction; in the case of MIB corresponding to target visible and invisible) provides a useful metaphor for understanding this effect (Deco and Romo, 2008). In this scheme, the stabilizing state change can be conceived as an active force (red arrow) transiently deepening the valleys. Only if the sensory input is ambiguous and, consequently, the perceptual interpretation meta-stable (i.e., during MIB), does this transient state change culminate in a perceptual stabilization: the stronger the state change (i.e., the longer the red arrow) during a perceptual transition, the longer the subsequent perceptual illusion. During Replay, the physical removal of the target stimulus instantaneously alters the energy landscape, thus overriding the effect of the internal state change and precluding a link to percept duration. Please note that we here use the term "state change" to refer to a change in the dynamics of cortical activity (i.e., the shape of

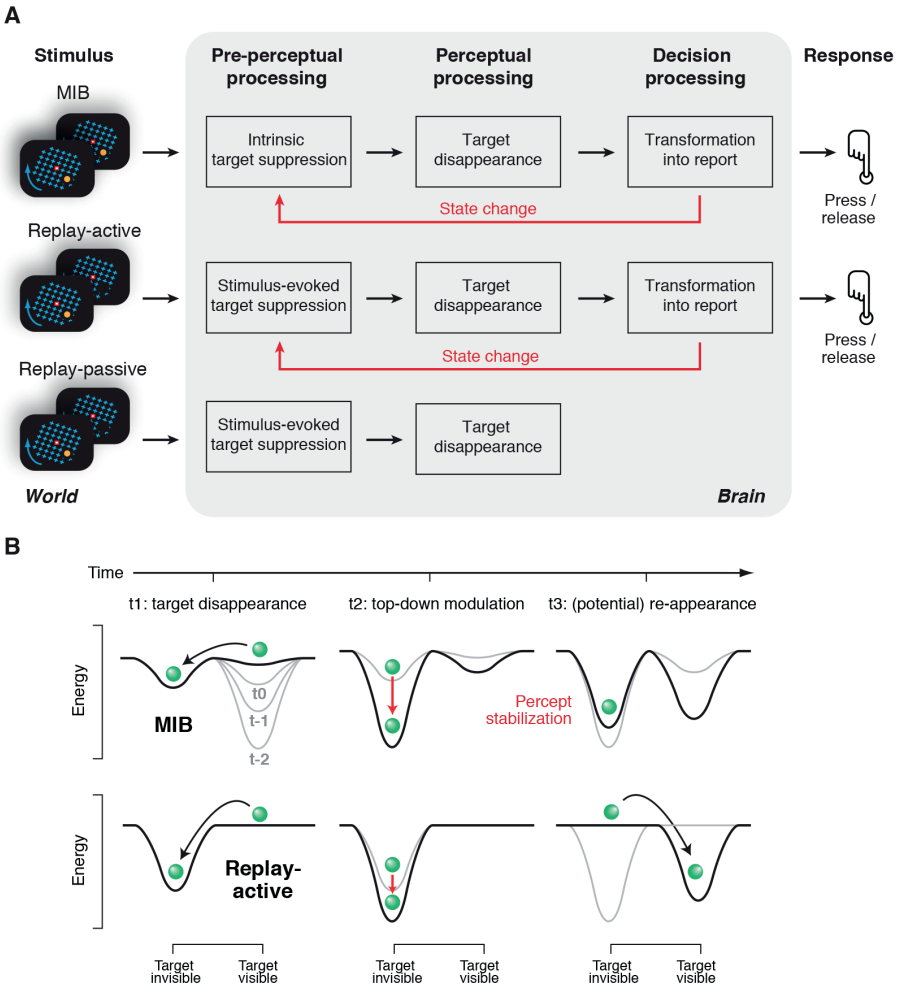

Figure 8 | Conceptual model of beta-power transient

A. Schematic of the hypothetical process driving the report-related beta-band modulation in visual cortex. During MIB, Replay-active, and Replay-passive, the cortical representation of the target is suppressed, leading to the target's disappearance. The suppression occurs either spontaneously (i.e., due to intrinsic cortical processing in MIB) or in response to the physical target offset (Replay). If the perceptual disappearance is task-relevant (MIB and Replay-active, but not Replay-passive), a central decision process transforms it into a behavioral report. This transformation induces the top-down modulation in visual cortex. The top-down modulation, in turn, alters the state of visual cortex and, hence, the target representation. **B.** Schematic of dynamical algorithm for cortical state change and perceptual stabilization. In both MIB (top) and Replay-active (bottom), the percept (green ball) is in the "target visible" valley. Adaption gradually flattens this valley before target disappearance (sequence: t_{-2}, t_{-1}, t_0). The ball then hops into the "target invisible" valley (perceptual switch, t_1). Behavioral report of this perceptual event induces a state change that deepens the target invisible valley (t_2, red arrows). This, in turn, stabilizes perception during MIB (t_3: top right): When the state change is strong, the percept variable is less likely to move back to the visible valley some time after the switch (t_3). By contrast, during Replay (t_3: bottom right), the physical target re-appearance alters the energy landscape (i.e., eliminates the target invisible valley), and thereby prevents the state change at t_2 from affecting the percept duration.

the energy landscapes in Figure 8 B) and not perception. The changes in perceptual state (i.e., target disappearances and re-appearances) experienced by the subject correspond to the hopping of the percept variable from one valley of this landscape to the other.

Different from other multistable illusions, the MIB illusion is asymmetric in the sense that it only entails a single non-veridical percept (target invisible). This might explain, why the top-down modulation is limited to the target disappearances. The power-enhancement differed functionally from the target re-appearance in that it also occurred during passive viewing of target stimulus onsets and depended on the presence of the mask. It seems likely that these functional differences are due to the inherent asymmetry of MIB and would not occur in symmetric bistable phenomena, such as binocular rivalry (Brascamp et al., 2006) or 3D-structure-from-motion (Klink et al., 2008). Despite the differences in symmetry, recent psychophysical work (Bonneh et al. 2014) establishes analogous dynamical properties for MIB as for the above two phenomena. We thus hypothesize that analogous beta-suppression effects as observed during MIB target disappearance will occur during all switches in these illusions. Future work should test this hypothesis.

Mounting evidence suggests that the widespread state change in visual cortex characterized here might be a general phenomenon. Several studies reported modulations of population activity in human and monkey early visual cortex, which were largely decoupled from cortical stimulus representations but linked to behaviorally relevant events (Jack et al., 2006; Wilke et al., 2006; Donner et al., 2008; Hsieh and Tse, 2009; Sirotin et al., 2009; Cardoso et al., 2012; de-Wit et al., 2012; Swallow et al., 2012; Donner et al., 2013; Choe et al., 2014). Specifically, several human fMRI studies reported retinotopically widespread modulations in V1 during perceptual reports in MIB (Donner et al., 2008; Hsieh and Tse, 2009; Kloosterman et al., 2015c), bistable motion binding (de-Wit et al., 2012), and visual discrimination tasks (Choe et al., 2014). Local field potential results from monkey visual cortex and thalamus (Gail et al., 2004; Wilke et al., 2006; Wilke et al., 2009) point to modulations in the alpha- and beta-bands as electrophysiological underpinning of the widespread fMRI-signal modulations associated with bistable perceptual dynamics. By establishing the retinotopically widespread nature and functional consequences of the switch-related beta-band modulations in the human brain, our current MEG results add critical new information to this emerging body of evidence.

What is the source of the beta-band modulation in visual cortex? At the functional level, the modulation could be a phasic arousal signal depending on the task demands (thus absent during passive viewing) and the timing of events that drive the modulation. It could also indicate that a response has been made. While these possibilities should be addressed in future work, we find that the modulation is specific for the type of the perceptual change (occurring specifically during target disappearance), and that it is dissociated from activity evident over motor cortex. Thus, our observations are inconsistent with a non-specific task- or response-related mechanism, or a direct copy of activity from the motor cortex. At the neural level, the beta-band modulation in visual cortex might originate from higher cortical areas (Nienborg and Cumming, 2009; Siegel et al., 2012), the thalamus (Wilke et al., 2009), neuromodulatory brainstem centers (Aston-Jones and Cohen, 2005; Parikh et al., 2007; Einhauser et al., 2008; Hupe et al., 2009; de Gee et al., 2014), or from a combination of cortical feedback and neuromodulation (Noudoost and Moore, 2011).

Indeed, neuromodulatory brainstem systems, such as the noradrenergic locus coeruleus and the cholinergic basal forebrain systems, also exhibit transient activity during perceptual reports, which can reflect the content of the report (Aston-Jones and Cohen, 2005; Parikh et al., 2007; Einhauser et al., 2008; Hupe et al., 2009; de Gee et al., 2014; Kloosterman et al., 2015b). Further evidence suggests that beta-band power modulations in visual cortex during visual stimulation might index changes in neuromodulatory state (Belitski et al., 2008; Donner and Siegel, 2011). If such beta-band modulation emerges from the interaction between neuromodulation and the bottom-up stimulus drive, this would explain why the beta-band modulation co-localizes with the response to the MIB stimulus, despite the more widespread neuromodulatory projections to the cortex.
Finally, neuromodulatory brainstem systems are in a position to stabilize the perceptual dynamics, because they can dynamically alter key cortical circuit parameters in profound ways. In particular, neuromodulators suppress cortical variability (Polack et al., 2013) and may amplify inhibitory interactions in cortical circuits (Haider et al., 2012). In competitive networks underlying multistable perception (Moreno-Bote et al., 2007; Braun and Mattia, 2010), a transient boost of mutual inhibition is equivalent into the deepening of valleys shown in Figure 7 B.

The cerebral cortex continuously undergoes changes in internal state (Steriade, 2000; Harris and Thiele, 2011; Lee and Dan, 2012). While these state changes have

traditionally been associated with slow fluctuations of arousal level (Steriade, 2000; Harris and Thiele, 2011; Haider et al., 2012) some of these state changes co-occur with rapid cognitive processes (Aston-Jones and Cohen, 2005; Gilbert and Sigman, 2007; Parikh et al., 2007). Our current results are consistent with the idea that the active report of perceptual changes triggers a cortical state change, which can stabilize an illusory percept. Future work should address whether the effect we have identified here for the MIB illusion generalizes to other perceptual phenomena (Jazayeri and Movshon, 2007; Stocker and Simoncelli, 2008; Fischer and Whitney, 2014), as well as to more complex decisions beyond the domain of perception (Festinger, 1957).

ACKNOWLEDGEMENTS

We thank David Heeger, Tomas Knapen, Mike X Cohen, Simon van Gaal, Tomas Knapen, Anouk van Loon, Sander Nieuwenhuis, Jan Brascamp, and all members of the Donner lab for comments on the manuscript. This work was supported by the European Research Council (V.A.F.L.: DEFCON1). The authors declare no competing financial interests.

Chapter 3

Modulation of Beta-Band Activity in Human Visual Cortex by Covert Perceptual Decisions

This chapter is based on:

Meindertsma, T.*, Kloosterman, N. A.*, Nolte, G., Engel, A. K., Donner, T. H. (* Shared first authorship). Modulation of Beta-Band Activity in Human Visual Cortex by Covert Perceptual Decisions. *In preparation.*

ABSTRACT

The cerebral cortex continuously undergoes changes in internal state. Such state changes occur during slow transitions from sleep to wakefulness, but also when awake, during cognitive acts operating at a sub-second timescale. Recent studies of simple perceptual decisions (reporting the presence or absence of visual targets) have identified a signature of such a rapid change in cortical state during the report of sudden target disappearances: a widespread suppression of neural population activity in the beta frequency range across early visual cortex. Several observations indicate that this modulation is a top-down signal caused by the perceptual decision. Here, we used magnetoencephalography (MEG) to further characterize this top-down modulation. Consistent with previous observations, reports of (spontaneous and stimulus-evoked) target disappearances were associated with widespread beta-power suppression over visual cortex. Importantly, when observers silently counted the disappearances, we observed the same beta-band suppression over visual cortex as when they reported the disappearances by button press. Taken together, our results indicate that the beta-band suppression is tightly linked to the perceptual decision process.

Keywords: beta-oscillations, bistable perception, brain dynamics, brain state, perceptual decision-making

INTRODUCTION

The cerebral cortex continuously undergoes changes in its internal state, as revealed by the temporal structure of cortical population activity (Steriade, 2000; Harris and Thiele, 2011; Lee and Dan, 2012). For example, strong and widespread changes in cortical state occur during the transition from sleep or anesthesia to wakefulness (Steriade, 2000; Harris and Thiele, 2011; Haider et al., 2012). However, mounting evidence points to the existence of more rapid cortical state changes during wakefulness, that are time-locked to cognitive acts like perceptual decisions (Ress et al., 2000; Aston-Jones and Cohen, 2005; Jack et al., 2006; Wilke et al., 2006; Gilbert and Sigman, 2007; Parikh et al., 2007; Donner et al., 2008; Wilke et al., 2009; Harris and Thiele, 2011; Choe et al., 2014; Kloosterman et al., 2014). One possible source of these rapid cortical state changes are neuromodulatory brainstem centers, such as the noradrenergic locus coeruleus (Aston-Jones and Cohen, 2005; Bouret and Sara, 2005) and the cholinergic basal forebrain (Sarter et al., 2009). These centers exhibit phasic activity during perceptual tasks and send widespread projections to the cortex.

A number of studies investigating simple visual decisions in humans and non-human primates have identified neurophysiological and neuroimaging signatures of cortical state changes in early visual cortex (Ress and Heeger, 2003; Jack et al., 2006; Wilke et al., 2006; Gilbert and Sigman, 2007; Donner et al., 2008; Wilke et al., 2009; Choe et al., 2014; Kloosterman et al., 2014). In line with signal detection theory (Green and Swets, 1966), we here define a simple perceptual decision as the transformation of a graded perceptual signal into a categorical proposition that can drive an (immediate or delayed) motor action. For example, one study found that the functional magnetic resonance imaging (fMRI) response in human V1 during a yes-no contrast detection task reflects only the observers' yes vs. no judgment, but not the physical stimulus (Ress and Heeger, 2003). Another line of studies reported a transient suppression of the fMRI-response and electrophysiological population activity in early visual cortex during observers' reports of the disappearance of a salient visual target. (Wilke et al., 2006; Donner et al., 2008; Maier et al., 2008; Wilke et al., 2009; Donner et al., 2013; Kloosterman et al., 2014). This transient suppression (i) is widespread across the retinotopic map of area V1, evident far beyond the sub-regions processing the stimulus (Donner et al., 2008), (ii) predominates in the 12-30 Hz (beta) frequency range of the local field potential (Wilke et al., 2006; Maier et al., 2008; Wilke

et al., 2009) and MEG (Kloosterman et al., 2014), (iii) occurs during both spontaneous (in perceptually bistable situations) and stimulus-evoked disappearance of the target (Wilke et al., 2006; Donner et al., 2008; Maier et al., 2008; Wilke et al., 2009; Donner et al., 2013; Kloosterman et al., 2014), and (iv) is not evident during passive viewing of the target disappearance (Wilke et al., 2006; Donner et al., 2008; Maier et al., 2008; Wilke et al., 2009; Donner et al., 2013; Kloosterman et al., 2014). Taken together, these observations suggest that the transient modulation in visual cortex reflects a widespread top-down modulation of the state of visual cortex that is triggered by the observer's decision to report a perceptual change (Kloosterman et al., 2014).

The goal of the present study was to further pinpoint the functional characteristics of this top-down modulation. The fact that the modulation occurs during the active report of perceptual changes, but not during passive viewing (Wilke et al., 2006; Donner et al., 2008; Maier et al., 2008; Wilke et al., 2009; Donner et al., 2013; Kloosterman et al., 2014), might indicate that the modulation is triggered by the motor response (button press) used for report, rather than by the perceptual decision per se (O'Connell et al., 2012). Indeed, motor responses are associated with beta-band modulations in the motor system (Donner et al., 2009; Engel and Fries, 2010). Although our previous findings suggest that the report-related beta-band modulation in visual cortex was decoupled from motor beta-band activity in several ways (Kloosterman et al., 2014), it remains an open question whether the same modulation occurs when subjects covertly form decisions about the perceptual changes without reporting them immediately by button press. Here, we addressed this question by instructing subjects to silently count the number of target disappearances and re-appearances and report the total after the end of an experimental block (O'Connell et al., 2012). We found that a similar beta-band modulation over visual cortex accompanied covert (silent counting) and overt (button press) perceptual decisions. Our results show that the beta-band suppression in visual cortex is closely linked to endogenous perceptual decision processes. (Kloosterman et al., 2014)

MATERIALS & METHODS

Subjects

22 subjects participated in the experiment. One subject was excluded due to failure to complete all the sessions and one subject was excluded after the first session due to bad pupil data quality. Thus, twenty subjects (11 female, age range 20 - 54 years, mean age 29.6, SD 10.7) were included in the analysis. All subjects had normal or corrected-to-normal vision and no known history of neurological disorders. The experiment was approved by the ethics committee of the Universitätsklinikum Hamburg Eppendorf, and each subject gave written informed consent.

Stimulus

Subjects viewed the continuous presentation of a static target (full contrast Gabor patch; diameter: 2°, two cycles) and reported target disappearance and re-appearance. The latter perceptual events were either induced spontaneously, by means of a bistable perceptual illusion called motion-induced blindness (MIB (Bonneh and Donner, 2011); see Figure 1), or they were evoked by the physical on- and offsets of the target, “replaying” the illusion. We used a number of these Replay conditions. By using a Gabor patch as the target, subjective (during the illusion) and physical (during its replay) stimulus luminance remained constant around the target onsets and offsets, so that pupil responses due the subjective or objective light and dark responses after perceptual reports would be as minimal as possible (Loewenfeld and Lowenstein, 1993). During the Replay conditions (see *Behavioral Tasks and Design*), the different parts of the Gabor modulated at opposite phase at a temporal frequency of 10 Hz. The resulting counter-phase flicker rendered the target more salient and thus minimized the number of illusory target disappearances during Replay. The target was located in either the lower left or lower right visual field quadrant (eccentricity: 5°, counterbalanced between subjects), surrounded by a rotating mask (17°x17° grid of white crosses) and superimposed on a gray background (Figure 1A). The mask rotated at a speed of 160°/s. The target was separated from the mask by a gray “protection zone” subtending about 2° around the target (Bonneh et al., 2001). Subjects fixated on a fixation mark (red outline, white inside, 0.8° width and length) centered on the mask in the middle of the screen. Stimuli were presented using the Presentation Software (NeuroBehavioral Systems, Albany, CA, USA). Stimuli were back-projected on

a transparent screen using a Sanyo PLC-XP51 projector with a resolution of 1024x768 pixels at 60 Hz. Subjects were seated 58 centimeters from the screen in a whole-head magnetoencephalography (MEG) scanner setup in a dimly lit room.

Behavioral Tasks and Design

The subjects participated in various tasks designed to determine the factors driving transient modulations of cortical activity around reports of perceptual switches. All subjects completed the MIB condition and the various Replay conditions; the Stimulus-on-off condition was completed by 17 of the subjects.

Stimulus-on-off

In this Stimulus-on-off condition, subjects viewed the full MIB stimulus (gray background, fixation, rotating mask and target) for 0.75 s, preceded and succeeded by only the background and fixation. This stimulus duration was too short to induce MIB target disappearance, but sufficiently long to measure the stimulus-induced modulation of cortical population activity (Figure 1D). Subjects were instructed to maintain fixation and passively view the stimulus on- and offsets.

MIB condition

The MIB stimulus (Figure 1A) was continuously presented for several runs of 3 min duration each. The subjects' task was to maintain stable fixation and report the spontaneous disappearance and re-appearance of the target by pressing a response button with their right index finger and middle finger, respectively.

Replay conditions

The "Replay" conditions were identical to MIB, except that the target was intermittently removed from the screen physically, so subjects reported physical instead of illusory target disappearances. The physical offsets and onsets of the target were always instantaneous, mimicking the typically abrupt quality of the perceptual switches in MIB.

The general purpose of the Replay conditions was to test whether transient modulations in cortical activity during MIB are related to the motor response to indicate decisions. In addition, different replay conditions contained different levels of temporal

surprise to investigate whether the transient beta-band modulation was affected by surprise. To test the first question, subjects reported switches either promptly (Replay-button condition) or silently counted target offsets (Replay-count condition). To test the second question, we manipulated the timing of the on- and offsets of the target in three levels of surprise (high, medium and low). These manipulations resulted in a 2x3 factorial design (report method x surprise level). The results of the surprise manipulation will be reported in a separate paper.

Replay-button: In this condition subjects had to report target disappearances and re-appearances in the same way as during MIB, by pressing a button with their right index finger and middle finger. Perceptual switches were evoked by physical target off- and onsets on the screen.

Replay-count: This condition was identical to Replay-button, except for the way subjects reported the perceptual changes. Instead of pressing buttons, subjects had to silently count the number of target offsets that occurred during the 3 minute run and report the total in a four alternative forced-choice (4AFC) question (Figure 1B). The 4AFC question was prompted on the screen after the run ended. The three incorrect 4AFC alternatives were generated by randomly subtracting or adding 1, 2 or 3 from the actual number of disappearances, under the constraint that the four alternatives were all different from each other. In each run, Replay-button or Replay-count conditions were randomly selected, under the constraint that 50% of the Replay runs were Replay-button. The corresponding instructions were displayed on the screen before the run started. Subjects could only start the next run after they confirmed the instructions to the experimenter over the intercom.

The experiment consisted of two sessions of ca. two hours. Over these sessions, subjects completed a total of 44 three-minute runs (MIB: 6, both Replay-button and -count: 19), divided over blocks of three runs. Subjects performed MIB and Replay in different blocks. The order of the blocks within a session was counterbalanced across subjects. The Stimulus-on-off condition was performed at the end of one of the two sessions.

MEG and eye tracking recordings

Magnetoencephalography (MEG) data were acquired on a CTF 275 MEG system (VSM/CTF Systems, Port Coquitlam, British Columbia, Canada) with a sample rate of 1200 Hz. Subjects were placed in a seated position inside the scanner. The location of the subjects' head was measured real-time using three fiducial markers placed in the both ears and on the nasal bridge to control for excessive movement. Furthermore, electrooculography (EOG) and electrocardiography (ECG) were recorded to aid artifact rejection.

Concurrently with the MEG recordings, the diameter of the left eye's pupil was sampled at 1000 Hz with an average spatial resolution of 15 to 30 min arc, using an EyeLink 1000 Long Range Mount (SR Research, Osgoode, Ontario, Canada). This MEG-compatible (non-ferromagnetic) setup was placed on a table under the stimulus presentation screen. The eye tracker was calibrated before every block of four runs. The eye tracking data are reported in Chapter 5 (Kloosterman et al., 2015b).

Data analysis

The MEG data were analyzed in MATLAB (The Mathworks, Natick, MA, USA) using the Fieldtrip (Oostenveld et al., 2011) and Chronux (Mitra and Bokil, 2008) toolboxes and custom-made software.

Trial extraction

For the Stimulus-on-off condition, we extracted trials of fixed durations, ranging from 0.2 s before to 0.75 s after stimulus onset.

For the MIB and Replay conditions involving subjects' reports, we extracted trials of variable duration, centered on subjects' button presses or releases, from the three-minute runs of continuous stimulation. For trial extraction we used the algorithm that we designed in our previous study (Kloosterman et al., 2014). Thus, in the case of MIB, the term "trial" refers to an epoch of constant stimulation and is solely defined based on subjects' subjective reports of target disappearance and re-appearance. We call this method for trial extraction "response-locked". The following constraints were used to avoid mixing data segments from different percepts when averaging across trials: (i) The maximum trial duration ranged from -1.5 s to 1.5 s relative to report; (ii) when another report occurred within this interval, the trial was terminated 0.5 s from this report; (iii) when

two reports succeeded one another within 0.5 s, no trial was defined; (iv) for the analysis of all Replay-button conditions, we included only those reports that were preceded by a physical change of the target stimulus within 0.2 to 1 s, thus discarding reports following illusory target disappearances.

In an alternative analysis of all Replay conditions, trials were defined in the same way as described above, but now aligned to physical target on- and offsets, eliminating the need to discard illusory target disappearances ("stimulus-locked"). In the Replay-count conditions, no button responses were given during the run, so stimulus-locked trial extraction was the only option. We used this method in every analysis that involved the Replay-count condition.

Preprocessing

The following preprocessing steps were performed: trial extraction (see *Trial extraction*), environmental, muscle, jump and eye artifact rejection, and resampling to 500 Hz.

Artifact rejection

All epochs that contained artifacts caused by environmental noise, eye, muscle activity or squid jumps were excluded from further analysis using standard automatic methods included in the Fieldtrip toolbox. Epochs that were marked as containing an artifact were discarded after every artifact detection step. For all artifact detection steps the artifact thresholds were set individually for all subjects. Both of these choices aimed at optimization of artifact exclusion. Line noise was removed by subtracting the 50, 100, 150 and 200 Hz Fourier components from the raw MEG time course of each trial.

Spectral analysis of MEG power

We used sliding window Fourier transform (Mitra and Pesaran, 1999) (window length: 400 ms, step size: 50 ms) to calculate time-frequency representations of the MEG power (spectrograms) for each sensor and each single trial. We used a single Hanning taper for the frequency range 3 - 35 Hz (frequency resolution: 2.5 Hz, bin size: 1 Hz) and the multi-taper technique for the frequency range 36 - 140 Hz (spectral smoothing: 8 Hz, bin size: 2 Hz, five tapers). After time-frequency analysis, the two orthogonal planar gradiometers of each sensor were combined by taking the sum of their power values.

Stimulus-induced power modulation

For Stimulus-on-off, spectrograms were averaged aligned to MIB stimulus onsets. For MIB and Replay conditions, spectrograms were averaged aligned to perceptual reports of target disappearances/re-appearances (MIB and Replay), or aligned to the corresponding target off-/onsets (Replay).

Switch-related power modulation

Power modulation (denoted as M(f,t) in the figures) were characterized as the percentage of power change at a given frequency bin and time point, relative to a "baseline" power value for each frequency bin. For Stimulus-on-off, the baseline was computed as the mean power across the pre-stimulus blank fixation interval (from -0.25 s to 0 s relative to stimulus onset). For MIB and Replay, the baseline was computed by averaging the power values across all time points within each trial (maximum time range -1.5 to 1.5 s around the event), and then across all variable-length trials (i.e., pooling across disappearance and re-appearance trials) within a recording day, but separately for each condition (i.e., MIB, Replay-button, Replay-count). As a result, the modulation around perceptual reports (MIB and Replay conditions) and stimulus changes (Replay conditions) were expressed as percentage of power change relative to the mean power across all artifact-free trials of each condition.

We focused our analysis of MEG power modulation around perceptual reports on those cortical regions that also processed the physical MIB stimulus (i.e. visual cortex). Therefore, before performing the statistical tests described in this and the following section, we averaged all power modulation across the 25 occipital sensors exhibiting the biggest stimulus-induced high-frequency response (60-120 Hz) during Stimulus-on-off (marked in Figure 1 C). See for a similar procedure Kloosterman et al. (2014).

Statistical tests of power modulation

We used a two-tailed permutation test (1000 permutations) (Efron and Tibshirani, 1998) to test the significance of the overall power modulation of the sensor group obtained in Stimulus-on-off. We tested the overall power modulation for (i) significant deviations from zero, and (ii) significant differences between disappearance and re-appearance. For all these tests, we used a cluster-based procedure (Maris and Oostenveld, 2007) to correct

for multiple comparisons. For time-frequency representations of power modulation (Figures 1, 2), this was done across all time-frequency bins. Because in our previous study we observed a transient modulation around the perceptual switches across the time window -0.3 to 0.3 s around report (Kloosterman et al., 2014), we averaged power modulation for all subsequent analyses across this time window before statistical tests. For statistical tests of the spectra of transient power modulation around report (Figure 3), we performed the permutation test with cluster-based multiple comparison correction across frequency bins. Based on our previous study, we defined our frequency band for further analyses based on the significant cluster around disappearance reports during MIB (12-30 Hz).

To test the effect of motor response on the power modulation around perceptual switches, we statistically compared the Replay-button and Replay-count conditions. The cluster-based permutation analysis was performed separately on both conditions and on the difference between conditions. Due to the lack of motor report during Replay-count, we performed this analysis time-locked to the stimulus onsets and offsets. We could not perform the corresponding analysis for MIB, because due to its illusionary nature there were no stimulus triggers in this condition.

RESULTS

Top-down modulation in visual cortex during report of perceptual change

First, consistent with previous studies, we found a decrease of ~8-40 Hz (alpha and beta) power and an increase of ~60-120 Hz (gamma) power in visual cortex (Figure 1C) during brief presentations of the MIB-stimulus in the Stimulus-on-off condition (Fries, 2009; Donner and Siegel, 2011; Kloosterman et al., 2014). We selected the 25 sensors with the strongest stimulus-evoked gamma power increase for further analyses (see dashed box in Figure 1C, top panel and *Materials & Methods*). All of the selected sensors were located over the occipital cortex (depicted as circles in the topographic plot in the top panel in Figure 1C).

Next, we investigated the power modulation in these sensors around reports of target disappearance and re-appearance during the continuous MIB and Replay-button

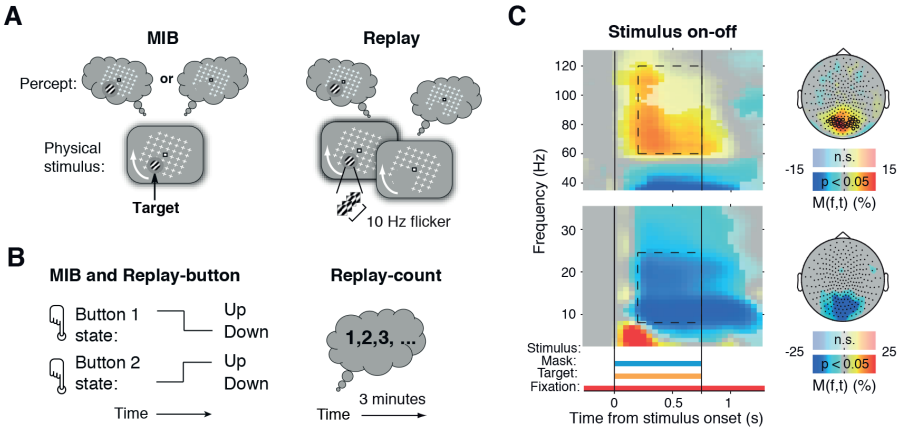

Figure 1 | Stimuli, behavioral tasks and stimulus response

A. Schematic snapshots of stimuli and alternating percepts. Left, bottom panel: MIB stimulus. A salient target stimulus (Gabor patch) was surrounded by a moving mask pattern (white), which appeared as a rotating grid. Top left panel, fluctuating perception of the target due to MIB. Right: Corresponding stimulus and alternating perception during Replay, in which the target flickered at 10 Hz. **B**. Behavioral response regimes. Left, MIB and Replay-button. Subjects reported perceptual switches by alternating button press of two buttons. Right, Replay-count. Subjects covertly counted the disappearances during the three-minute run, and reported the total after the end of the run in a 4AFC question. **C**. Cortical response to the MIB stimulus during Stimulus on-off. Scalp maps, topography of 8-25 Hz and 60-120 Hz modulations (0.25-0.75 s after stimulus onset; see dashed outlines on time frequency representations). Fully saturated colors indicate clusters of significant modulation ($p < 0.05$, two-sided permutation test across subjects, cluster-corrected, N = 17 subjects). Highlighted circles in high frequency scalp map (top right): MEG sensors showing the biggest stimulus response. These sensors were used for the subsequent analyses of overall power modulation.

conditions. We found a decrease in power in the beta band (~12-30 Hz) around the reports of target disappearances in the MIB condition (Figure 2A). The transient modulation of power was specific to this frequency band, sparing out the alpha and gamma bands. We observed a positive modulation during re-appearances to the target in the MIB condition (Figure 2D). Similar power modulations occurred during Replay-button, in which perceptual switches were evoked by physical target offsets and onsets (Figure 2B and 2E). This finding indicates that the transient beta modulations are not the cause of the perceptual switches, but instead are their consequence (otherwise they would only occur during MIB). In addition, there was significant alpha-band (~10 Hz) suppression around target disappearance during Replay-button (Figure 2B), but not MIB (Figure 2A). This alpha suppression presumably reflects attention capture by the physical target offsets in Replay-button.

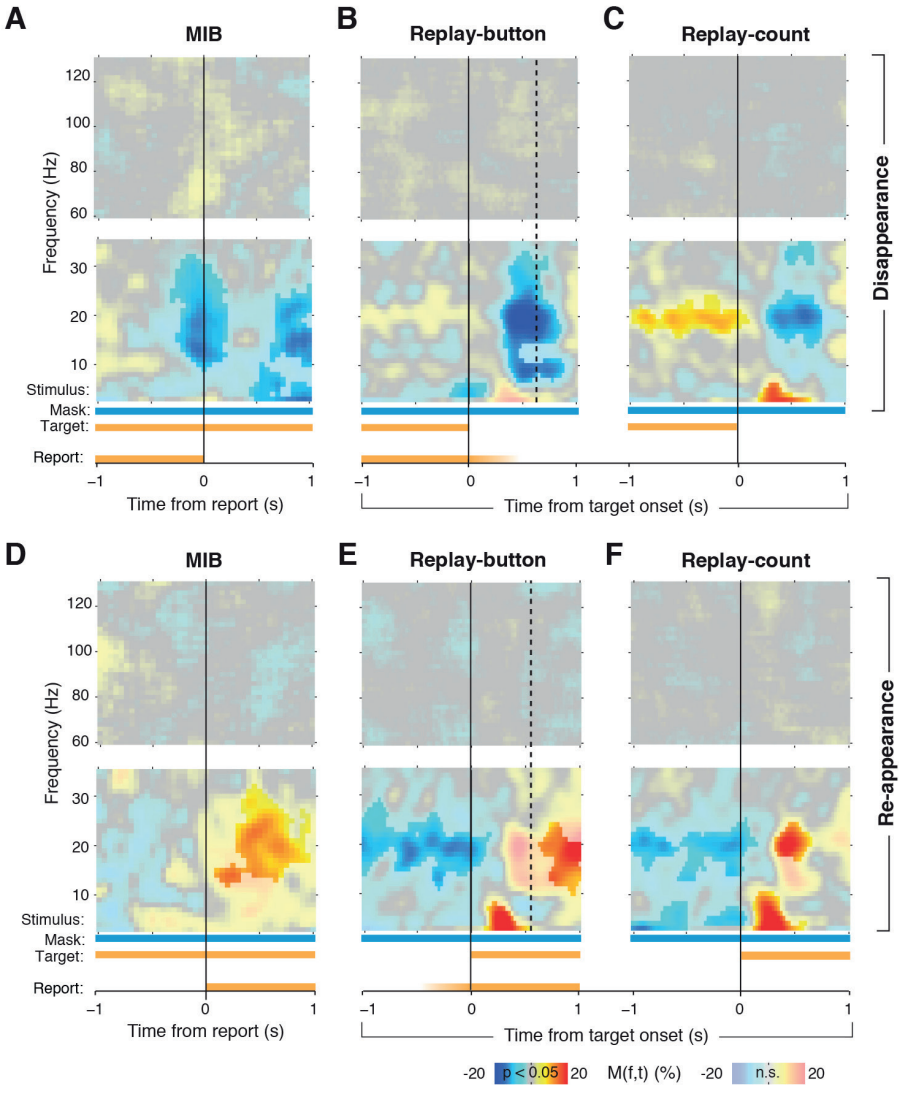

Figure 2 | Switch-related power modulation in visual cortex is independent of immediate motor report

MEG power modulations are shown as time-frequency representations, averaged across trials within each subject and then across subjects. Fully saturated colors highlight clusters of significant modulation ($p < 0.05$, two-sided permutation test, cluster-corrected). In each panel, the first and middle rows correspond to high- and low-frequency ranges, respectively. Bottom row corresponds to time course of stimulus components and subjects' reports. Fading indicates variable timing of the instantaneous stimulus changes with respect to the trigger. Different panels correspond to different experimental conditions and different trigger events. **A**. MIB, aligned to disappearance report. **B**. Replay-button, aligned to stimulus offset. Dashed line indicates median reaction time. **C**. Replay-count, aligned to stimulus offset. **D-F.** Corresponding modulation aligned to re-appearance report.

In contrast to the percept-specific modulation around target disappearance and re-appearance over occipital cortex (positive for re-appearance, negative for disappearance), the beta modulation over parietal cortex was negative during both disappearance and re-appearance. Subtracting the two topographical maps effectively isolated the percept-specific beta modulation over occipital cortex, while the modulations over parietal cortex were cancelled out (Figures 3G and 3H). This finding suggests that the beta suppressions over visual and parietal cortices around disappearance reflect functionally distinct processes. Taken together, the beta modulation observed here is consistent with our previous findings (Kloosterman et al., 2014) of a top-down modulation across visual cortex around perceptual switches. The current findings provide an important replication, using a different MEG system and a new group of subjects.

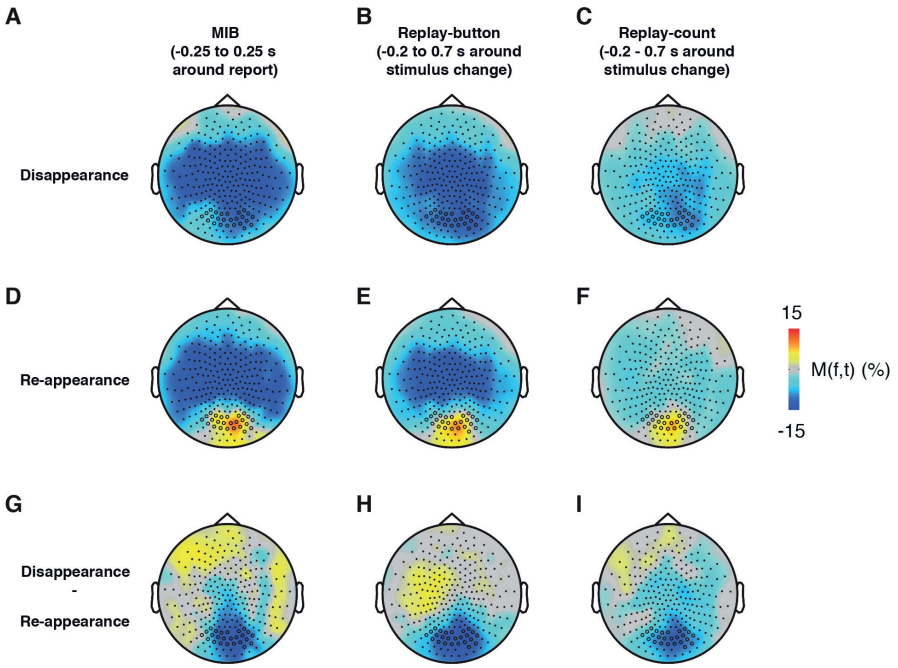

Figure 3 | Switch-related power modulation in visual cortex is independent of motor-response-related activity in parietal cortex

Topographical scalp maps of 12-30 Hz modulations and disappearance - re-appearance differences. **A**. MIB disappearance. **B**. Replay-button disappearance. **C**. Replay-count disappearance. **D-F**. Corresponding scalp maps for re-appearance. **G-I**. Corresponding scalp maps for disappearance - re-appearance difference.

Beta-band modulation in visual cortex reflects the decision to report switches

In our previous studies, we observed the modulation in visual cortex during immediate motor report of the perceptual switches, but not when subjects passively viewed target onsets and offsets during Replay (Donner et al., 2008; Kloosterman et al., 2014). The lack of modulation during passive viewing can either be explained by the absence of an immediate button press to indicate switches, the absence of an active decision about the stimulus change, or a combination of the two. To disentangle decision-related from motor-related modulation around perceptual switches, we asked subjects in the Replay-count condition to silently count target disappearances and report the total at the end of the run (see *Materials & Methods*). As during MIB and Replay-button, also during Replay-count subjects were required to actively decide whether their perception switched, but any motor-related component around the switches was eliminated.

Indeed, despite the lack of an immediate motor response, we also found significant transient beta-band modulation over visual cortex around perceptual switches during Replay-count (Figures 2C, 2F, 3C and 3F), with a similar difference map between disappearance and re-appearance as for MIB and Replay-button (Figure 3I, compare with Figures 3G and 3H). In contrast to MIB and Replay-button, there was no beta suppression over parietal cortex around the perceptual switches in Replay-count (Figures 3C and 3F), indicating that parietal modulations during MIB and Replay-button are related to the motor response to report the switches. Although the beta modulation was weaker than during MIB and Replay-button, this difference was not statistically significant. Taken together, these findings indicate that a considerable component of the transient beta-band modulation around the switches can be ascribed to the decision to report the perceptual switch, even when the actual report of the switch is delayed in time. This conclusion is in line with our interpretation of the modulation as a top-down signal triggered by perceptual decisions (see *Discussion*).

DISCUSSION

Here, we show that simple perceptual decisions about salient visual targets trigger a modulation of beta-band activity in visual cortex. The modulation is widespread and unrelated to the location of the visual target, its sign encodes the content of perceptual

reports, and a significant component of it reflects the endogenous decision, rather than the ensuing motor response. In sum, our current results, in line with the results from previous studies, indicate that the beta-band modulation in visual cortex reflects a top-down signal that changes the internal state of the cortex during perceptual decision-making.

Although we observed significant report-related beta-band modulation during target disappearance in Replay-count, the modulation was weaker than during Replay-button (Figure 2B, 2C). In addition, our previous study showed that the modulation was completely absent during passive viewing of target offsets. The difference between Replay-button and Replay-count might be explained by the additional motor-related activity required during Replay-button. In general, the difference in strength of the modulation around disappearance across these three replay conditions might reflect the differences in behavioral relevance of the perceptual switches imposed by the task instructions to the observers. Behavioral relevance of the perceptual switches is most direct during immediate report in Replay-button, whereas it is more indirect during Replay-count and completely absent during Replay-passive. Thus, our findings suggest that the strength of the beta-band modulation around target disappearance tracks the level of behavioral relevance of the stimulus changes (note that we here define a perceptual decision as the transformation of a perceptual signal into a categorical proposition that can drive an (immediate or delayed) motor action, see *Introduction*).

Which neural events cause the widespread, decision-related state change in visual cortex that manifests itself as a suppression of beta-band power? Our current study shows that the beta-band suppression in visual cortex can be associated with a decision in the absence of motor response. But we find no other cortical brain region exhibiting a similar modulation during covert decisions (Figure 3I). Deeper regions in frontal cortex (Aston-Jones and Cohen, 2005) or the thalamus (Wilke et al., 2009), for which MEG has little sensitivity, are one candidate source. Neuromodulatory brainstem centers are another candidate source of the state change (Aston-Jones and Cohen, 2005; Nieuwenhuis and Donner, 2011). These neuromodulatory centers, such as the noradrenergic locus coeruleus and the cholinergic basal forebrain systems, also exhibit transient activity during perceptual reports, which can reflect the content of the report (Aston-Jones and Cohen, 2005; Parikh et al., 2007; Einhauser et al., 2008; Hupe et al., 2009; de Gee et al., 2014; Kloosterman et al., 2015b). The activity of these neuromodulatory systems can be

measured non-invasively in the dilation of the pupil (Einhauser et al., 2008; de Gee et al., 2014). We next plan to analyze our simultaneously acquired pupillometry data to explore the link between pupil dilation and the beta modulations over visual cortex.

The cerebral cortex continuously undergoes changes in internal state (Steriade 2000; Harris and Thiele 2011; Lee and Dan 2012). While these state changes have traditionally been associated with slow fluctuations of arousal level (Steriade 2000; Harris and Thiele 2011; Haider et al. 2012) some of these state changes co-occur with rapid cognitive processes (Aston-Jones and Cohen 2005; Gilbert and Sigman 2007; Parikh et al. 2007). Our current results provide further support for the idea that a task-relevant perceptual transition triggers a cortical state change, independent of whether this transition is associated with an immediate action. Future work should address whether similar state changes occur during other perceptual tasks, for example during auditory decisions (Kloosterman et al., 2015d) and during more complex decisions beyond the domain of perception (Festinger, 1957).

Chapter 4

Short-term Stabilization in Bistable Visual Perception

This chapter is based on:

Kloosterman N. A., Lamme V. A. F., Donner T. H. Short-term Stabilization in Bistable Visual Perception. *In preparation.*

ABSTRACT

In bistable perceptual illusions, perception alternates spontaneously and unpredictably between distinct interpretations of a constant sensory stimulus. Distributions of percept durations reported by psychophysical observers in these illusions are typically asymmetric, with a rapid growth and a long tail. Remarkably, the mode (most frequent percept duration) and shape of the distributions vary widely across individuals, while being highly reproducible within individuals. What causes these individual differences? Specifically, observers typically report only very few percepts that are shorter than their mode. Here, we explored two alternative scenarios that could explain the lack of very short percepts. In the first scenario, observers do in fact experience these short percepts, but some are better able to accurately track and report them than others (motor latency scenario). Alternatively, observers might experience a genuine lack of short percepts, indicating that perception briefly stabilizes after a perceptual switch (perceptual stabilization scenario). Both these scenarios could result in the observed individual differences in percept duration modes. To arbitrate between them, we asked 33 observers to report perceptual switches during two bistable visual illusions (Motion-Induced Blindness and Structure-from-Motion) as well as during a physical replay of these illusions containing percept durations reported by the fastest switching ("reference") observer. We found that all observers were well able to accurately report percept durations shorter than their mode reported during the illusion, supporting the perceptual stabilization scenario. Thus, our results suggest a stabilizing mechanism preventing immediate return transitions during bistable visual illusions, which varies in strength across individuals. Such stabilization might occur through a combination of sensory adaptation and active top-down modulation of neural activity.

Keywords: bistable perception, psychophysics, individual differences

INTRODUCTION

Perception sometimes alternates spontaneously between distinct interpretations of the same sensory input, a phenomenon referred to as bistable perception (Blake and Logothetis, 2002; Deco and Romo, 2008). For example, in "motion-induced blindness" (MIB) (Bonneh et al., 2001; Donner et al., 2008; Bonneh and Donner, 2011; Donner et al., 2013; Bonneh et al., 2014), a salient visual target spontaneously disappears when surrounded by a moving mask, only to re-appear after some period of time. In "3D-structure-from-motion" (SfM) (Klink et al., 2008) a cloud of dots is perceived as a sphere rotating around its vertical axis. When viewing this stimulus for an extended period of time, the perceived direction of rotation alternates spontaneously. Different bistable perceptual phenomena are governed by common dynamical principles (Brascamp et al., 2006; Klink et al., 2008; Bonneh et al., 2014).

Computational models of bistable perception posit that the spontaneous perceptual dynamics result from intrinsic (independent of stimulus changes) fluctuations in the activity of stimulus-selective populations of neurons (Blake and Logothetis, 2002; Laing and Chow, 2002; Wilson, 2003; Freeman, 2005; Kim et al., 2006; Moreno-Bote et al., 2007; Noest et al., 2007; Gigante et al., 2009; Pastukhov et al., 2013). These intrinsic activity fluctuations emerge from the interplay of random fluctuations ("noise") of neuronal activity and competitive interactions between neuronal populations processing the distinct stimulus features (Moreno-Bote et al., 2007; Donner et al., 2013; van Loon et al., 2013). In the absence of any mechanism promoting the stability of a given perceptual dominance state, neuronal competition models of bistable perception predict exponentially distributed durations of perceptual dominance states (Moreno-Bote et al., 2007) (see Figure 1A, gray line, for an example). By contrast, the percept duration distributions reported by psychophysical observers are asymmetric, with a rapid growth and a long tail (see Figure 1A, black line, for an example), often modeled as a gamma distribution (Leopold and Logothetis, 1999). Remarkably, the center of mass (typically quantified by the mode) and shape of the percept duration distribution vary widely across individuals, while being highly reproducible within individuals (Leopold and Logothetis, 1999; Donner et al., 2013; van Loon et al., 2013).

What causes the individual differences in the perceptual dynamics? More specifically: what causes the individual differences in the center of mass of the percept

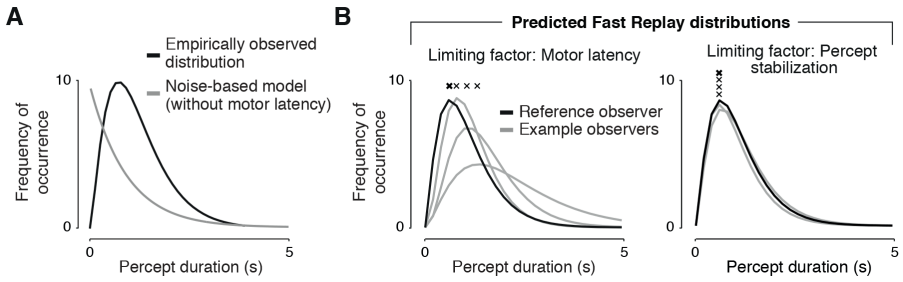

Figure 1 | Experimental predictions

A. Empirically observed versus noise-based modeled percept duration distributions. In the absence of a factor limiting the subject's ability to track short percepts, noise-based models produce exponential distributions, in contrast to the typically observed gamma-shaped distribution. **B**. Predictions by two alternative scenarios for the limiting factor determining the location of the peak of the individual illusory distributions. Left, "motor latency": Similar peak location during Fast replay and its corresponding illusion. Right, "percept stabilization": Individual peak locations during Fast replay should match the one of the actual stimulus alternation. Individual distributions are scaled copies of each other for visibility. Crosses above distributions, mode percept durations of example observers and the reference observer (bold).

duration distributions? Here, we explored two alternative scenarios. First, observers, in fact, experience many short percepts (corresponding to the gray distribution in Figure 1A) but some are better able to report them behaviorally than others. In other words, the individual differences in the center of mass reflect different latencies of motor response (typically button presses). In the following we refer to this scenario as "motor latency". Alternatively, the individual differences in the center of mass reflect actual differences in the perceptual dynamics due to a mechanism that stabilizes the newly selected percept for some time, thereby preventing rapid return transitions. When this short-term stabilizing mechanism has a strong effect, the observer only rarely experiences short percepts. In the following, we refer to this scenario as "percept stabilization". Note that the term is neutral with respect to the underlying mechanism: it comprises both local adaptation (Blake et al., 2003; Noest et al., 2007) as well as active ("top-down") forms of stabilization (Leopold et al., 2002; Einhauser et al., 2008; Kloosterman et al., 2014).

The goal of the present study was to arbitrate between the motor latency and the percept stabilization scenarios, to shed light on the origin of individual differences in bistable perception. To this end, we asked observers to report their alternations of perception in two conditions: (i) during a bistable visual illusion (MIB or SfM); and (ii) during a sequence of physical stimulus changes, which evoked perceptual alternations that

resembled those in the illusions in terms of their phenomenal appearance, but occurred more rapidly than the alternations they reported during the illusions. This was achieved by replaying the spontaneous perceptual alternations reported during the illusions by the observer who exhibited the fastest perceptual dynamics in our sample of observers. We, henceforth, refer to this observer as the "reference observer" and to condition (ii) as the "Fast Replay" and contrast it with the "corresponding illusion", i.e., condition (i). The "Fast Replay" condition eliminated the effect of a possible percept stabilization mechanism (due to the presentation of salient physical stimulus events) and thereby isolated the effect of motor (report) latency.

The "Fast Replay" condition elicited a large fraction of short percepts (i.e., more akin to the gray than to the black distribution in Figure 1A), while still allowing for accurate behavioral report by at least one observer within our sample (the reference observer). If the differences in center of mass between the reference observer and the other observers were determined by longer motor latencies, then the other observers should not be able to track the Fast replay alternations with their behavioral reports. In other words, the center of mass in the Fast replay should be more similar to each observer's own center of mass in the corresponding illusion than to the center of mass of the reference observer (Figure 1B, left). In contrast, if the individual differences in the center of mass were determined by differences in percept stabilization, then each observer's center of mass in the Fast replay should be more similar to the center of mass of the reference observer (Figure 1B, right). Our results support the second scenario.

MATERIALS AND METHODS

Subjects

33 observers (20 female, age range: 18 - 35 years) participated in the experiment. All observers had normal or corrected-to-normal vision and gave written informed consent. The experiment was conducted in two groups of observers. One group (N = 10) performed the illusion and Fast replay conditions with only the MIB stimulus. The other group (N = 23) performed both conditions with both the MIB and the SfM stimuli. Two observers of this group were excluded due to not responding at all in at least two trials. Thus, 21 observers of this group were entered in the analysis. The experiment was approved by

the ethics committees of the Department of Psychology at the University of Amsterdam and the VU University Medical Center, Amsterdam.

Stimuli

MIB illusion

The ten MIB-only observers viewed an MIB stimulus consisting of a yellow target and a blue mask on a black background (Figure 2A). The target was a salient yellow disc (full contrast, diameter: 0.12 or 0.2° of visual angle) surrounded by a moving mask (square, equally spaced grid of 9 by 9 blue crosses, 17° width/length), both superimposed on a black background and centered on a fixation mark (red outline, white inside, 0.8° width and length) (Figure 2A, left). The target was located on one of the four visual field diagonals at an eccentricity of 3°. Target size and location (visual field quadrant) were individually selected for each subject prior to the experiment, to yield a percentage of target invisible time of at least 20%. The mask rotated around the fixation square (speed: 120°/s). The target was separated from the mask by a black "protection zone" subtending about 2° around the target (Bonneh et al., 2001). Stimuli were presented using the Presentation Software (NeuroBehavioral Systems, Albany, CA, USA).

During the illusory MIB condition, observers were supinely placed in a whole-head magneto-encephalograpy (MEG) scanner setup (Elekta Neuromag Oy, Helsinki, Finland). The MEG data are reported in Chapter 2 (Kloosterman et al., 2014). The stimulus was projected via two mirrors onto the ceiling of the MEG scanner room by an LCD projector (BarcoData 8200 LC, Barco Projection Systems, Kuurne, Belgium) with a pixel resolution of 800 x 600 and 60 Hz refresh rate (field of view of 18 x 23°).

The 21 MIB-and-SfM observers viewed the same MIB stimulus during the illusory condition as described above, with the following exceptions: the target was a black-and-white Gabor patch (diameter: 2°; location: 5° eccentricity in one of the four visual field quadrants), the mask was white and the stimulus background was gray.

SfM illusion

The SfM stimulus consisted of an array of black and white dots (dot diameter: 0.1°), centered on a fixation circle (red outline, green inside, 0,5° diameter) in the middle of a gray screen and limited to a circular aperture (diameter: 10°) (Figure 2A, right). The

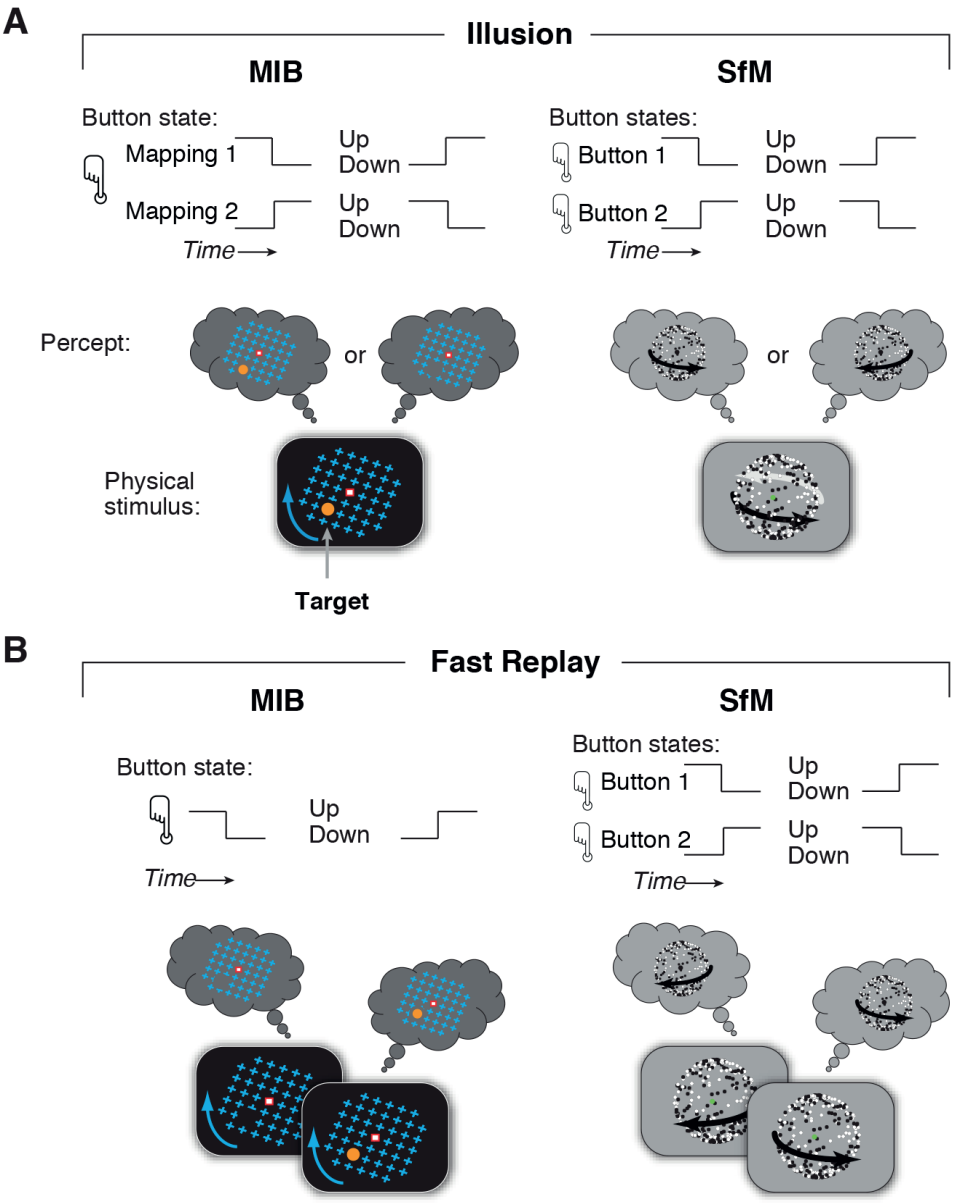
A
Illusion
MIB
SfM
Button state:
Mapping 1
Up
Down
Mapping 2
Up
Down
Time
Button states:
Button 1
Up
Down
Button 2
Up
Down
Time
Percept:
or
or
Physical
stimulus:
Target
B
Fast Replay
MIB
SfM
Button state:
Up
Down
Time
Button states:
Button 1
Up
Down
Button 2
Up
Down
Time

Figure 2 | Motion-Induced Blindness (MIB) and Structure-from-Motion (SfM) perceptual phenomena and report regimes

Stimuli (bottom panels), perception (middle panels) and motor response regimes (top panels) in the different illusions. **A**. Illusion conditions. Left, MIB. A salient target stimulus (yellow dot) was surrounded by a moving mask pattern (blue on black background), which appeared as a rotating grid. Observers continuously reported their alternating perception of the target stimulus (disappearance and re-appearance) by either pressing and holding (Mapping 1) or releasing (Mapping 2) a button. Right, SfM. bottom, schematic of the physical SfM stimulus. The coordinated movement of a circular cloud of dots produces the percept of a sphere, whose rotation direction is bistable. Observers continuously reported their perceived left- or rightward rotation direction with two response buttons. **B**. Corresponding stimuli for the Fast replay condition, in which observers reported physical stimulus changes that were a replay of the fastest-switching observer's illusory percept durations. Left, Fast replay of MIB. Observers reported rapid target offsets and onsets. Right, Fast replay of SfM. Sphere rotation direction was disambiguated by manipulating dot luminance, contrast and size (see *Materials and Methods*). Observers reported rapid alternations in stimulus rotation direction.

coordinated movement of the dots on the x-, y- and z-axes on a two-dimensional plane created the impression of a three-dimensional sphere rotating around its vertical axis. The peak dot velocity was in the center of the sphere and decreased towards the edges. The perceived rotation direction of the sphere was bistable, such that a constantly moving stimulus gave rise to an alternating subjective perception of left- and rightward rotation.

The 21 MIB-and-SfM observers were seated in a silent and dimly lit room, 50 cm in front of the computer screen. Stimuli were displayed on a 32-bit LaCie Electron Blue 4 CRT monitor with a resolution of 1024x768 pixels at a refresh rate of 85 Hz. Observers were seated in a silent and dark room, with their head positioned on a chin rest, 50 cm in front of the computer screen. During the experiment, the left eye was tracked at 1000 Hz with an average spatial resolution of 15 to 30 min arc, using an EyeLink 1000 697 Desktop Mount (SR Research, Osgoode, Ontario, Canada). The eye tracking data are not reported in this chapter.

Fast replay

During the Fast Replay conditions, observers reported their perception of a sequence of physical stimulus changes that mimicked the phenomenal appearance of the illusions (MIB, SfM) (Figure 2B), but were, for all but one observer (the reference observer), faster than the spontaneous perceptual alternations reported during the illusions. This sequence was a replay of the spontaneous alternations reported by the one observer who reported the fastest alternations during the illusions. We selected the observer with the highest

switch rate as the reference observer, defined as the total number of switches divided by the total stimulus duration) (Figure 3A and B, thick black line).

Perceptual switches during Fast replay of MIB were evoked by actual onsets and offsets of the target on the screen. This sequence was a replay of illusory target disappearances and re-appearances reported by the reference observer. The same reference observer was used for the ten MIB-only and the 21 MIB-and-SfM observers. The target viewed by the MIB-only observers during Fast replay was identical to the target used during the corresponding MIB, but enlarged (4° of visual angle) to minimize the occurrence of illusory target disappearances due to MIB. The Fast replay MIB stimulus was displayed on a 22 inch LCD monitor (Asus VW222U) with a resolution of 800x600 pixels at a refresh rate of 60 Hz. Observers were seated in a silent and dark room during this condition.

The Gabor target viewed by the MIB-and-SfM observers during Fast replay of MIB was initially the same size as during the illusory MIB condition. Thus, observers were not able to visually track the target offsets and onsets during Fast replay due to MIB (data not shown). Twelve of the 21 observers of this group were available for an extra session, in which they performed the Fast replay again, but now with a bigger target (4° of visual angle). In Figure 3A and B, left panels, we report the data of these twelve observers combined with the ten MIB-only observers. Both groups analyzed separately show the same qualitative results (data not shown). In Figure 3A and B, right panels, we report the data of the SfM illusion and its Fast replay for all 21 MIB-and-SfM observers that initially performed the experiment. In Figure 4, we also report the illusory conditions of all MIB-and-SfM observers.

During the Fast replay of SfM, the ambiguity of the sphere's rotation direction was resolved by decreasing the luminance, contrast and size of each dot as a function of its location on the z-axis (depth). Reversing the presentation order of the array of frames evoked alternations in perceived rotation direction.

Task and procedure

The ten MIB-only observers performed the MIB condition and its Fast replay over three days: MIB (days 1 and 2), followed by Fast replay (day 3). During MIB, observers reported the spontaneous disappearance and re-appearance of the target by pressing or releasing

a response button with their index finger (left or right, counterbalanced across observers). The mapping between perceptual switch and motor response was flipped between the two recording days (Figure 2A, top left): button press for indicating target disappearance (release for re-appearance) on day 1, and button release for disappearance (press for re-appearance) on day 2. During Fast Replay, observers continuously depressed the space bar on a keyboard when the target was removed from the screen and released it when the target was replaced. Observers completed 32 runs of 2 min duration of MIB and twelve runs of Fast Replay.

The 21 MIB-and-SfM observers indicated their current percept during the MIB and SfM illusion and corresponding Fast replay by pressing the "." or "/" button on a keyboard with their index or middle finger respectively. The mapping between perceptual switch during MIB (disappearance, re-appearance) and motor response was counterbalanced across observers. During SfM, these observers continuously reported the spontaneous or stimulus-evoked alternations of perceived rotation direction. All observers reported leftward rotation with their right index finger, and rightward rotation with their right middle finger. Observers completed ten runs of 2 minutes for the illusory conditions and 5 runs of 2 minutes for Fast replay in randomized order. Observers performed the MIB and SfM conditions in two distinct blocks. Block order was counterbalanced across observers. Twelve of the 21 observers performed an extra session in which they performed Fast Replay of MIB with a bigger target (see *Fast replay* section).

Data analysis

The aim of our analyses was to quantify and compare the centers of mass of observers' percept durations during the MIB and SfM visual illusions and their corresponding Fast replay conditions. We defined the center of mass as the mode percept duration. We extracted the mode for each subject and condition by first binning the percept durations (see below for bin sizes used) and selecting the most often-occurring duration. If there were multiple percept durations occurring equally frequently, we selected the smallest of those values as the mode. Thus, the mode corresponds to the first peak in the frequency distribution of percept durations (indicated by crosses in Figures 1B, 3A and 3B). We normalized distributions within each subject by dividing the number of occurrences in each bin by the total number of switches reported by the subject.

Similarity between percept duration distributions from illusion and Fast Replay

As a measure of overall similarity between percept duration distributions during illusions and Fast replay plotted in Figure 3A, we computed the Pearson correlation between each subject's Fast replay percept duration distribution and (i) their own percept duration distribution for the illusion and (ii) the percept duration distribution of the reference observer (Figure 3C). Due to the generally shorter percept durations in MIB than in SfM, we used bin sizes of 0.1 s for MIB and 0.5 s for SfM, respectively, as well as their corresponding Fast Replay. We tested whether the two correlations, averaged across observers, were significantly different using a permutation (shuffling) procedure (see *Statistical comparisons*).

Similarity of center of mass during illusion and Fast Replay

The motor latency scenario predicts that each observer's mode percept duration during Fast replay is more similar to their mode in the corresponding illusion than to the reference observer's mode (Figure 1B, left). The percept stabilization scenario predicts the opposite (Figure 1B, right). To test these predictions, we computed for each subject the mode percept duration during the illusory conditions and their corresponding Fast replay and statistically tested these modes against each other across observers using a permutation procedure (see *Statistical comparisons*). We used bin sizes of 0.025 s for MIB and 0.25 s for SfM and its corresponding Fast replay for computing the mode.

Correlation between median percept durations across illusions

To test whether observers produced similar perceptual dynamics across different bistable illusions, we pooled within each subject all percept durations of the MIB and SfM illusions in Experiment 2 and computed the median. We then Pearson-correlated these median durations across observers and tested significance of the correlations with a permutation procedure (see *Statistical comparisons*). We used the median instead of the mode or mean in this analysis, because the median captures the typical percept duration better than the mode or mean due to the skewedness of percept duration distributions. In addition, the median is less sensitive to outliers than the mean.

Statistical comparisons

We used two-tailed non-parametric permutation procedures across observers (Efron and Tibshirani, 1998) for testing significance of the correlation between illusion and Fast replay distributions against the correlation between Reference and Fast replay distributions (Figure 3C), as well as testing the modes during the illusory conditions against the Fast replay modes (Figure 3D). All statistical tests were performed across observers. For each comparison, we randomly permuted the labels of the observations (e.g., the condition labels of mode percept durations), and recalculated the difference between the two group means (1000 permutations). The p-value associated with the original difference between the means was given by the fraction of shuffles in which the original difference was exceeded by the difference between the means obtained for the shuffled data.

RESULTS

All observers, including those with the slowest spontaneous perceptual dynamics (i.e., a mode of several seconds longer than the one of the reference observer), were able to accurately report the rapid stimulus alternations during Fast replay of both the MIB and SfM illusions (Figure 3). In other words, the observers produced percept duration distributions that closely resembled the distribution produced by the reference observer during the illusory condition (black lines Figure 3A and 3B) and not their own illusory distribution (Figure 3A).

We used Pearson correlation to quantify the overall similarity of observers' percept duration distributions from the Fast replay with both the reference distribution and their own distribution during the illusion. For both MIB and SfM, there was a significantly stronger correlation between each subject's Fast replay distribution and the distribution of the reference subject than between Fast replay and the subject's own illusory distribution (MIB, $p = 0.008$; SfM, $p < 0.001$; Figure 3C). Thus, observers' Fast replay distributions were more similar to the reference observer's distribution than to each observer's own illusory distributions.

We then tested the key prediction of the percept stabilization scenario: that each observer's center of mass (defined as the mode percept duration) during Fast replay would be more similar to the center of mass of the reference observer than to their own

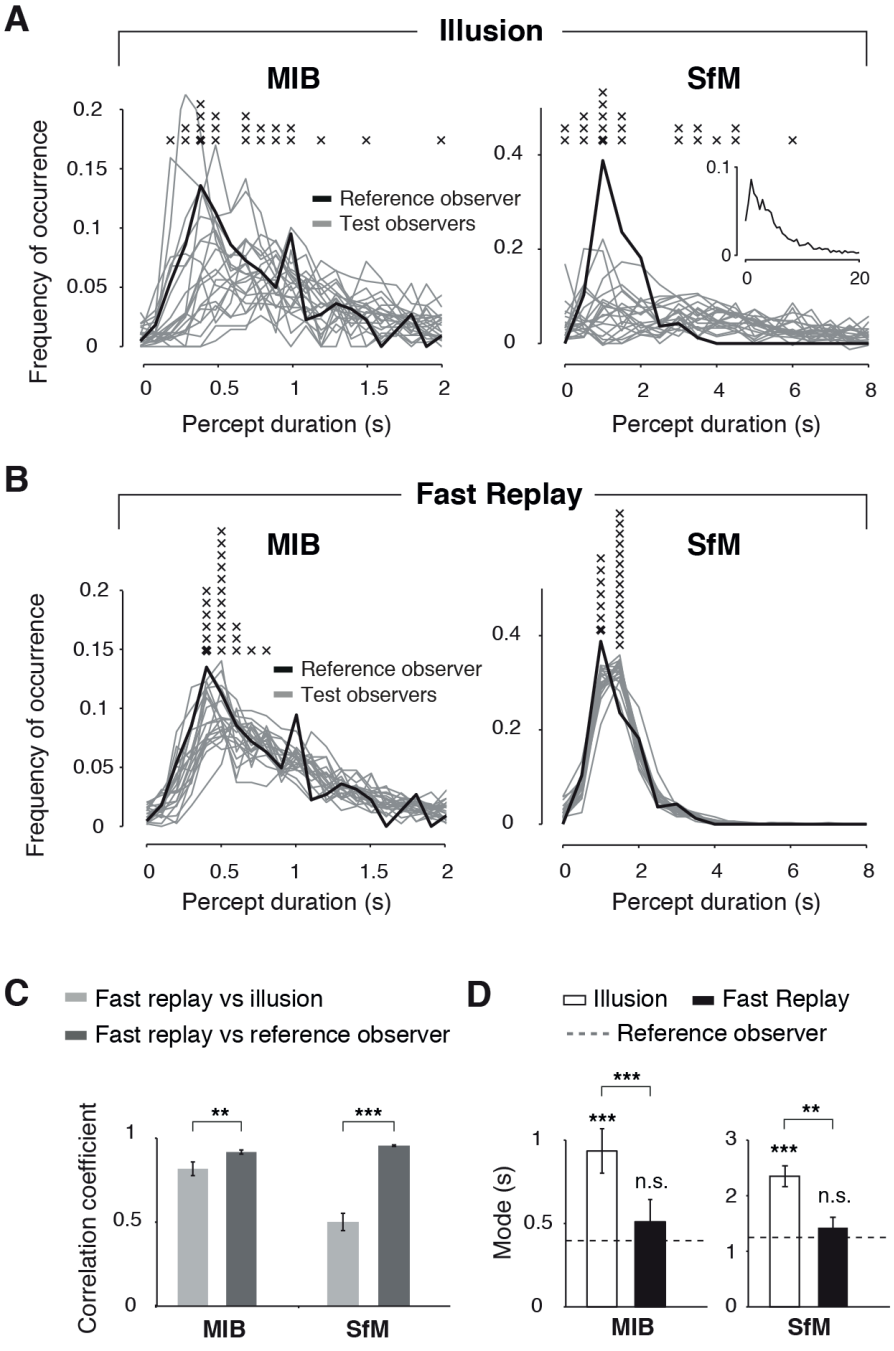
A
Illusion
MIB
SfM
Frequency of occurrence
Reference observer
Test observers
Percept duration (s)
B
Fast Replay
MIB
SfM
Frequency of occurrence
Reference observer
Test observers
Percept duration (s)
C
Fast replay vs illusion
Fast replay vs reference observer
Correlation coefficient
MIB
SfM
D
Illusion
Fast Replay
Reference observer
Mode (s)
n.s.
MIB
SfM

Figure 3 | Lack of short percepts is not explained by motor latency

A. Frequency distributions of percept durations reported during the illusory conditions Left, MIB (target disappearance). Data are collapsed over the two types of MIB stimuli (N = 21 observers). Right, SfM (left and right rotation percepts pooled). Thick black lines, distribution of the reference observer, which was used for generating the sequence of stimulus alternations in the Fast replay conditions. Crosses above distributions, mode percept durations of single observers and reference observer (bold). Inset, SfM distribution averaged across observers, showing the long tail of the distribution. **B.** Percept duration distributions for button states during Fast Replay. The distributions match the ones predicted under percept stabilization. **C.** Correlations between observers' own illusory distributions and their Fast replay and between the reference observer's distribution and their Fast Replay. *, $p < 0.05$, **, $p < 0.01$, ***, $p < 0.001$. Error bars, s.e.m. **D.** Mode percept duration averaged across observers during MIB and SfM and corresponding Fast Replay. Dotted line, mode percept duration of the reference observer.

center of mass in the corresponding illusion. This is indeed what we found: for both MIB and SfM, the average mode across observers during Fast replay was significantly closer to the mode of the reference observer than to the average mode during the illusion (MIB, $p < 0.001$, SfM, $p = 0.004$; permutation tests across observers)(Figure 3D). There was significant difference between the mode produced during Fast Replay and the mode of the reference observer (MIB, $p = 0.57$, SfM, $p = 0.39$). Taken together, our results indicate that observers were in fact well able to report shorter percept durations than they typically do during bistable illusions.

Finally, we assessed whether individual differences in the perceptual dynamics (specifically: the median percept duration) are correlated between different bistable illusions. To this end, we correlated the median perceptual dominance durations observed in MIB to those observed in SfM across observers and found a significant positive correlation ($r = 0.48$, $p = 0.02$, permutation test) (Figure 4), indicating that observers who generally experience longer percepts in one illusion, also have longer percepts in another illusion. In other words, the perceptual state dynamics do not only differ markedly across individuals, but they are also highly consistent across different phenomena within an individual.

DISCUSSION

Here, we assessed the origin of the large individual differences in the dynamics of bistable visual perception. In the absence of any mechanism stabilizing the newly selected perceptual state (Moreno-Bote et al., 2007), the only factor limiting the report of very short percepts is the inability to track these short percepts by means of behavioral reports

$$\tau_A \partial A_i = -A_i + \alpha S[X_i],$$
$$i, j \in \{1,2\}$$

Figure 4 | Perceptual state dynamics within individuals are consistent across bistable phenomena

Correlation across observers between median percept durations reported during the MIB and SfM illusions (N = 21 observers).

(motor latency). In contrast, our current results show that all observers were well able to report percepts much shorter than their own mode percept duration during two different illusions. This result is independent of the specific type of motor regime (using one or two response buttons, Figure 2) that observers use to indicate perceptual switches. In sum, noise and motor latency combined are not sufficient to explain the reported perceptual dynamics. Thus, our results are consistent with the existence of a stabilizing mechanism that prevents immediate return transitions during bistable visual illusions.

What is this stabilizing mechanism? Adaptation of stimulus-selective sensory neurons is one candidate (Noest et al., 2007). When combined with noise and competition, adaptation can qualitatively re-produce the empirically observed asymmetric percept duration distributions (Moreno-Bote et al., 2007). Indeed, there is paramount evidence for the effects of adaptation in primate visual cortex (Kohn, 2007) and there is fMRI evidence for a role of target-specific neuronal dynamics in human V1 (presumably linked to adaptation) in the stability of MIB target disappearance (Donner et al., 2013). Notably, adaptation predicts some degree of history-dependence in the perceptual dynamics (i.e., correlation between the duration for which a percept is suppressed and the following period in which it is dominant) (Leopold and Logothetis, 1999; Pastukhov et al., 2013), which is subtle in empirical data (Pastukhov and Braun, 2007; van Ee, 2009). While the existence of stimulus-selective adaptation mechanisms in visual cortex is unquestionable, it remains to be seen whether their effects are sufficiently strong and variable across people to account for the striking individual differences in the perceptual dynamics in bistable visual illusions.

Another candidate is an active top-down mechanism triggered by the perceptual switch (Einhauser et al., 2008; Kloosterman et al., 2014).}. Indirect evidence from pupillometry shows a correlation between pupil dilation during perceptual switches and the duration of the newly selected perceptual state (Einhauser et al., 2008). Based on the putative link between pupil dilation and brain-wide noradrenaline release (Aston-Jones and Cohen, 2005), this finding could be interpreted as evidence for a role of noradrenergic neuromodulation in perceptual stabilization. During MIB, transient modulations of beta-band activity in visual cortex around perceptual report of target disappearance also predict the duration of the subsequent MIB state (Kloosterman et al., 2014). Finally, the phenomenon of protracted repetition of perceptual judgments during intermittent presentation of ambiguous stimuli has also been interpreted as evidence for an active stabilization mechanism (Leopold et al., 2002) (but see Noest et al. (2007)). Adaptation and top-down factors might conspire to determine the stability of a perceptual state.

It is tempting to speculate that the stabilization mechanism characterized here during bistable visual perception generalizes to higher-order thought, as well as its disturbances in psychiatric conditions. The perceptual dynamics in these illusions are altered in depression and autism (Leopold and Logothetis, 1999; Pettigrew, 2001; Robertson et al., 2013) and they resemble the dynamics of fixation durations – a proxy of the durations of individual thoughts – during challenging cognitive tasks (Suppes et al., 1983). In sum, the bistable perceptual dynamics investigated here may be a fingerprint of an individual's general "stream of thought". Uncovering the underlying mechanism may thus prove instrumental for understanding individual differences in the dynamics of cognition.

ACKNOWLEDGMENTS

We thank Berend Kirch and Bart van Loenen for help with data collection. V.A.F.L. was supported by an advanced investigator grant from the European Research Council.

Chapter 5

Pupil Size Tracks Perceptual Content and Surprise

This chapter is based on:

Kloosterman, N. A., Meindertsma, T., Loon, A. M., Lamme, V. A., Bonneh, Y. S., & Donner, T. H. (2015). Pupil Size Tracks Perceptual Content and Surprise. *European Journal of Neuroscience*, 41(8), 1068-1078.

ABSTRACT

Changes in pupil size at constant light levels reflect the activity of neuromodulatory brainstem centers that control global brain state. These endogenously driven pupil dynamics can be synchronized with cognitive acts. For example, the pupil dilates during the spontaneous switches of perception of a constant sensory input in bistable perceptual illusions. It is unknown whether this pupil dilation only indicates the occurrence of perceptual switches, or also their content. Here, we measured pupil diameter in human subjects reporting the subjective disappearance and re-appearance of a physically constant visual target surrounded by a moving pattern ("motion-induced blindness" illusion). We show that the pupil dilates during the perceptual switches in the illusion and a stimulus-evoked "replay" of that illusion. Critically, the switch-related pupil dilation encodes perceptual content, with larger amplitude for disappearance than re-appearance. This difference in pupil response amplitude enables prediction of the type of report (disappearance vs. re-appearance) on individual switches (receiver operating characteristic: 61%). The amplitude difference is independent of the relative durations of target-visible and target-invisible intervals and subjects' overt behavioral report of the perceptual switches. Further, we show that pupil dilation during the replay also scales with the level of surprise about the timing of switches, but there is no evidence for an interaction between the effects of surprise and perceptual content on the pupil response. Taken together, our results suggest that pupil-linked brain systems track both the content of, and surprise about perceptual events.

Keywords: pupillometry, perceptual bistability, perceptual decision-making, brain state, human

INTRODUCTION

It has long been known that the diameter of one's pupil changes during cognitive acts (Hess and Polt, 1964; Kahneman and Beatty, 1966). Specifically, the pupil dilates when subjects engage in cognitive tasks, independent of the level of retinal illumination (Einhauser et al., 2010; Preuschoff et al., 2011; Fiedler and Glockner, 2012; Wierda et al., 2012; Zylberberg et al., 2012; Shalom et al., 2013; de Gee et al., 2014). These pupil responses are associated with changes in the gain of neural interactions in the cerebral cortex (Eldar et al., 2013; Reimer et al., 2014). Indeed, mounting evidence suggests that the same brainstem centers that control fast changes in cortical state also control non-luminance mediated pupil dynamics - in particular the noradrenergic system (Aston-Jones and Cohen, 2005; Murphy et al., 2014). Other brainstem systems such as the cholinergic system (Sarter et al., 2009; Lee and Dan, 2012; Yu, 2012) and the superior colliculus (Wang et al., 2012) involved in attentional control may also contribute to task-related pupil dynamics. Task-related pupil responses, therefore, provide a window into fast fluctuations in global brain state during cognitive processing.

In particular, the pupil dilates during illusory perceptual switches in so-called multi-stable perceptual phenomena, in which a constant sensory input induces illusory switches in perception (Einhauser et al., 2008; Hupe et al., 2009; Frassle et al., 2014). Similar dilation occurs during the stimulus-evoked replay of the perceptual switches (Einhauser et al., 2008; Hupe et al., 2009; Frassle et al., 2014). While the button press typically used for reporting the perceptual switches can account for part of the pupil dilation, significant dilation remains in the absence of any overt motor response (Hupe et al., 2009).

Here, we asked whether the switch-related pupil dilations only track the occurrence of perceptual switches, or if they also contain information about the content of perception. In some illusions, perception alternates between two asymmetric states. For example, in "motion-induced blindness" (MIB), a salient visual target surrounded by a moving mask spontaneously disappears from perception, and then reappears after some time (Bonneh et al., 2001; Bonneh and Donner, 2011; Bonneh et al., 2014). This subjective target disappearance and re-appearance might be associated with different levels of cognitive engagement, which, in turn, might be reflected in the activity of pupil-linked brainstem systems.

We monitored pupil diameter of human subjects reporting their perceptual switches during MIB (Figure 1A, left) and a physical replay of that illusion (Figure 1A, right). We tested whether the subjective difference between target disappearance and re-appearance might be reflected in a difference of the associated pupil dilation. Because surprise about behaviorally relevant events has been shown to drive pupil dilation (Preuschoff et al., 2011; Nassar et al., 2012; Naber et al., 2013) and the timing of perceptual switches in bistable illusions is typically unpredictable and hence surprising, we also investigated whether pupil dilation amplitude during replay tracked surprise about switch timing and if this surprise effect might interact with the effect of perceptual content.

MATERIALS AND METHODS

General stimuli and procedure

We measured pupil diameter during the MIB illusion (Figure 1A, left) as well as during a number of control conditions collectively referred to as Replay, in which the target was intermittently removed from the screen for some period of time (Figure 1A, right, and see below for details). The target was a full contrast black-and-white Gabor patch (diameter: 2°) located at 5° eccentricity in one of the four visual field quadrants selected individually for each subject to yield the maximum percentage of target invisible time. Because the mean luminance of the Gabor patch was equal to the luminance of the gray background, overall stimulus luminance remained constant during the target onsets and offsets in the Replay conditions. The target was surrounded by a rotating mask (17° x 17° grid of white crosses), separated from the target by a gray "protection zone" subtending about 2° around the target. The fixation mark at the center of the screen was a square with red outline and white inside (0.8° width/length). Subjects were asked to monitor and report the disappearance and reappearance of the target via various motor response regimes (Figure 1B, and see below for details). Stimuli were presented and responses recorded by means of the Presentation software (NeuroBehavioral Systems, Albany, CA, USA). The diameter of the left eye's pupil was sampled at 1000 Hz with an average spatial resolution of 15 to 30 min arc, using an EyeLink 1000 697 Desktop Mount (SR Research, Osgoode, Ontario, Canada).

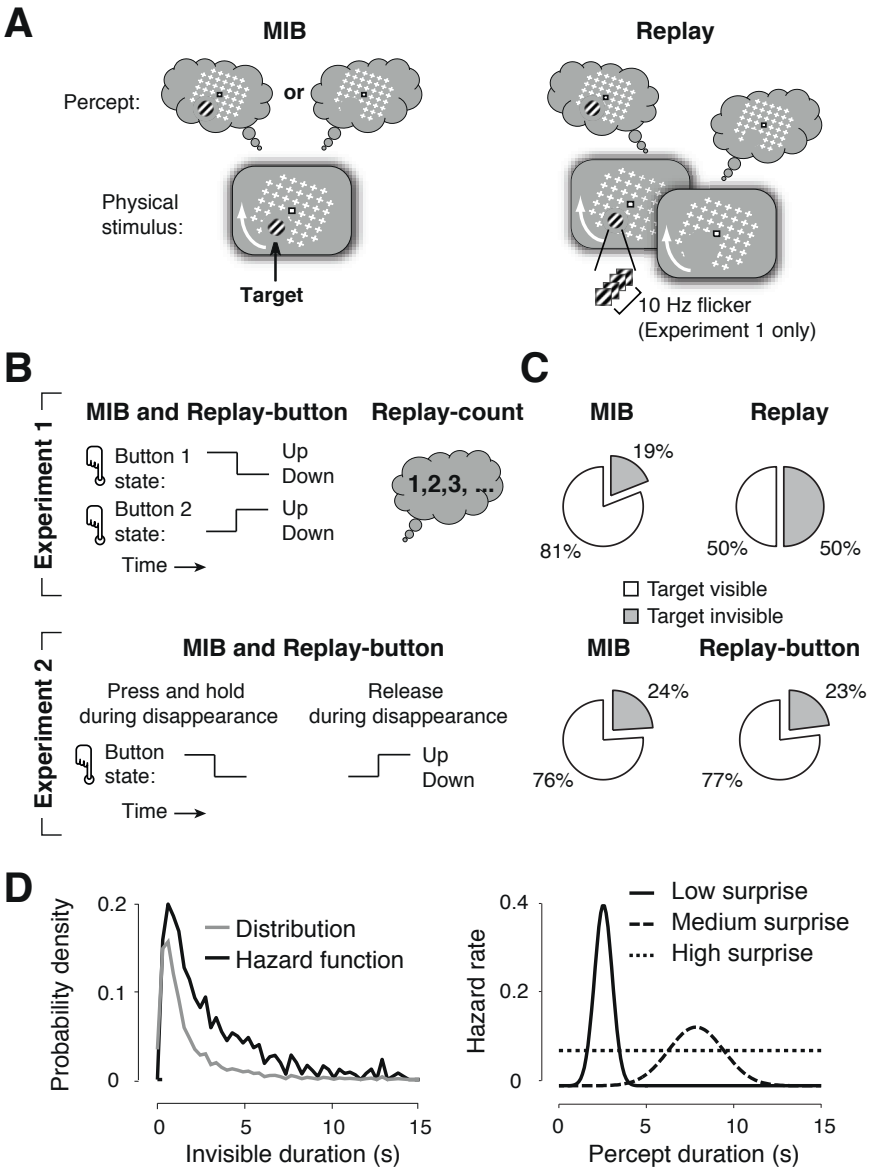
A
MIB
Replay
Percept:
or
Physical stimulus:
Target
10 Hz flicker
(Experiment 1 only)
B
C
Experiment 1
MIB and Replay-button
Replay-count
Button 1 state:
Button 2 state:
Up
Down
Time
1,2,3, ...
MIB
Replay
19%
81%
50%
50%
Target visible
Target invisible
Experiment 2
MIB and Replay-button
Press and hold during disappearance
Release during disappearance
Button state:
Up
Down
Time
MIB
Replay-button
24%
76%
23%
77%
D
Probability density
0.2
0.1
0
Distribution
Hazard function
0
5
10
15
Invisible duration (s)
Hazard rate
0.4
0.2
0
Low surprise
Medium surprise
High surprise
0
5
10
15
Percept duration (s)

Figure 1 | Stimuli and behavioral tasks

A. Schematic snapshots of stimuli and alternating percepts. Bottom left: MIB stimulus. A salient target stimulus (Gabor patch) was surrounded by a moving mask pattern (white), which appeared as a rotating grid. Top left, fluctuating perception of the target due to MIB. Right: Corresponding stimulus and alternating perception during Replay. Replay stimuli were identical in Experiments 1 and 2, except that the target flickered at 10 Hz in Experiment 1. **B.** Behavioral response regimes. Top, Experiment 1: During MIB and Replay-button, subjects switched button press of two buttons. During Replay-count, subjects covertly counted the disappearances during the three-minute run, and reported the total after the end of the run in a 4AFC question. Bottom, Experiment 2. Subjects either pressed and held or released to report target disappearance (complementary for re-appearance). **C.** Corresponding fraction of total target visible and invisible percept durations in the MIB and Replay conditions. Target onset and offset durations in Replay in Experiment 1 (top right) were sampled from the same distributions. **D.** Left: Distributions and corresponding hazard function of MIB durations in Experiment 1. Right: Hazard functions used for generating percept durations during Replay in Experiment 1. The intervals between events were drawn from the probability distributions (not shown) corresponding to the three hazard functions shown here. Because subjects' expectation of event timing follows the hazard rate, events occurring around the mean interval in both conditions will elicit different levels of surprise.

In this paper, we report data from two experiments. The main experiment was designed to assess the modulation of the pupil response by (i) perceptual content, (ii) surprise about switch timing, and (iii) motor response. It also entailed magneto-encephalography (MEG) recordings, which will be reported in a separate paper. The analyses of the main experiment showed a robust modulation of pupil response by perceptual content, which has not previously been shown. To replicate this effect in an independent sample, we also analyzed data from a previously reported, within-subjects, placebo-controlled, pharmacological study of the perceptual dynamics in MIB (van Loon et al., 2013). In this study, subjects were administered either a placebo or 1.5 mg of the GABA-A receptor agonist lorazepam in each of two sessions (double-blind; session order counterbalanced across sessions). Because we found no differences between pupil responses in the two pharmacological conditions during MIB (Figure S1), we collapsed across these conditions in the pupil results reported in this paper.

Experiment 1 (main experiment)

Subjects

22 subjects participated in the experiment (10 female, age range 20-54 years). Three subjects were excluded: one subject due to failure to complete all the sessions, one due to bad quality of the eye tracking data, and one due to reaction times consistently being longer than 1 s during one of Replay conditions. Thus, nineteen subjects (10 female, age

range 20-54 years) were included in the analysis. All subjects had normal or corrected-to-normal vision and gave written informed consent. The experiment was approved by the ethics committee of the Universitätsklinikum Hamburg Eppendorf in accordance with the Declaration of Helsinki.

Stimulus

The Gabor target contained 2 spatial cycles. During the Replay conditions, the different parts of the Gabor modulated at opposite phase at a temporal frequency of 10 Hz. The resulting counter-phase flicker rendered the target more salient and thus minimized the number of illusory target disappearances during Replay. The mask rotated at a speed of 160 °/s. Stimuli were back-projected on a transparent screen using a Sanyo PLC-XP51 projector with a resolution of 1024 x 768 pixels at 60 Hz. Subjects were seated 58 cm from the screen in a dimly lit room.

Task

During the MIB and half of the Replay runs (henceforth called Replay-button condition), subjects were asked to press and hold a button with their right index finger during target disappearance and another button with their right middle finger during target re-appearance (Figure 1B, top panel, left). In the other half of the Replay runs (henceforth called Replay-count condition), subjects were instructed to silently count the number of target offsets and report the total in a four alternative forced-choice question displayed on the screen after the end of the run (Figure 1B, top panel, right). There were always one correct and three incorrect numbers; the incorrect numbers were generated by randomly subtracting or adding 1, 2 or 3 from the actual number of disappearances, under the constraint that the four alternatives were all different from each other. Replay-button or Replay-count conditions were randomly selected before each run, under the constraint that each would occur equally often. The corresponding instructions were displayed on the screen and communicated verbally by the experimenter before each run. Each run had a duration of 3 min.

To test for an effect of surprise on the pupil dilation amplitudes, the predictability of the timing of perceptual events (stimulus disappearance or re-appearance) was manipulated during three different Replay conditions. To this end, the intervals between physical target offsets and onsets were randomly sampled from three different

distributions, corresponding to narrow, intermediate and broad hazard functions (Figure 1D). The hazard function describes the probability that an event will occur at a particular point in time, given that it has not occurred yet (Luce, 1986), and is computed as

$$\lambda(t) = \frac{f(t)}{1-F(t)}, \qquad \text{eq. 1}$$

where $f(t)$ is the value of distribution f at time t, $\lambda(t)$ is the value of the hazard function at t, and $F(t)$ is the area under the curve of f until t. Varying the hazard function changes the overall level of surprise elicited by stimulus changes, which can be formalized as the negative logarithm of the probability of an event (Friston, 2010). Thus, most events in the narrow, intermediate and broad hazard function conditions (i.e., those that occur around the center of mass of the corresponding distribution) are associated with low, medium, and high surprise, respectively. For simplicity, we here refer to these conditions overall as “low surprise”, “medium surprise”, and “high surprise” conditions, respectively (Figure 1D). Splitting up individual events by the level of the associated surprise (which varies from event to event within each condition) might enable a more sensitive analysis; because we found significant modulation of the pupil dilation amplitude by the surprise condition (see Results), the analysis reported here seemed sufficiently sensitive.

Procedure. The experiment consisted of two sessions of approximately two hours duration each, and subjects completed a total of 44 3-min runs (MIB: 6, Replay: 38). Subjects completed 16 low, 16 medium and 6 high surprise Replay runs. Different numbers of runs per hazard function were used to obtain a similar number of trials for each of the three conditions (the high surprise condition yielded more trials per unit time). Subjects performed the MIB and high surprise Replay conditions in one session and the medium and low surprise Replay conditions in the other session. The two types of runs in each session were presented within two separate blocks to allow subjects to learn the event distributions of each condition as much as possible. The order of blocks within a session and the order of sessions were counterbalanced across subjects.

Experiment 2 (replication)

Subjects

Nineteen subjects (12 female, age range 21-39 years) participated in the experiment. All subjects had normal or corrected-to-normal vision and gave written informed consent.

Four subjects were excluded due to excessive blinking. The experiment was approved by the ethics committee of the Department of Psychology at the University of Amsterdam in accordance with the Declaration of Helsinki.

Stimulus, task, and procedure

The Gabor target contained 4 spatial cycles. The mask rotated at a speed of 120 °/s. Stimuli were displayed on a 32-bit LaCie Electron Blue 4 CRT monitor with a resolution of 1024 x 768 pixels at a refresh rate of 85 Hz. Subjects were seated in a silent and dark room, with their head positioned on a chin rest, 50 cm in front of the computer screen. Subjects reported perceptual switches by pressing or releasing the space bar on a keyboard, using their preferred hand. The mapping between perceptual switch and motor response was flipped between two blocks of six runs of about 15 min each: button press for indicating target disappearance (release for re-appearance) in one block, and button release for disappearance (press for re-appearance) in the other block (Figure 1B, bottom panel). Block order was counterbalanced across subjects. During the Replay-button condition, the target was physically removed from the screen in the same temporal sequence as it had previously disappeared during one of several previous MIB runs completed by that same subject. The design ensured that each Replay-button run would be preceded by at least two MIB runs. Replay-button was otherwise identical to MIB. Each run lasted 2 min.

Data analysis

Periods of blinks were detected using the manufacturer's standard algorithms with default settings. All the remaining data analyses were performed using custom made MATLAB (The Mathworks, Natick, MA, USA) software and the Fieldtrip toolbox (Oostenveld et al., 2011).

Preprocessing

Blinks were removed by linear interpolation of values measured just before and after each identified blink (interpolation time window: from 0.1 s before until 0.1 s after blink). Fixation errors were defined as gaze positions outside of a permissible window of 4.5 deg from fixation mark. Pupil responses during cognitive events are sluggish and confined to a frequency range below 4 Hz (Hoeks and Levelt, 1993; Loewenfeld and Lowenstein, 1993). Consequently, signal fluctuations above 4 Hz reflect mainly measurement noise. To

remove the high-frequency noise, we low-pass filtered the interpolated pupil time series from each block of runs using a 3rd order Butterworth filter with a cutoff of 4 Hz. We obtained qualitatively identical results without filtering (data not shown), but we found that removing high-frequency noise increased the reliability of our single-trial pupil amplitude estimates, thus quantitatively boosting single-trial decoding of perceptual report type from the pupil response (see *Statistical tests of modulations of the pupil response* below).

Event-related analysis of pupil responses

Epochs for event-related analysis of pupil diameter changes around perceptual switches were extracted from the low-pass filtered pupil time series. In the following, we refer to the extracted epochs as "trials", noting that the actual stimulus presentation was continuous (except for the target offsets and onsets in the Replay conditions). For MIB, trials were always aligned to subjects' behavioral report of target disappearance and re-appearance (button presses, releases, or button switches). For Replay-count, trials were always aligned to the physical stimulus change. For Replay-button, we performed two separate analyses: one in which trials were aligned to the physical stimulus change and one in which trials were aligned to behavioral report.

In all report-locked analyses (MIB, Replay-button), the following constraints were used for trial extraction: (i) The maximum trial duration ranged from -1 s to 1.5 s relative to report (response-locked analysis) or -0.5 to 2 s relative to physical target on- and offsets (stimulus-locked analysis); (ii) when another report occurred within this interval, the trial was terminated 0.5 s from this report; and (iii) when two reports succeeded one another within 0.5 s, no trial was defined. For the analysis of Replay-button, we included only those reports that were preceded by a physical change of the target stimulus within 0.2 to 1 s, thus discarding reports following illusory target disappearances or button press errors and re-appearances. In Experiment 1, 8 % of disappearance trials and 9 % of re-appearance reports were discarded for Replay-button due to this constraint. When analyzed separately, the pupil time courses of these discarded trials were similar as during the main analysis (data not shown).

In the stimulus-locked analysis of all the Replay conditions, trials were aligned to physical target on- and offsets. Trials in which either blinks or fixation errors occurred for more than 10% of the time occurred during the interval from 1 s before until 1 s after the trigger event were excluded from further analysis. After trial extraction, we down-

sampled the data to 50 Hz to boost the sensitivity of our (sample-by-sample) statistical comparisons of pupil time courses (see below).

We used established procedures (Hupe et al., 2009; de Gee et al., 2014) to normalize the raw pupil diameter time courses. We subtracted the baseline pupil diameter value at the start of each trial from each sample of the time course and divided the time course by the mean pupil diameter across the experiment (i.e., all samples and trials pooled across two experimental sessions from a given subject). This normalization procedure transformed the pupil diameter time courses into units of percent modulation.

As baseline intervals, we used the following intervals for the report-locked and stimulus-locked analyses, respectively: from 1 (or later) to 0.6 s before report and from 0.5 (or later) to 0.1 s before stimulus change. The difference of 0.5 s between the intervals for the two analyses corresponds to the median reaction time measured during the Replay-button conditions. As a consequence, the baseline interval for both analyses contained predominantly pupil measurements preceding the (illusory or stimulus-evoked) perceptual switch. The above described trial extraction procedure caused the start of the baseline intervals to be later (i.e., closer to the trigger event) for some trials.

Quantification of pupil response amplitudes

Because the pupil response is sluggish, any transient neural input will be smeared out in time (Hoeks and Levelt, 1993). Hence, the quantification of the response amplitude should take into account the entire pupil response time course rather than only the peak. We used a linear projection (de Gee et al., 2014) procedure to collapse each single-trial time course into a single measure of response amplitude, according to

$$a_i = r_i \frac{\bar{r}}{\|\bar{r}\|^2}, \qquad \text{eq. 2}$$

where a_i is the scalar amplitude estimate for trial i, r_i is a row vector containing the pupil response time course of that trial and $\bar{r}$ is a column vector containing the average pupil response time course across all trials of all conditions for a given subject. The term $\frac{\bar{r}}{\|\bar{r}\|^2}$ normalized the mean response vector to be of unit length. In words, we computed the inner product between each trial's pupil response and a "template", which was each individual's normalized mean response. This procedure is well established for the quantification of fMRI response amplitudes (e.g., Ress et al. (2000)). It yields robust estimates of single-trial amplitudes. By using a separate template per subject, it also

accounts for the individual differences in the pupil impulse response function in a data-driven fashion (de Gee et al., 2014).

We used two different time windows, for linear projection in the report-locked and stimulus-locked analysis, again shifted by 0.5 s to account for the median reaction time from the Replay-button conditions. In the report-locked analysis, we used the time window 0 to 1.5 s from report. For the stimulus-locked analysis, we used the time window 0.5 to 2 s from the stimulus change. These time windows consistently included the peak of all individual pupil dilation responses.

If a given trial was shorter than the above time windows (due to the trial extraction), then *r* was clipped to the length of the trial. Because the resulting amplitude values calculated according to eq. 2 scales with the number of samples per trial (due to the addition of the products of individual samples), we divided each trial's amplitude value by the number of samples. A control analysis in which we computed the projection over the interval from 0 to 1 s (response-locked) or 0.5 s to 1.5 s (stimulus-locked) included only trials of complete length. This analysis yielded similar results as the analysis including all the trials (Figure S6).

Removing the effect of baseline pupil diameter

There is a known negative correlation between the baseline pupil diameter and the amplitude of phasic pupil responses (Gilzenrat et al., 2010; Murphy et al., 2011; de Gee et al., 2014), which we also observed in the present data (Figure S2). Because of this statistical dependence, differences in pupil response amplitudes between conditions (e.g., disappearance and re-appearance) could be "inherited from" differences already existing during the baseline interval, even after subtraction of the baseline diameter when computing the response (de Gee et al., 2014). We addressed this concern in a control analysis, in which we used linear regression to remove the effect of baseline pupil diameter on the single-trial amplitudes a_i before testing for differences between disappearance and re-appearance.

Statistical tests of modulations of the pupil response

We used two-tailed nonparametric permutation tests to test for differences between the pupil response time courses and amplitudes (Efron and Tibshirani, 1998). These tests

were performed across subjects. For each test, we randomly permuted the labels of the observations (e.g., the condition labels of pupil response amplitudes), and recalculated the difference between the two group means (1000 permutations). The p-value associated with the original difference between the means was given by the fraction of shuffles in which the original difference was exceeded by the difference between the means obtained for the permuted data. For the pupil modulation time courses, we performed permutation tests at each time point with cluster-based multiple comparison correction across time points, as implemented in the Fieldtrip toolbox (Maris and Oostenveld, 2007). For testing significance of the correlations, we computed the correlation after each permutation of the labels of the observations, and obtained the p-value by comparing the correlations found after each permutation to the observed correlation, as explained above.

We used receiver operating characteristic (ROC) analysis (Green and Swets, 1966) to compare the distributions of pupil modulation values from individual trials between the two types of perceptual reports (disappearance and re-appearance). The ROC index ranges between 0 and 1 and quantifies the probability with which one can predict the report type based on the pupil response measured during individual trials. An index of 0.5 implies chance level prediction. The index was first computed for the interval 0 to 1.5 s after report within each individual subject, averaged across subjects, and tested for significant deviation from chance (i.e., 0.5) with a two-tailed permutation test across subjects (1000 permutations).

For testing whether the modulation amplitudes differed significantly across the three surprise conditions we used a 1-way ANOVA across subjects. To quantify the overall surprise effect in each subject with a scalar value (collapsing across Replay-count and Replay-button), we averaged the following two amplitude differences: high-surprise – medium-surprise and medium-surprise – low-surprise. We then correlated (across subjects) the magnitude of this overall surprise effect to the magnitude of the perceptual modulation (i.e. difference between disappearance and re-appearance amplitudes, pooled across MIB and Replay-button/Replay-count).

For testing whether reaction times and pupil amplitudes differed between disappearance and re-appearance across surprise conditions, we used a two-way ANOVA across subjects.

Eye position control analysis

The measurement of pupil diameter in video-based eye trackers depends on eye position. Although we found that subjects fixated well on the fixation mark at the center of the screen throughout all experiments (Figure 2), we wondered whether the observed differences in pupil modulation could be explained by differences in eye position between target disappearance and re-appearance trials. We computed three-dimensional histograms of the subject's gaze behavior in Experiment 1 across the complete stimulus screen consisting of 1024x768 pixels. We normalized each subject's eye position data by dividing the number of observations per x,y bin by the total number of x,y observations. Then, we subtracted the re-appearance from the disappearance maps for both MIB and Replay, and tested these maps across subjects against zero with a permutation test using a cluster-based procedure (Oostenveld et al., 2011) to correct for multiple comparisons (Figure 2). We found no significant differences (all $p > 0.05$, cluster-corrected for multiple comparisons). To assess whether subjects fixated equally well during target disappearances and re-appearances, we quantified the similarity between the eye position distribution maps of the two types of perceptual switches. The spatial correlations between these maps were high for both MIB and Replay ($r = 0.73$ and $r = 0.82$, respectively) and significantly different from zero ($p < 0.001$, permutation test). Taken together, these analyses rule out the concern that the difference between pupil responses for target disappearance and re-appearance reported in the Results section might be due to differences in eye position.

RESULTS

Pupil dilation response reflects content of perceptual switch events

We linked pupil dynamics to perceptual switches during the MIB illusion and a physical replay of that illusion (Figure 1). We used a Gabor patch as the target to ensure that the overall stimulus luminance remained constant around targets offsets and onsets during the Replay condition. This was intended to minimize, as much as possible, the effect of pupillary response due to subjective (Laeng and Endestad, 2012) or physical stimulus changes during the perceptual switches. The pupil dilated from the time of subjects'

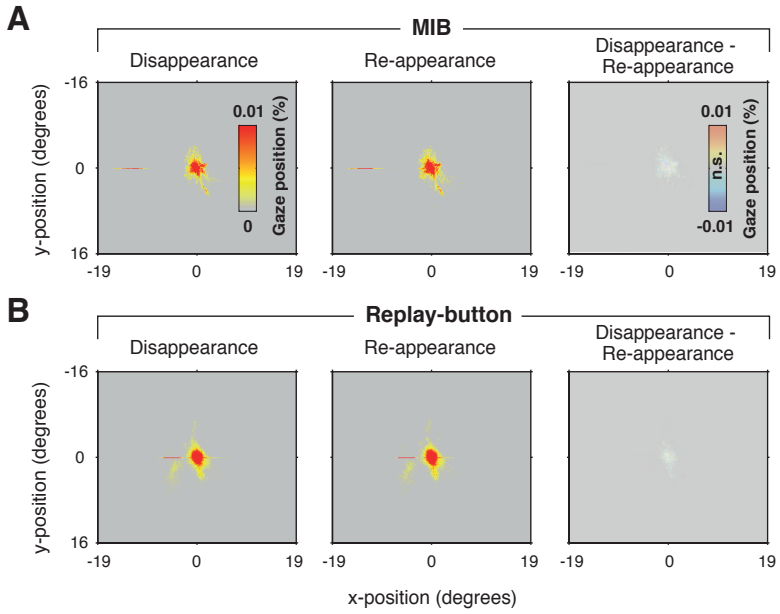

Figure 2 | No difference in eye position during target disappearance and re-appearance

Gaze fixation histograms averaged across subjects, indicating proportion of fixation time spent at each position on the screen around perceptual reports during MIB and Replay-button in Experiment 1. **A.** Left, MIB disappearance; middle, re-appearance; right, disappearance – re-appearance. Transparency level highlights clusters of significant modulation ($p < 0.05$, two-sided permutation test, cluster-corrected for multiple comparisons). **B.** Corresponding histograms for Replay-button.

perceptual report to around 1 s after report (Figure 3). This was the case during the MIB illusion (i.e., in the absence of any physical change in the stimulus; Figure 3A) and during Replay (Figure 3B). The similar responses during the MIB illusion and Replay indicate that the pupil dilation during MIB did not reflect the endogenous neural events causing the spontaneous perceptual switches (then it should have occurred only during the illusion), but was a consequence of these switches. This is consistent with pupil dilation responses observed across a range of bistable perceptual phenomena other than MIB (Einhauser et al., 2008; Hupe et al., 2009; Naber et al., 2011).

Critically, we found that the switch-related pupil dilation was significantly larger for disappearance than re-appearance (Figure 3). We henceforth refer to this amplitude difference between disappearance and re-appearance as the perceptual content effect. This effect was evident in the main experiment (Experiment 1; left panels of Figure 3A,B)

conducted in a group of 19 subjects as well as in an independent replication (Experiment 2) conducted in another group of 15 subjects. For both the pupil response time courses as well as the response amplitudes (see bar graphs), the perceptual content effect was statistically highly significant for MIB in both experiments (Figure 3A), and it was statistically highly significant for Replay in Experiment 1 (Figure 3B). In Experiment 1, subjects needed on average 60 ms longer to report target offsets than onsets, and the perceptual content effect was significant both when time-locked to the perceptual report (Figure 3B, left panel) and to the physical stimulus change (Figure 3C, left panel). Importantly, the occurrence of the perceptual content effect in the pupil response during the MIB condition implies that this effect is due to the subjective interpretation of the stimulus, rather than the physical stimulus itself.

We also assessed the impact of the temporal context of the disappearance and re-appearance events on the perceptual content effect. During the MIB illusion, subjects spent, on average, a smaller proportion of time in the target invisible than the target visible percept (Figure 1C), as is commonly observed in this illusion when only a single target is presented (Bonneh et al., 2001; Donner et al., 2008; Bonneh and Donner, 2011; Bonneh et al., 2014). This asymmetry might have rendered target disappearances more salient. We used two approaches to test whether this might explain the larger pupil dilation during disappearance. First, we selectively analyzed those subjects who spontaneously produced balanced percept durations, or a dominance of the duration of the target invisible percept. All three subjects satisfying this criterion exhibited larger pupil dilation around target disappearance than re-appearance; this effect was statistically significant within two of the subjects (Figure S3). Second, in the Replay of Experiment 1, we matched (by design) the mean durations of the two percepts (Figure 1C, top panel). Nonetheless, we observed the same perceptual effect in the pupil response (Figure 3B, left panel, and Figure 3C). Taken together, these observations suggest that the perceptual content effect is also unlikely to be caused by the asymmetry between the mean percept durations. We turn to the effect of the distribution of the intervals between events on the pupil response below (*Surprise about event timing also affects pupil response*).

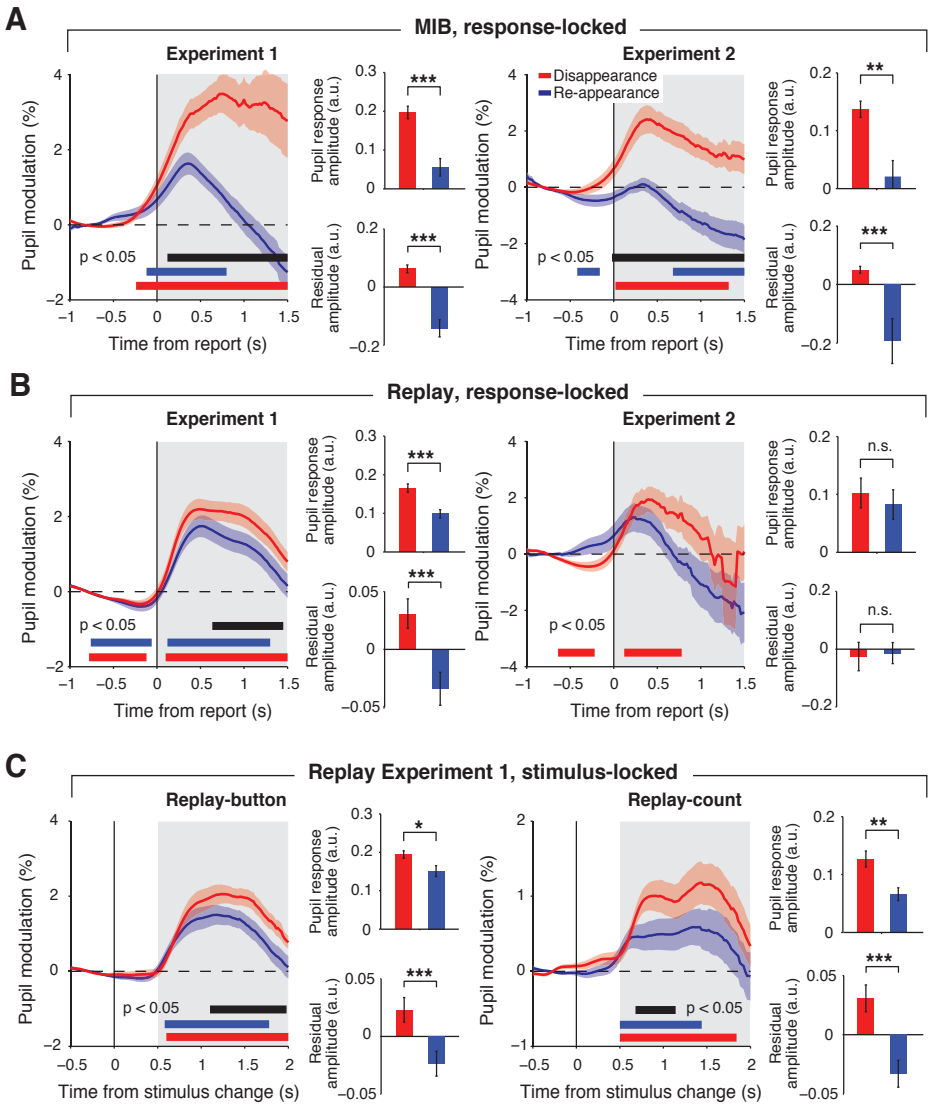

Figure 3 | Pupil dilation reflects content of perceptual report

Time courses of pupil diameter modulation around target disappearance and re-appearance. In each panel, the bar graphs on the right show scalar pupil response amplitudes in the time window indicated by the gray area underlying the time courses. Top, total pupil response amplitude. Bottom, residual response amplitudes after removing the effect of baseline pupil diameter. Colored bars indicate clusters of significant modulation; black bar indicates significant differences between colored traces ($p < 0.05$, cluster-corrected, Experiment 1: N = 19; Experiment 2: N = 15). Shaded areas time courses, s.e.m. across subjects. Gray shaded area, interval used for estimation of response amplitude. Bar graphs: baseline pupil diameter, averaged over subjects. *, $p < 0.05$; **, $p < 0.01$; ***, $p < 0.001$; n.s., not significant. **A.** MIB Experiments 1 and 2, time-locked to behavioral report. **B.** Replay Experiments 1 and 2, time-locked to behavioral report. **C.** Replay Experiment 1, separately for active and count conditions, time-locked to stimulus change.

Perceptual content effect is not explained by baseline pupil diameter

Our analyses focused on the transient pupil responses around the perceptual switches, by subtracting the pupil diameter at the start of each trial from the response time courses (see Materials and Methods). In a control analysis, we calculated the overall pupil diameter modulations around perceptual switches, thereby preserving potential differences between disappearance and re-appearance already in the "baseline" pupil diameter (here defined as pupil diameter before the trigger event). Indeed, we found larger baseline pupil diameter values before target re-appearance than target disappearance during MIB (Figure S4). This difference might be due to the above-described asymmetry between percept durations (on average, there was more time for the pupil diameter to decrease before disappearance than before re-appearance events). This indicates that the approach used in all the main figures was more suitable for isolating the event-related pupil responses. Nonetheless, we wondered whether the difference in baseline in combination with the correlation between baseline diameter and subsequent pupil response amplitude (Figure S2) might account for the perceptual content effect. In a control analysis, we removed (via linear regression) the component of the response amplitudes explained by the baseline diameter. The residual amplitudes exhibited the same perceptual content effect, with highly significantly larger amplitudes for disappearance than re-appearance (Figure 3; see bottom right bar graphs in each panel).

Pupil response reflects perceptual content at single-trial level

The analyses presented so far have shown that the subjects' mean pupil responses differed significantly between target disappearance and re-appearance. How reliable are the pupil responses as a predictor of the content of individual perceptual switches? We applied ROC analysis (see *Materials and Methods*) to the distributions of single-trial pupil response amplitudes sorted by the subjects' disappearance vs. re-appearance reports. The group mean ROC index for the post-report pupil dilation for the MIB condition was 0.61 ($N = 34$ across both experiments), which was significantly different from the 0.5 chance level ($p < 0.001$, two-sided permutation test). Thus, not only did the average pupil response amplitudes reflect the content of perceptual reports, but the single-trial pupil responses also enabled prediction of the content of individual reports.

Perceptual content effect is independent of motor report

Hupe et al. (2009) showed that a significant proportion of the switch-related pupil response in a bistable perceptual illusion could be accounted for by the button press used to report the switch. In the Replay-count condition of the main Experiment 1, we asked subjects to silently count the number of target disappearances. In line with Hupe et al. (2009), the overall pupil response in this condition was smaller than in the standard Replay-button condition (Figure 4). But, critically, the perceptual content effect in the pupil was evident across a range of different report regimens. In Experiment 1, pupil responses were significantly larger for disappearance than re-appearance during Replay-count (Figure 3C, right panel). In Experiment 2, we asked subjects to indicate target disappearance by means of button press in one half of the experiment and by means of button release in the other half (the converse for re-appearance; Figure 1B, bottom). Pupil responses were similar across both button press regimes (Figure S5) and, consequently, the perceptual content effect was significant after collapsing across these two response regimens (Figure 3A,B, right panels). In sum, the perceptual modulation of pupil diameter was consistent across a range of different mappings between perceptual switch and motor response, and even in the complete absence of a motor response.

Surprise about timing of stimulus-evoked perceptual events also affects pupil response

The timing of perceptual switches in bistable illusions and their replay is typically unpredictable. Therefore, the perceptual switches may elicit surprise. Other forms of surprise have been shown to engage pupil-linked brainstem systems (Preuschoff et al., 2011; Nassar et al., 2012; Naber et al., 2013). We wondered if the pupil dilation around the perceptual switches also reflected temporal surprise. It is difficult to experimentally control temporal surprise during MIB due to the spontaneous nature of the perceptual switches. Therefore, we focused this analysis on the Replay conditions in Experiment 1, in which we systematically manipulated the predictability of the target onsets and offsets (Figure 1D; see *Materials and Methods* for details). This manipulation affected subjects' behavior: Reaction times to the perceptual events occurring under these so-called low, medium and high surprise conditions increased as a function of surprise level (490, 590 and 630 ms, respectively).

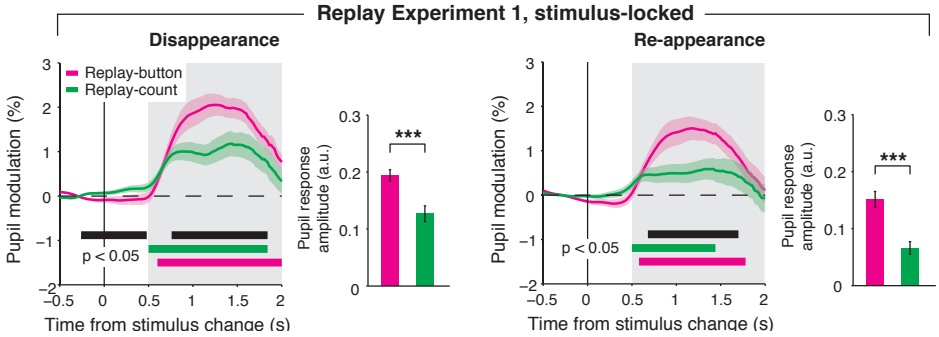

Figure 4 | Pupil dilation is larger for button pressing than for counting

Pupil diameter time courses around target disappearance (left) and re-appearance (right) during Replay-button versus Replay-count. Conventions as in Figure 3.

The pupil responses during target disappearances reflected surprise about event timing during Replay, in particular during the Replay-count condition (Figure 5). Response amplitudes were largest for the high surprise condition and decreased in the medium and low surprise conditions during Replay-count (Figure 5A: disappearance: $F_{2, 56} = 4.6$; $p < 0.05$; re-appearance: $F_{2, 56} = 7.58$; $p < 0.01$, 1-way ANOVA). During Replay-button, response amplitudes were also larger in high than low surprise, but similar for high and medium surprise.

Importantly, the effects of surprise level and perceptual content were independent of each other during the Replay conditions, both for reaction times and pupil responses. Both the main effects of surprise level and type of perceptual switch on reaction time were significant (2-way ANOVA: surprise level, $F_{2, 113} = 27.2$, $p < 0.001$; perceptual switch type, $F_{1,113} = 14.3$, $p < 0.001$), but there was no significant interaction ($F_{2,113} = 0.06$, $p = 0.94$). These main effects were also significant for the pupil responses (surprise level, $F_{2, 113} = 14.9$, $p < 0.001$; perceptual switch type, $F_{1,113} = 5.4$, $p = 0.02$), again with no significant interaction ($F_{2,113} = 0.06$, $p = 0.94$). Consistent with this finding, the overall effect of surprise (quantified as described in *Materials and Methods*) on the pupil in a given subject did not predict the strength of the perceptual content effect (quantified as the amplitude difference between disappearance and re-appearance; $r = 0.13$, $p = 0.59$, permutation test, N=19). In sum, despite clear effects of both effects of surprise and perceptual content on pupil and subjects' response behavior during Replay, we found no evidence for a relationship between these effects.

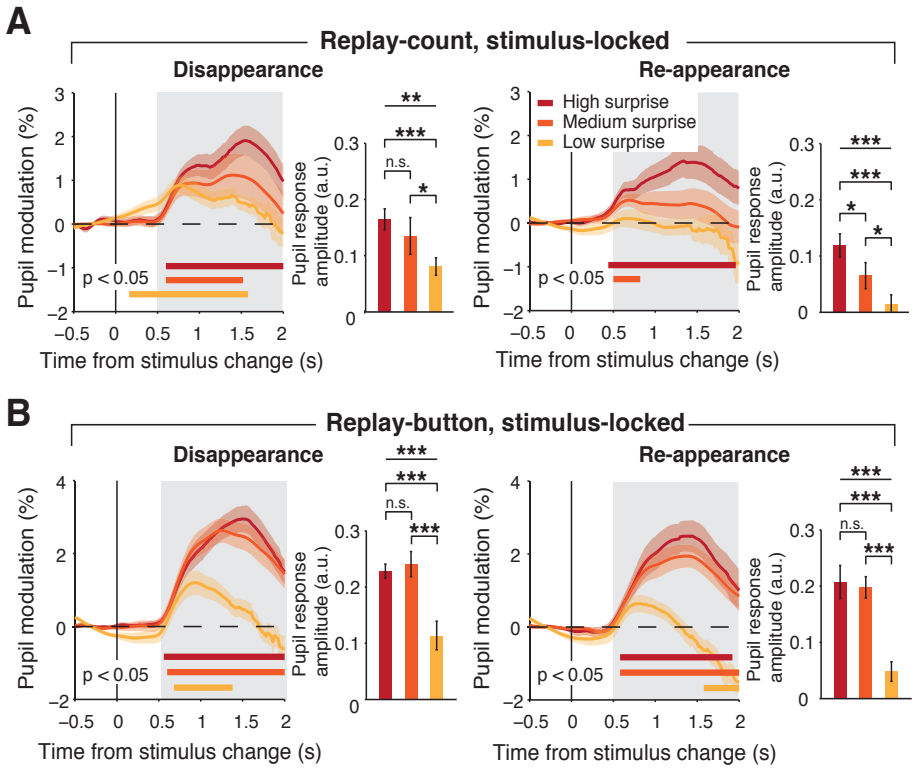

Figure 5 | Pupil dilation reflects surprise about timing of perceptual switches

Pupil diameter time courses around target offset and onset during low, medium and high surprise Replay conditions. Conventions as in Figure 3. **A.** Replay-count. **B.** Replay-button.

DISCUSSION

A number of recent studies have linked modulations of pupil to surprise about behaviorally relevant events (Preuschoff et al., 2011; Nassar et al., 2012; Naber et al., 2013), the content of perceptual decisions (Shalom et al., 2013; de Gee et al., 2014), and to the spontaneous perceptual switches in bistable illusions as well as the corresponding stimulus-evoked perceptual switches in replays of the illusions (Einhauser et al., 2008; Hupe et al., 2009; Naber et al., 2011). Here, we show that pupil dilations following alternations in a visual stimulus can reflect the content of the perceptual switches as well as the level of subjects' surprise about the timing of the switches, both independent of motor response. Further, the effects of perceptual content and surprise on the pupil dilation during Replay seem to be distinct from one another.

The similar pupil dilations during the MIB illusion and its replay indicate that the pupil dilation during MIB does not reflect the endogenous neural processes that initiate the spontaneous perceptual switch in the MIB illusion (Donner et al., 2008, 2013) – in this case, the effect should be specific for MIB (Donner et al., 2008). Rather, the switch-related pupil dilation during both conditions reflects a process that is triggered by the switch, regardless of whether this switch is endogenously generated or evoked by a physical stimulus change. This result is in line with previous studies of pupil dynamics in bistable perception (Einhauser et al., 2008; Hupe et al., 2009). Further, while the dilation is small during passive viewing of a replay of an illusion (Hupe et al., 2009), we here show robust dilation in the absence of immediate motor report, provided that subjects count the switches. The concomitant pupil dilation might reflect the updating of working memory. All the present results indicate that a substantial component (~ 65% of the report-locked pupil response during disappearance in Replay-button) of the pupil dilation measured during perceptual switches reflect elementary decision-making: the decision to report the switch by button press, or the decision to update (or not, in case of re-appearance) working memory.

The most notable aspect of the current results is that the pupil dilation does not only indicate the occurrence of perceptual switches, but also reliably differentiates between target disappearance and re-appearance (even at the level of individual reports). Some pupillometry studies of other types of perceptual decision-making have reported modulations of pupil responses by perceptual content (Shalom et al., 2013; de Gee et al., 2014; Laeng and Sulutvedt, 2014). Pupillometry studies of binocular rivalry have shown that the pupil tracks the luminance of the image seen by the currently dominant eye (Fahle et al., 2011; Naber et al., 2011) and older work indicates that a light flash in the dominant eye yields a larger pupil response than a flash in the suppressed eye (Bárány and Halldén, 1948; Lowe and Ogle, 1966). However, a perceptual content effect in pupil dilation during bistable perception has not been shown previously without manipulating luminance of the bistable stimulus (Einhauser et al., 2008; Hupe et al., 2009).

Although objective luminance was constant in our experiments, it is possible that the stronger pupil dilation around target disappearance than re-appearance may be due to concomitant changes in the perceived visual properties (brightness or contrast) of the disappearing and re-appearing target. Indeed, the pupil also responds to subjective changes in perceived brightness of large, centrally presented, black-and-white stimuli

during constant physical luminance (Laeng and Endestad, 2012). However, we think that this possibility is unlikely to account for our findings for three reasons. First, the subjective pupil brightness response in Laeng and Endestad's study scales with the strength of the Kanisza illusion, which is determined by the stimulus configuration. In contrast, a uniformly gray patch does not appear to be brighter than the Gabor target, so it seems unlikely that a perceived brightness increase underlies the stronger pupil dilation around target disappearance. Second, our gray, peripherally presented target stimulus was very small compared to the large and salient stimuli used by Laeng and Endestad. It seems unlikely that any subjective change in luminance around disappearance of the small target would have a large effect on pupil dilation. Third, the perceptual content effect seems also unlikely due to changes in perceived contrast, because stronger contrast of visual targets induces, at least under certain stimulus and task conditions, larger pupil dilations (Wang and Munoz, 2014). This effect would result in a stronger dilation around target re-appearance, in contrast with our results. Future work should test the effects of visual contrast and perceived brightness under the stimulus and task conditions used here.

We propose that the perceptual content effect in the pupil response reflects a difference in engagement that depends on the behavioral context. The effect might reflect a difference in the subjective saliency assigned to the disappearance and re-appearance events, or, relatedly, a (stronger or more reliable) shift in covert attention towards the target triggered by the sudden target disappearance. Indeed, shifts in attention modulate the pupil response under certain conditions (Mathot et al., 2013), and microstimulation of an important node in the attentional control network, the superior colliculus, induces transient pupil responses (Wang et al., 2012). While neither physical stimulus properties nor the temporal context of the switch events seem sufficient to account the perceptual content effect, one relevant aspect might be that only one of the two perceptual interpretations in MIB is illusory (target absent) whereas the other is veridical (target present). Future work should compare different types of perceptual illusions to determine the factors governing the subjective salience of the perceptual switch events.

Our findings indicate that the phasic activation of pupil-linked brainstem systems can be driven by purely subjective perceptual changes in a content-specific fashion. This conclusion has important implications for neurophysiological and neuroimaging studies of perception. Phasic brainstem activation is rapidly followed by changes in cortical state (Parikh et al., 2007; Pinto et al., 2013). Thus, our current and previous (Einhauser

et al., 2008; Hupe et al., 2009; Naber et al., 2011) pupillometry results may, at least in part, account for retinotopically global modulations of population activity that have been observed in early visual cortex during perceptual switches in various illusions (Donner et al., 2008; de-Wit et al., 2012; Donner et al., 2013; Kloosterman et al., 2014) (N. Rubin, personal communication). In particular, in MIB, this global activity modulation exhibits similar characteristics as the pupil diameter modulation reported here, occurring during both the illusion and its physical replay and differentiating between target disappearance and re-appearance. An important difference, however, is that the activity modulation during MIB differs in sign between target disappearance and re-appearance (Donner et al., 2008; Kloosterman et al., 2014), as opposed to the scaling of the (generally positive) pupil response amplitude by perceptual content observed here.

In conclusion, our findings point to an intriguing feedback interaction between subjective perception and global brain state. Pupil-linked brainstem systems are phasically activated by changes in subjective perception. We here show that the amplitude of this phasic activation can depend on the contents of the perceptual changes. Because this phasic activation, in turn, causes widespread changes in cortical state, our finding implies that subsequent perception and cognition is affected in a way that depends on the contents of preceding perceptual changes.

ACKNOWLEDGEMENTS

We thank all members of the Donner lab for comments and discussion. The authors declare no conflict of interest.

SUPPLEMENT 1

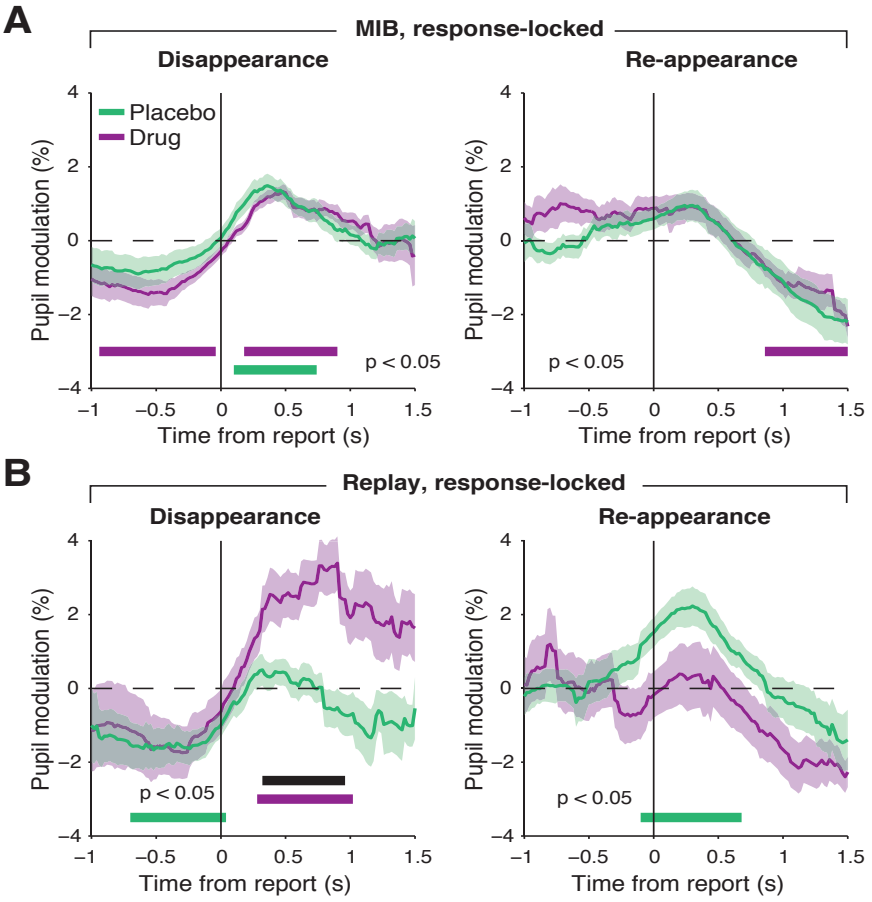

Figure S1 | Pupil dilation during MIB is independent of drug manipulation

Pupil time courses around target disappearance and re-appearance during placebo/drug manipulations in Experiment 2. Conventions as in Figure 3. **A.** MIB. **B.** Replay.

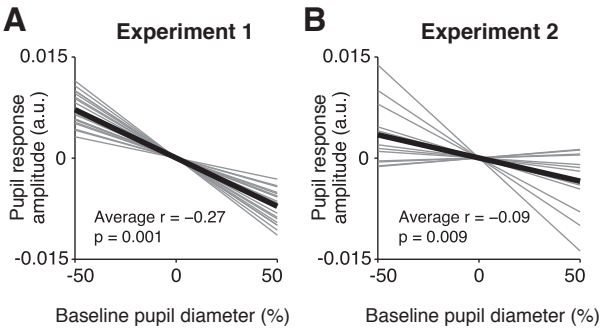

Figure S2 | Correlation between baseline pupil diameter and subsequent pupil response

Linear regression of baseline pupil diameter to phasic pupil response. Thin gray lines, individual subjects. Thick black line, group average. P-values indicate significance of permutation test against zero. **A.** Experiment 1. **B.** Experiment 2.

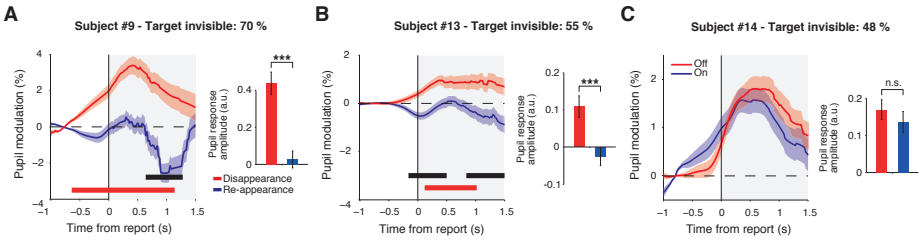

Figure S3 | Pupil dilation reflects content of perceptual report also in subjects for whom target-visible durations are not longer than target-invisible durations

A-C. Time course of pupil diameter modulation around target disappearance and re-appearance for three subjects showing ca. 50 % or more target invisible time. Shaded areas time courses and error bars on amplitude bars, s.e.m. across trials. Conventions as in Figure 3.

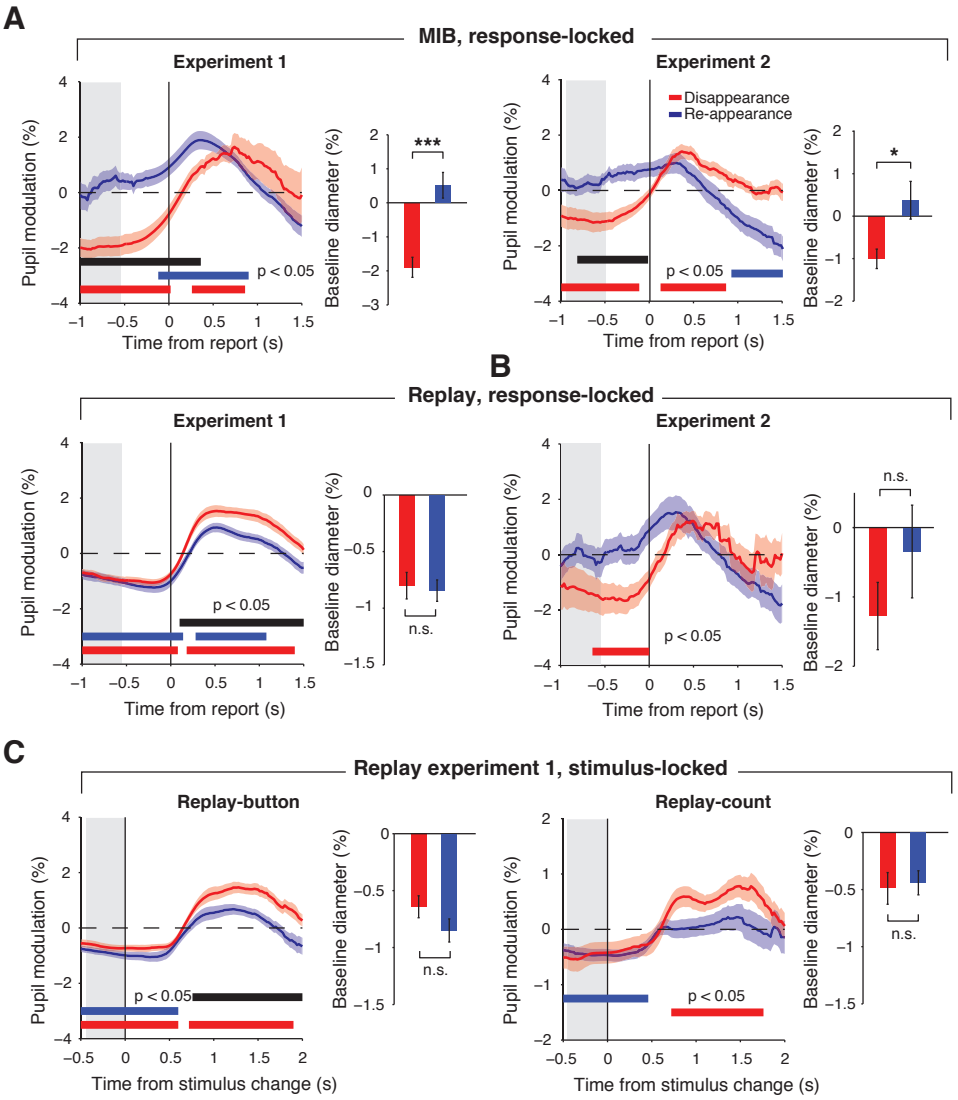

Figure S4 | Baseline pupil diameter and overall modulation around perceptual switches

Pupil diameter time courses around target disappearance versus re-appearance, normalized with respect to the complete time course. In this control analysis, we computed the baseline as the mean pupil diameter value across all samples and trials from a given condition (MIB or Replay). We then used this number as the baseline value in the percent signal change conversion. This yields the overall modulations of the pupil diameter around the perceptual switches, including systematic differences before the trigger event. For an analogous procedure, see (Einhauser et al., 2008). Conventions as in Figure 3. Gray shaded area, time period for pre-trigger interval calculation. Bar graphs: average modulation values of the pre-trigger interval. **A.** MIB Experiments 1 and 2, time-locked to behavioral report. **B.** Replay Experiments 1 and 2, time-locked to behavioral report. **C.** Replay Experiment 1, separately for button and count conditions, time-locked to stimulus change.

Pupil modulations were significantly larger during the intervals preceding re-appearance than disappearance reports in both experiments. Because the pupil response to a switch is sluggish, it is possible that this difference was due to the fact that target invisible intervals were shorter than visible intervals during MIB (both experiments) and Replay (Experiment 2) (median invisible and visible durations, respectively, averaged across subjects in Experiment 1: 1.77 s versus 4.98 s (MIB); Experiment 2: 1.69 s versus 2.65 s (MIB), and 1.79 versus 2.73 s (Replay). In line with this notion, there was no difference between disappearance and re-appearance pupil modulations during Replay in Experiment 1 (in which visible and invisible durations were equated, Figure 1C) in the pre-trigger interval. To rule out this confound, we focus all analyses in the main paper on the transient pupil responses following the trigger events, by subtracting from each trial the pupil diameter values in the pre-trigger interval.

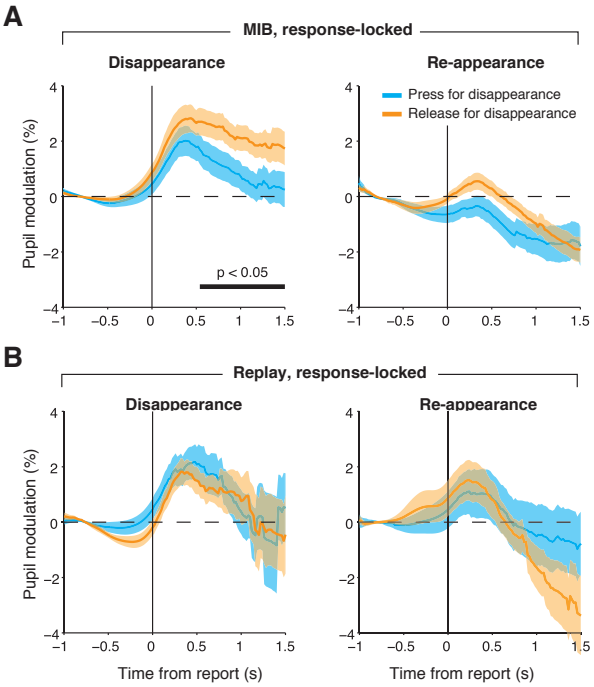

Figure S5 | Pupil dilation is independent of motor response regime

Pupil time courses around target disappearance and re-appearance during the two motor response regimes in Experiment 2. Conventions as in Figure 3. **A.** MIB. **B.** Replay.

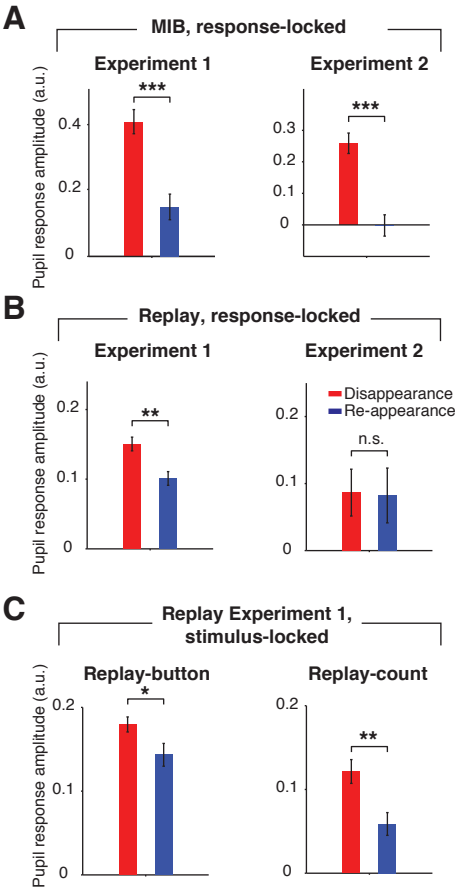

Figure S6 | Pupil response amplitudes for disappearance and re-appearance trials of equal duration

Linear projection amplitudes pupil diameter around target disappearance versus re-appearance, averaged over subjects. In this control analysis, only trials were included that contained data at every sample within the projection interval (here, 0 to 1 s for response-locked or 0.5 s to 1.5 s for stimulus-locked).

Chapter 6

Pupil-linked Modulation of Decision-related Signals in Human Primary Visual Cortex

This chapter is based on:

Kloosterman N. A., Lindh D., de Gee J. W., Knapen T., Lamme V. A. F., Donner T. H. Pupil-linked Modulation of Decision-Related Signals in Human Primary Visual Cortex. *In preparation.*

ABSTRACT

The cerebral cortex continuously undergoes changes in its internal state. Such state changes do not only occur during the slow transitions from sleep to wakefulness, but also at a sub-second timescale while subjects are awake. These rapid state changes are often precisely synchronized with specific cognitive acts, such as perceptual decisions. Signatures of state changes are evident in a widespread modulation of task-related hemodynamic and electrophysiological population signals that are retinotopically decoupled from the cortical response to the stimulus. Here we tested, if these retinotopically "global" decision-related modulations in visual cortex are associated with the activation of neuromodulatory brainstem systems. This hypothesis predicts that the amplitude of the modulations in visual cortex should be linked to the dilation of the pupil, which is a peripheral proxy of neuromodulatory activity. We simultaneously monitored pupil diameter and fMRI activity in human subjects reporting their subjective changes of perception during a bistable visual illusion called motion-induced blindness (MIB). In MIB, a salient (and constantly present) visual target surrounded by a moving pattern repeatedly disappears and reappears in conscious perception. Time-locked to subjects' behavioral reports of these spontaneous perceptual changes, we found a modulation of fMRI activity in a peripheral, non-stimulated region of primary visual cortex (area V1) and anterior cingulate cortex (ACC). The modulation encodes the type of perceptual report (disappearance vs. re-appearance) in terms of its polarity and also occurs during a stimulus-evoked "replay" of the illusion. Crucially, these decision-related modulations in V1 and ACC are linked with stronger concomitant pupil dilation. Taken together, these results support an active role of phasic neuromodulation in fast changes in brain state during elementary perceptual decisions.

Keywords: fMRI, perceptual bistability, perceptual decision-making, brain state, human

INTRODUCTION

The internal state of the brain changes constantly, shaping the way in which the cerebral cortex processes incoming information about the outside world (Harris and Thiele, 2011; Zagha and McCormick, 2014). Changes in cortical state during slow transitions between sleep and wakefulness are a long established phenomenon (Steriade, 2006). More recent evidence indicates that cortical state changes also occur on a faster time scale during full wakefulness. Intriguingly, these fast state changes are often synchronized with rapid cognitive processes, such as perceptual decisions (Gilbert and Sigman, 2007; Kloosterman et al., 2014; Meindertsma et al., 2014). In line with signal detection theory (Green and Swets, 1966), we here define a simple perceptual decision as the transformation of a graded perceptual signal into a categorical proposition that can drive an (immediate or delayed) motor action.

An increasing number of neuroimaging studies report candidate signatures of these rapid state changes in monkey or human visual cortex during elementary perceptual tasks. These signatures are evident in widespread fMRI response modulations across the retinotopic map of visual cortex that are spatially decoupled from the stimulus responses, but precisely time-locked to the subjects' behavioral report or other task-relevant events (Jack et al., 2006; Wilke et al., 2006; Donner et al., 2008; Hsieh and Tse, 2009; Sirotin and Das, 2009; Cardoso et al., 2012; de-Wit et al., 2012; Swallow et al., 2012; Donner et al., 2013; Choe et al., 2014). Local field potential recordings from monkey (Gail et al., 2004; Wilke et al., 2006; Wilke et al., 2009) and magnetoencephalography from human visual cortex (Kloosterman et al., 2014; Meindertsma et al., 2014) indicate that modulations in the beta-band and lower frequency ranges (< 8 Hz) are the electrophysiological underpinning of these widespread fMRI-signal modulations.

Multi-stable perceptual phenomena, in which a constant sensory input induces illusory switches in perception, are excellent tools for studying rapid cortical state changes linked to cognition. For example, during motion-induced blindness (MIB), a salient visual target surrounded by a rotating mask suddenly disappears from perception, only to re-appear after some time (Figure 1A) (Bonneh et al., 2001; Bonneh and Donner, 2011). Subjects' behavioral reports of these perceptual switches are associated with a widespread modulation of the fMRI signal (Donner et al., 2008, 2013) as well as beta-band activity (Kloosterman et al., 2014; Meindertsma et al., 2014) across visual cortex.

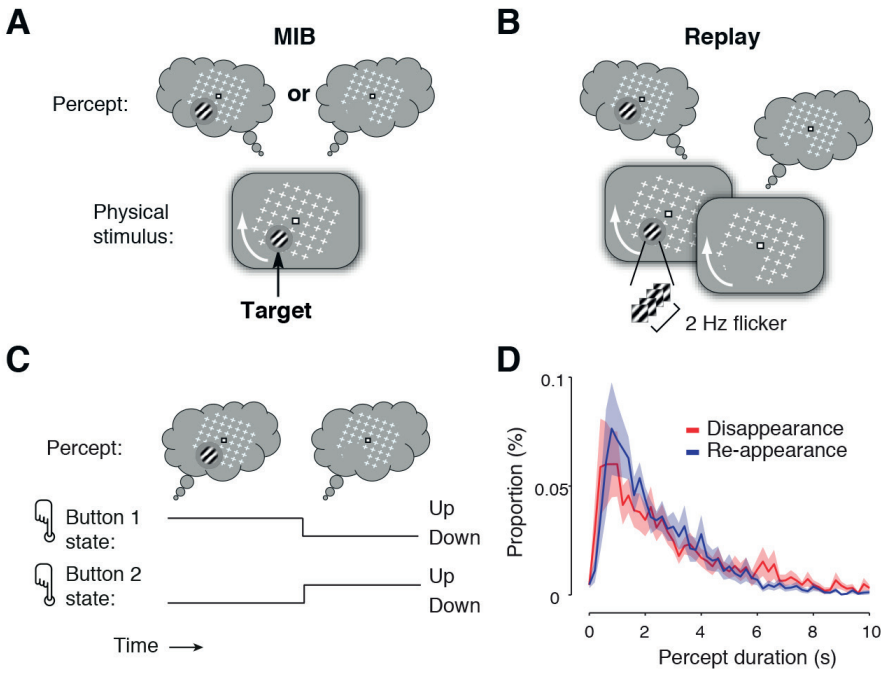

Figure 1 | MIB stimulus, task and behavorial results

A. Schematic snapshots of stimuli and alternating percepts. Left: MIB stimulus. A salient target stimulus (Gabor patch) was surrounded by a moving mask pattern (white), which appeared as a rotating grid. Top left, fluctuating perception of the target due to MIB. **B.** Corresponding stimulus and alternating perception during Replay. The target flickered at 2 Hz. **C.** Behavioral response regime. Subjects switched button press of two buttons to report target disappearance and re-appearance. **D.** Group average distributions of target invisible and target visible durations (N = 9 subjects). Shaded areas, s.e.m. across subjects.

This modulation is (i) precisely time-locked to perceptual report, (ii) reflects the content of the perceptual decision (negative sign for target disappearance and positive sign for re-appearance), (iii) occurs irrespective of whether the perceptual switches occur spontaneously or are evoked by the physical stimulus, (iv) neither depends on physical stimulus properties, such as stimulus location and presence of the mask, nor the type of motor response, but (v) is contingent on the behavioral relevance of the perceptual switch. Taken together, these characteristics indicate that the modulation is a non-sensory (top-down) signal linked to the perceptual decision process that transforms a perceptual event into a behavioral report (Donner et al., 2008; Kloosterman et al., 2014; Meindertsma et al., 2014). While similar modulations have been observed in the visual thalamus (Wilke et

al., 2009), the brain-wide distribution of these decision-related top-down modulations is, so far, unknown.

Neuromodulatory brainstem systems, such as the noradrenergic locus coeruleus (LC-NA) and the cholinergic basal forebrain systems are candidate sources of these decision-related modulations in visual cortex. These brainstem systems have widespread projections to the cerebral cortex (including visual cortex) and receive top-down input from frontal cortical areas, in particular the anterior cingulate cortex (Aston-Jones and Cohen, 2005). Further, in animals, they have been found to exhibit transient ("phasic") bursts of activity during elementary sensory-motor tasks (Aston-Jones and Cohen, 2005; Parikh et al., 2007). Activation of these systems is associated with changes in pupil diameter (Aston-Jones and Cohen, 2005; Murphy et al., 2014). Pupil dilation also closely tracks mental effort, arousal, surprise, and decision processes (Hess and Polt, 1964; Kahneman and Beatty, 1966; Beatty, 1982; Einhauser et al., 2008; Einhauser et al., 2010; de Gee et al., 2014). In particular, pupil dilation also reflects the content of perceptual reports during MIB, with larger pupil dilation during disappearance than re-appearance (Kloosterman et al., 2015b). If neuromodulatory brainstem systems are involved in the top-down modulation, then their activity should affect both population responses in visual cortex and pupil dilation. This hypothesis predicts that greater pupil dilation around perceptual decisions is associated with stronger modulation of fMRI-activity.

The goals of the present study were (i) to characterize the brain-wide distribution of the decision-related top-down modulation evident in primary visual cortex (V1) and (ii) to test for a relationship between its amplitude and the amplitude of the concomitant pupil dilation. To this end, we performed concurrent fMRI and pupillometry measurements during MIB. We isolated the decision-related modulation in V1 by focusing on a retinotopic sub-region in the far-periphery representation of the visual field map. This sub-region is located well beyond the one driven by the MIB stimulus while exhibiting strong widespread top-down modulations (Jack et al., 2006; Donner et al., 2008)).

MATERIALS AND METHODS

Subjects

Data were acquired from nine healthy subjects with normal or corrected-to-normal vision (4 female, age range: 25 - 32 years). Subjects received 15 euros per hour for their participation. The experiment was approved by the ethics committee of the Dept. of Psychology at the University of Amsterdam. Each subject gave written informed consent. Each subject participated in three scanning sessions: one to define retinotopically organized cortical visual areas (ca. 75 minutes) and two sessions to measure fMRI responses in the main experiment (MIB, replay and an auditory detection task, two hours per session). The results from the auditory task are not reported in this chapter.

Stimulus, task and procedure

Stimuli

The display consisted of a static target (full contrast gray-scale Gabor patch); diameter: 2°; location: 3° eccentricity in one of the four visual field quadrants). The target was surrounded by a rotating mask (10° x 10° grid of white crosses), superimposed on a gray background with a fixation mark (red outline, white inside, 0.8° width and length) centered on the mask in the middle of the screen (Figure 1A). The target Gabor patch contained 2 spatial cycles. The mask rotated at a speed of 140 °/s. Target location (visual field quadrant) was individually selected for each subject to maximize the percentage of target invisible time (at least 40%). The target was separated from the mask by a gray "protection zone" subtending about 2° around the target (Bonneh et al., 2001) (Figure 1A).

During the MIB condition, all features of the physical stimulus remained constant for each fMRI scanning run of 3 min duration. During the Replay condition, all features of the stimulus were the same as in MIB, except for the following changes to the target: (i) the target flickered at a temporal frequency of 2 Hz (by alternating the black and white parts of the Gabor patch); (ii) target size was increased to 4° diameter; and (iii) the target was physically removed in the same temporal sequence as reported by the corresponding subject in one of the preceding MIB runs. While (i) and (ii) rendered the target more salient and thus helped minimize its illusory disappearance due to MIB (Bonneh et al., 2001; Bonneh and Donner, 2011), (iii) yielded the critical experimental events (physical target

offset and onset) to be compared with the spontaneous perceptual switches during the MIB illusion.

Stimuli were back-projected on a transparent screen at the back of the scanner bore by a DLP projector (Projectiondesign F22 WUXGA, Fredrikstad, Norway) at a resolution of 1,024 × 768 pixels and a refresh rate of 60 Hz. Subjects viewed the screen in the MRI scanner from 121 cm distance via a mirror attached to the head coil (8 cm from eyes to mirror, 113 cm from mirror to screen). Stimuli were presented and subjects responses recorded by the Presentation software (version 14, NeuroBehavioral Systems, Albany, CA, USA).

Task

In both the MIB and the Replay conditions, the subjects' task was to report the target disappearance and re-appearance while maintaining stable fixation. To do so, subjects pressed a button with their left index finger or right index finger for as long as the percept lasted. The mapping of response button (left vs. right) to type of perceptual report (target disappearance vs. re-appearance) was counterbalanced across subjects. The experiment consisted of two sessions on separate days of approximately two hours duration each, in which subjects completed a total of 12-14 runs (MIB: 8-10, Replay: 4).

Data acquisition

Magnetic resonance imaging (MRI) data were acquired on a 3T Philips Achieva XT MRI scanner using a 32-channel head coil. During the MIB sessions, 2D echo planar imaging (EPI) scans were acquired parallel to the line between the most anterior and posterior parts of the corpus callosum with thirty-five slices (thickness 3.29 mm, in-plane resolution of 1.79 mm2) (field of view (FOV) = 160 × 200 × 105 mm, TR = 2 s, TE = 27.63 ms, flip angle = 76.1°). A structural T1-weighted anatomical scan was acquired with an resolution of 1 x 1 x 1 mm (FOV = 240 x 188 x 220, TR = 8.4 ms, TE = 3.8 ms, flip-angle = 8°). For registration purposes, an additional T2-weighted scan was acquired with twice the resolution of the functional EPI-scans (voxel size: 0.89 mm × 0.89 mm × 1.65 mm). A B0 field map was acquired at the end of each session.

Scan settings were identical in the retinotopy sessions, with the following exceptions. EPI scans were acquired with twenty-nine 2.74 mm slices with an in-plane resolution of

2.5 mm2 (field of view = 240 × 240 × 80 mm, TR = 1.5 s, TE = 27.63 ms, flip-angle = 70°). The voxel size of the T2-weighted scan was 1.25 mm × 1.25 mm × 1.37 mm.

Concurrently with the fMRI measurements, the position of the left eye's pupil was sampled at 1000 Hz with an average spatial resolution of 15 to 30 min arc, using an MRI-compatible EyeLink 1000 Long Range Mount (SR Research, Osgoode, Ontario, Canada) placed outside the scanner bore. The subject's eye was tracked via the mirror attached to the head coil. The eye tracker was calibrated before every fMRI recording. In addition, cardiac and respiratory activity was recorded at a sampling rate of 500 Hz using a pulse oximeter on the left index finger and a chest belt, respectively.

fMRI data analysis

MRI data was analyzed using FSL (Smith et al., 2004), FreeSurfer (Fischl et al., 1999; Fischl et al., 2004), as well as custom-made Python software.

Preprocessing

The first eight volumes of each functional run were discarded to minimize the effect of transient magnetic saturation and to allow the hemodynamic response to reach steady state baseline. For the analysis of the MIB and Replay data (see next section), we then applied the following preprocessing steps to the data from each run: (1) Removal of non-brain tissue (brain extraction) using the BET tool in FSL (2) unwarping using the B0 field map and FUGUE (FMRIB's Utility for Geometrically Unwarping EPIs), (3) image realignment to compensate for head movements (Jenkinson et al., 2002) (for improved precision we used as the target volume the high-resolution, brain-extracted T2 weighted anatomical scan; afterwards, images were down-sampled to their original dimensions), and (4) temporal filtering of each voxel's time series, using a high-pass filter (cutoff, 0.02 Hz) to remove slow drift. For computing event-related responses for different regions of interest (ROIs), we removed physiological artifacts using an extension of RETROICOR (Glover et al., 2000), as implemented in the PNM tool in FSL. This method assigns cardiac and respiratory phases to each volume in a participant's fMRI time-series post-hoc, and statistically controls for their effects by including them as regressors of no interest in the first-level general linear model (GLM). This procedure yielded a total of 36 physiological regressors (three regressors for cardiac, two for respiratory, three for the interaction from

cardiac to respiratory and two for the interaction from respiratory to cardiac). Finally, we Z-scored the residual voxel time series.

Preprocessing was identical for the whole brain analysis, except that the physiological regressors of no interest were included in the general linear model (GLM) in FEAT, and the data were slice time corrected and spatially smoothed (5 mm full width at half maximum Gaussian kernel). For visualization purposes, T1 weighted anatomical scans acquired at the beginning of each scanning session were automatically segmented and inflated using FreeSurfer.

ROI-based analysis of event-related responses during perceptual reports

We performed a deconvolution analysis (Dale, 1999) to estimate the mean fMRI response time course for the reports of target disappearance and reappearance. The preprocessed fMRI time series were averaged across gray matter voxels within the region of interest (ROI) in the periphery of V1 (see *Retinotopic mapping*). The time series were then concatenated across runs and session within each subject. The resulting mean time series was up-sampled by a factor of four (sampling rate: 0.5 s). We then computed ordinary least-squares estimates of the mean responses to each type of perceptual report of interest, according to:

$$\boldsymbol{h} = (\boldsymbol{X}^{\mathrm{T}}\boldsymbol{X})^{-1}\boldsymbol{X}^{\mathrm{T}}\boldsymbol{y}, \qquad \text{eq. 1}$$

Where $\boldsymbol{y}$ was the measured time series, $\boldsymbol{h} = [\boldsymbol{h}_1{}^{\mathrm{T}}\ \boldsymbol{h}_2\ \boldsymbol{h}_x{}^{\mathrm{T}}]^{\mathrm{T}}$ was a vertical concatenation of estimated responses to the event types of interest, the design matrix $\boldsymbol{X} = [\boldsymbol{X}_1\ \boldsymbol{X}_2\ \boldsymbol{X}_x]$ was a horizontal concatenation of the convolution matrices corresponding to the two event types, and superscript T indicates matrix transpose. Each $\boldsymbol{X}_i$ had dimensions *M x N*, where *M* was the number of samples in $\boldsymbol{y}$ and *N* was the number of time points in the estimated $\boldsymbol{h}_i$. The first column of each $\boldsymbol{X}_i$ contained 1's at the samples of the corresponding switch event and 0's elsewhere. Each of the *N* x 1 subsequent columns contained a copy of this event sequence, shifted by the corresponding lag. To create the discrete event sequences, we rounded subjects' reports (button presses sampled at 1 ms resolution) to the nearest sample (0.05 s resolution) of the pupil diameter time series. See Donner et al. (2008) for a detailed description.

We estimated 20 parameters (from the time of report until 10 s after report) for each type of perceptual switch. Successive perceptual reports within 0.5 s and eye blink

events were included as regressors of no interest. Sequences of blink events occurring < 0.1 s from each other were modeled as one blink event occurring at the time of the first event. The resulting deconvolved responses for disappearance and re-appearance were baseline-corrected by subtracting the value at time 0 from all time points for each subject, before computing the mean and SEM across subjects.

We also performed a separate deconvolution of the fMRI time courses estimating separate responses time-locked to disappearance and re-appearance for the high and low pupil response amplitude conditions (see below).

Statistical tests of event-related fMRI response time courses

We performed statistical tests of the fMRI response amplitudes across subjects by splitting the deconvolved response time courses into an early and a late interval with respect to the time of report and averaging the time series within each time window for each subject. The early interval ranged from 0 to 5 s and the late interval ranged from 5 to 10 s from report. We chose these intervals because a previous fMRI study of MIB showed a percept-specific modulation in V1 specifically in the late period, whereas there was no effect in the early period (Donner et al., 2008).

We used a two-tailed permutation test (10.000 permutations) (Efron and Tibshirani, 1998) to test the significance of the overall fMRI response amplitude and of the difference in fMRI response between the early and late intervals across subjects. We averaged (integrated) the fMRI response time courses across each interval and tested for (i) significant deviations of the integrated response from zero, (ii) significant differences between early and late intervals, and (iii) for differences between the disappearance/ reappearance (MIB/Replay). We also compared the fMRI response amplitudes between of high and low pupil response amplitude conditions.

To study the combined effects of the factors report type (target disappearance vs. re-appearance) and interval (early vs. late), we performed a parametric 2-way (2 x 2) repeated measures ANOVA. We studied the combined effects of the factors report type (target disappearance vs. re-appearance), time interval (early vs. late), and pupil response amplitude (high vs. low) with a parametric 3-way (2 x 2 x 2) repeated measures ANOVA.

Whole brain fMRI analysis of event-related responses during perceptual reports

For the analysis of the whole brain fMRI data we used a mixed effects approach within the framework of the general linear model, as implemented within the FEAT tool in FSL 5.6 (Jenkinson et al., 2012). For each run of the MIB and Replay conditions, we included separate regressors for target disappearance and reappearance reports as regressors of interest. We added the onset of the physical MIB stimulus, eye blink events, perceptual reports occurring within 0.5 s from each other and the 36 RETROICOR regressors as regressors of no interest. The eye blink regressor was orthogonalized with respect to the perceptual report regressors. We convolved each regressor with a hemodynamic response function (double-gamma variate preset in FEAT). Contrasts were computed at the single run-level for each of the regressors of interest, with the following comparisons: perceptual disappearance and re-appearance versus baseline and disappearance versus re-appearance.

We pooled the fMRI runs for each condition across the two sessions using a second-level (within-subject) fixed effects analysis. A third-level (across-subject) analysis was performed within a mixed-effects (FLAME 1 + 2) analysis in FSL, treating subjects as a random effect. To project the data onto the reconstructed and inflated surface, the second-level z-stats from each subject's were registered back from MNI-space to the anatomical space of the first run of the first session using FLIRT. Then, the data were registered to each subject's inflated T1 image using FreeSurfer. Finally, the images were projected on the MNI standard surface and averaged across subjects. For visualization (Figures 2, 3), statistical maps were thresholded using clusters determined by $p < 0.05$ and a corrected cluster significance threshold of $p < 0.05$.

Retinotopic mapping

We used standard population receptive field (pRF) mapping of the visual field to identify the borders of retinotopically organized visual areas (Dumoulin and Wandell, 2008; Lee et al., 2013). A pRF map is as a set of weights that can be estimated by solving a linear model that predicts the fMRI-signal in visual cortex for each location in the visual field (Wandell et al., 2007). The pRF stimulus consisted of moving bars (width 1.2°) of randomly oriented Gabor patches (100% contrast), presented across a circle-shaped aperture of 18° diameter. Four bar orientations (0°, 45°, 90°, 135°) and two different motion directions

for each bar were used, yielding a total of eight different bar configurations within a given scan. Subjects fixated a small gray fixation dot at the center of the screen. At random time points, the fixation dot briefly turned white. Subjects were instructed to press a button with their right index finger when they detected a color change.

After fitting a GLM to the pRF data, we extracted the polar angle and eccentricity location parameters (x, y) for each subject and projected these values onto the flattened cortical surface. We used the polar angel and eccentricity maps to delineate the borders of multiple retinotopic visual cortical areas as defined by Wandell and colleagues (Wandell et al., 2007; Dumoulin and Wandell, 2008; Lee et al., 2013).

The present report focuses on the non-stimulated, far-periphery sub-region (during MIB and Replay) of area V1. This ROI was defined as the region of visual cortex beyond the region stimulated by the round aperture in which the moving bars of the pRF stimulus moved, constrained by the borders of anatomical V1 as provided by the FreeSurfer package. In an alternative analysis, we delineated the non-stimulated from the stimulated portion of V1 using a localizer stimulus specifically tailored to the MIB stimulus. This localizer consisted of a circle shaped checkerboard pattern with the same diameter (7.6°) as the rotating mask, which flickered at 4 Hz by alternating its black and white parts. This central stimulus was alternated every 12 s with a ring-shaped stimulus surrounding the location of the central stimulus (ring width 1.4°), positioned 1.2° outside the central stimulus. Using this localizer for ROI selection yielded similar results (data not shown). We used the pRF-based ROI definition, because this stimulus ranged until the edge of the screen, whereas the center-surround stimulus did not. Hence, the pRF-based ROI provided us with a far periphery sub-region of V1 that corresponds to eccentricities larger than the ones that can be mapped out with our visual stimulation equipment.

Pupillometry data analysis

Preprocessing of pupil data

Eye tracking data was analyzed using custom-made Python and Matlab (MathWorks, Natick, MA, USA) software. Periods of blinks were detected using the manufacturer's standard algorithms with default settings. Blinks and periods of missing data were removed by linear interpolation of values measured just before and after each identified blink (interpolation time window, from 0.1 s before until 0.1 s after blink). The pupil data

was bandpass-filtered (passband 0.02 – 4 Hz, 2nd order Butterworth filter). Finally, we down-sampled the data to 20 Hz to make the deconvolution analysis computationally feasible (see next section).

Event-related pupil responses time-locked to perceptual reports

To obtain time courses for the pupil responses around perceptual reports we implemented the same deconvolution analysis as described above for the fMRI data. Time series of raw pupil diameter responses of each run were Z-scored and then concatenated across runs and sessions within each subject. For MIB and Replay, we estimated 120 parameters, corresponding to 1 s before report until 5 s after report. We simultaneously estimated blink event time courses as events of no interest. We baseline-corrected the resulting pupil response time courses for each subject by subtracting the average response in the interval from 1 s to 0.5 s before report from the complete time course before computing the average and SEM over subjects (Figure 2B).

Classification of high and low pupil dilation trials

We used a GLM to obtain a scalar measure of the amplitude of pupil responses around single perceptual reports. In this GLM, we modeled each trial as a separate regressor. We used as a kernel the deconvolved pupil response time course (computed as described above) collapsed over both disappearance and re-appearance switch reports. This kernel was then convolved with the time course of the corresponding individual perceptual switch events (i.e., a vector of 0's with a 1 at the time point of the switch) to yield the single-trial regressors that were entered in the design matrix. Blink time stamps were convolved with the deconvolved blink response function (computed as described in the previous section) and added as a regressor of no interest. The beta weights estimated in the linear regression were classified as either of high or low pupil amplitude by a median split, separately within each type of perceptual report (disappearance and reappearance). Figure 2 plots the report-locked pupil response time courses, separately for the trials classified as high vs. low pupil dilation by our GLM procedure, validating the procedure.

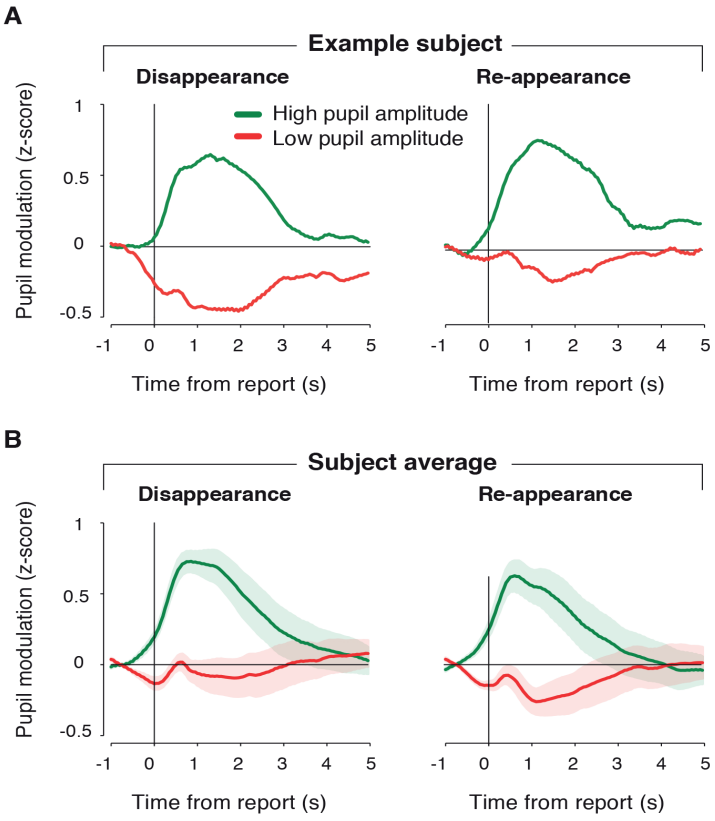

Figure 2 | Deconvolved time courses of pupil diameter modulation around perceptual reports

Deconvolved pupil modulation time courses classified into high and low amplitude by a median split of single trial estimates of the pupil dilation amplitude around perceptual reports. Left panels, MIB disappearance; right panel, MIB re-appearance. **A.** Example subject. **B.** Group average. Shaded areas, s.e.m. across subjects.

RESULTS

Nine healthy subjects reported their alternating perception of the target stimulus during MIB (Figure 1A, left panel) and its Replay (Figure 1B) by pressing and holding one of two response buttons (Figure 1C) while whole-brain fMRI-activity and pupil diameter were simultaneously recorded. During Replay, subjects reported the physical replay of previously reported target disappearances and re-appearances. We used a Gabor patch as the target to ensure that the overall stimulus luminance remained constant around targets offsets and onsets during the Replay condition. This was intended to minimize, as

much as possible, the effect of pupillary response due to subjective or physical stimulus changes during the perceptual switches (see Kloosterman et al. (2015b) for a similar procedure). As typically observed in bistable illusions (Leopold and Logothetis, 1999; Donner et al., 2008; Kloosterman et al., 2014), the durations of MIB target disappearances and re-appearances varied widely, following an asymmetric distribution (Figure 1D).

fMRI-activity in V1 periphery reflects contents of perceptual reports

To isolate report-related top-down modulations in visual cortex from (spontaneous or stimulus-evoked) modulations of stimulus responses in V1 (Donner et al., 2008, 2013), we focused on a far-periphery V1 sub-region that was far beyond those stimulated by any part (target or mask) of the MIB stimulus. In what follows, we refer to this region as "V1 periphery" (Figure 3A). As previously reported (Donner et al., 2008), fMRI-activity in this region decreased around target disappearance reports and increased around target re-appearance during MIB (Figure 3A). We split the time courses of the report-triggered modulations into early (0 to 5 s with respect to report) and late (5 to 10 s) intervals and averaged the modulation within these intervals (see bar graphs on the right of panels in Figures 3B and 3C). We chose these intervals based on a previous MIB fMRI study that showed the strongest percept-specific response modulation in the late, compared to the early interval (Donner et al., 2008). The difference between disappearance and re-appearance was significant across both intervals (early, $p = 0.008$; late, $p = 0.001$, two-sided permutation test). Accordingly, a two-way ANOVA with factors interval (early vs. late) and switch type (disappearance vs. re-appearance) showed a main effect of switch type ($F_{1,8} = 17.5$, $p = 0.003$,). There was no main effect of time interval on the modulation ($F_{1,8} = 0.8$, $p = 0.41$), but a trend towards an interaction ($F_{1,8} = 4.4$, $p = 0.07$), suggesting that the modulation indeed more strongly reflected perceptual content in the late interval.

As expected based on earlier results (Donner et al., 2008), we also observed an activity decrease during reports of physical target disappearances in the Replay condition, indicating that this modulation was not related to any process that causes the target to perceptually disappear during the illusion (Figure 3C). In contrast to this previous study, however, there was no significant modulation around reports of target onset (main effects of interval and event type $F1,8 = 1.1$, $p = 0.33$ and $F1,8 = 1.3$, $p = 0.28$, respectively, interaction $F1,8 = 0.294$, $p = 0.6$) (Figure 3C). Taken together, although the periphery

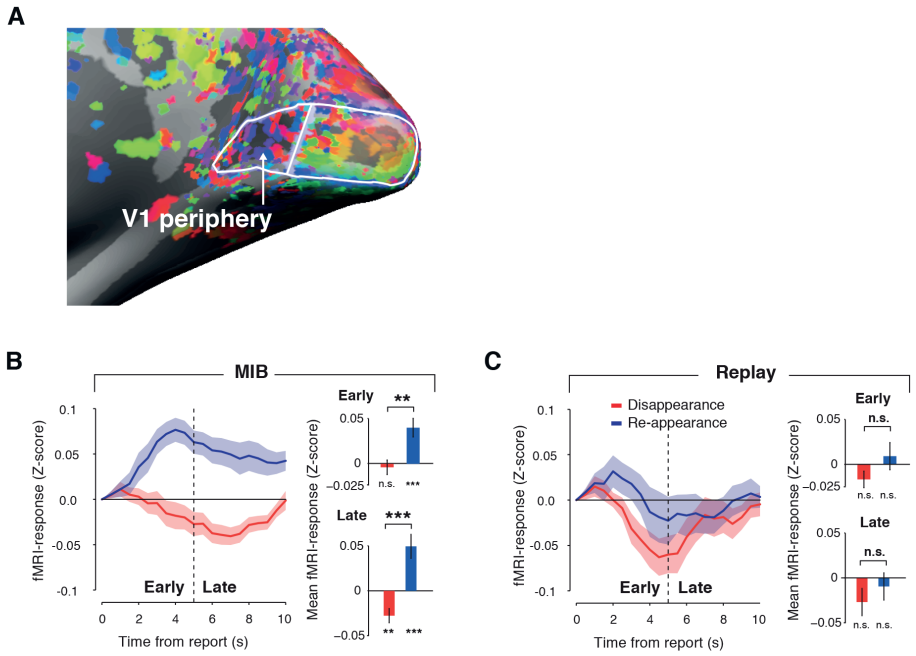

Figure 3 | fMRI activity in V1 periphery reflects content of perceptual reports

A. Region of interest (ROI) in V1 representing the periphery of the visual field. ROI was determined by both a localizer stimulus and anatomical landmarks (see *Materials and Methods*) **B.** Time courses of fMRI-activity modulation in V1 periphery following MIB target disappearance and re-appearance report. Dotted vertical line, border between early and late time intervals with respect to report. Bar graph insets, mean fMRI modulation in the early and late intervals. Shaded areas, s.e.m. across subjects. **C.** Corresponding time courses for Replay.

of V1 was not processing any component of the MIB stimulus, its activity during MIB, but not Replay, robustly reflected the type of perceptual switch that subjects reported. In particular, target disappearance reports were associated with widespread activity suppression during both MIB and Replay, regardless of whether the target disappearance was illusory or due to physical target offset.

Cortex-wide distribution of report-related fMRI modulations

We also assessed the detailed spatial distribution of the top-down signal in visual cortex as well as of its co-modulations in other brain regions (Figure 4, Table 1). This showed that the report-related opposite modulation of fMRI activity in visual cortex was largely homogenous throughout the midline within V1 and neighboring cortex. We also found

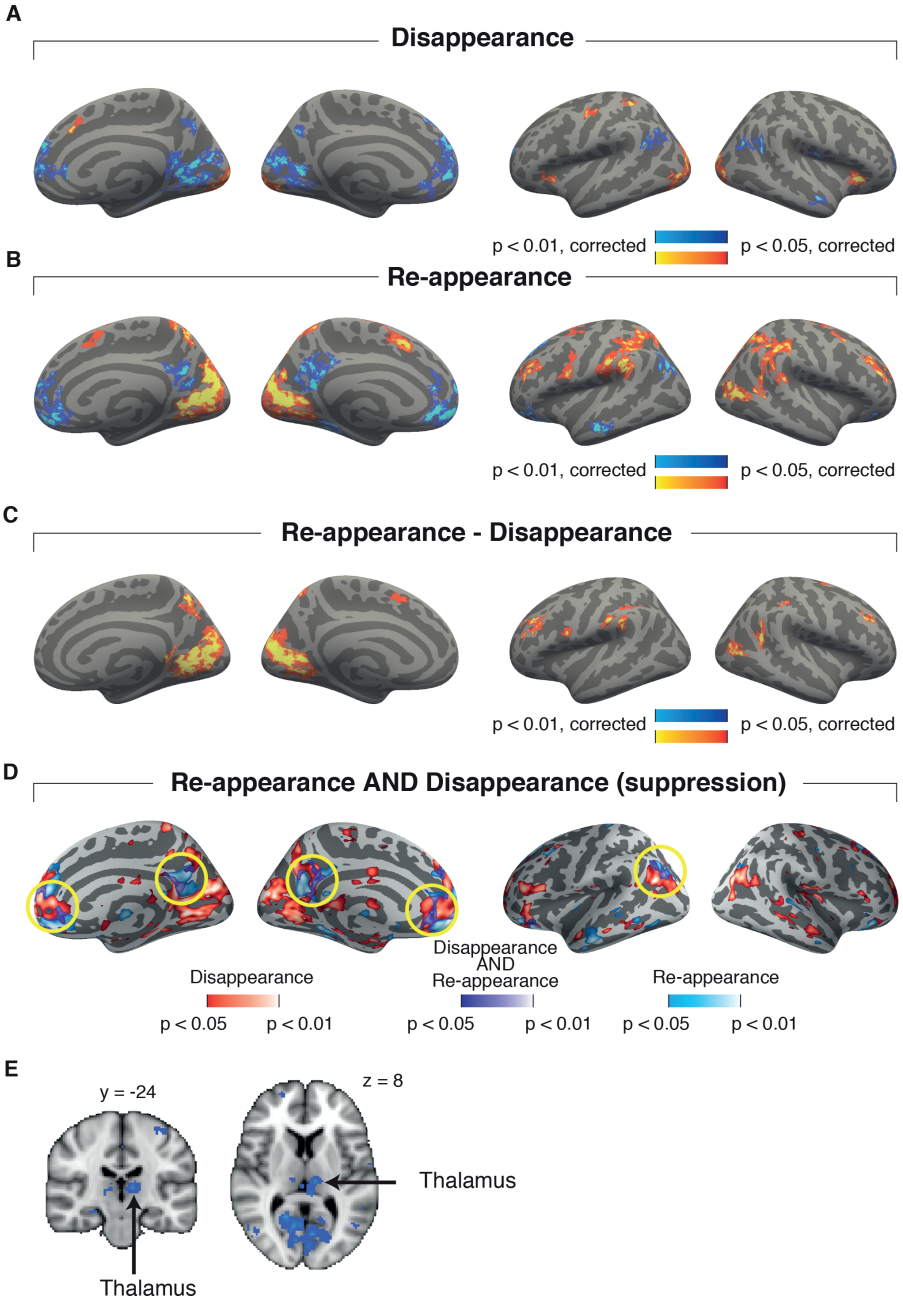
A
Disappearance
p < 0.01, corrected
p < 0.05, corrected
B
Re-appearance
p < 0.01, corrected
p < 0.05, corrected
C
Re-appearance - Disappearance
p < 0.01, corrected
p < 0.05, corrected
D
Re-appearance AND Disappearance (suppression)
Disappearance
p < 0.05
p < 0.01
Disappearance
AND
Re-appearance
p < 0.05
p < 0.01
Re-appearance
p < 0.05
p < 0.01
E
y = -24
Thalamus
z = 8
Thalamus

Figure 4 | Distributions of fMRI activity across the cerebral cortex during MIB and Replay

Flattened cortical surface maps showing significant activity around perceptual reports with respect to baseline. Maps are corrected for comparisons by cluster-based permutation testing across subjects (N = 9 subjects). Left two panels, medial views of the left and right hemispheres; Right two panels, corresponding lateral views. **A.** Disappearance **B.** Re-appearance **C.** Re-appearance – disappearance difference. **D.** Overlay of negative modulation during disappearance and re-appearance. Yellow circles highlight overlapping (purple) regions. E. Cross-section showing suppression of fMRI activity in the thalamus.

suppression of fMRI activity in the frontal midline, including parts of anterior cingulate cortex (ACC), during both disappearance and re-appearance (Figure 4A and B). Parietal and lateral frontal regions showed increased activity during re-appearance (Figure 4B), but not disappearance (Figure 4A). Subtracting the disappearance and re-appearance activation maps revealed the content-specific modulation in visual cortex (Figure 4C). A conjunction analysis of these two maps showed overlap in the midline of V1 and parietal cortex and ACC (purple areas in Figure 4D, outlined by yellow circles). In addition, we observed a suppression of fMRI-activity in the thalamus around disappearance (Figure 4E), consistent with electrophysiological measurements in monkeys showing that the thalamus reflects perceptual suppression (Wilke et al., 2009). Brain-wide fMRI-activity was less pronounced during disappearance in the Replay condition, but the same suppression in peripheral visual cortex was present (data not shown). Tables 1-4 list all activated regions during MIB and Replay target disappearance and re-appearance. In sum, a number of brain regions, including those located in the frontal midline, showed a modulation during the perceptual reports.

Phasic pupil dilation around perceptual decisions is linked to fMRI-activity in V1 periphery

Next, we wondered to what extent the modulation of fMRI activity around perceptual reports is linked to phasic activation of neuromodulatory brainstem systems. Phasic dilation of the pupil indexes the activity of these systems, most notably the LC-NA system (Aston-Jones and Cohen, 2005; Murphy et al., 2014). The ACC, which shows a modulation of activity during both MIB disappearance and re-appearance (Figure 4), has been proposed to control the activation of the LC-NA system (Aston-Jones and Cohen, 2005). We therefore estimated the amplitude of single trial pupil dilation responses, classified each trial as either of high or low pupil amplitude (Figure 2) and assessed the fMRI-activity in both classes.

The time course and amplitude of the top-down modulation in V1 around target disappearance was linked to the amplitude of the concomitant pupil response. In the early interval, there was stronger suppression for the low than high pupil trials, whereas the opposite effect occurred in the late interval (Figure 5). Around target re-appearance, the modulation was also slightly more positive for high than for low pupil trials, but there was no difference in the late interval. A three-way ANOVA with factors interval (early vs. late), pupil amplitude (low vs. high) and switch type (disappearance vs. re-appearance) revealed a significant interaction between these three factors ($F_{1,8} = 7.9$, $p = 0.02$). This interaction highlights the specificity of the link between pupil size and fMRI-activity for MIB target disappearance, with opposite effects during the early and late intervals (Figure 5A and 5B). None of the other main or interaction effects was significant (interval, $F_{1,8} = 0.77$, $p = 0.41$; pupil, $F_{1,8} = 0.61$, $p = 0.46$; interval x pupil, $F_{1,8} = 2.37$, $p = 0.162$; pupil x switch type, $F_{1,8} = 0.004$, $p = 0.95$, interval x switch type ($F_{1,8} = 4.4$, $p = 0.07$), besides the main effect of perceptual switch type reported above.

Interestingly, the suppression of fMRI-modulation in the ACC around target disappearance showed a similar dependence on pupil amplitude (Figure 5C). Whereas the suppression was stronger for low than high pupil trials in the early interval, the opposite was true for the late interval (two-way interaction between pupil and interval, F1,8 = 4.49, p = 0.07) (Figure 5D). In contrast to V1 periphery, the modulation was negative for both disappearance and re-appearance in ACC, so there was no three-way interaction between switch type, pupil amplitude and interval (F1,8 = 1.8, p = 0.21), but the two-way interaction between switch type and interval did reach significance (F1,8 = 7.02, p = 0.03), indicating that the suppression in the early interval was stronger for disappearance than re-appearance. Taken together, these results suggest that pupil-linked neuromodulatory systems are involved in the global modulation of fMRI-activity around target disappearance report.

DISCUSSION

Several previous studies have reported a new type of top-down modulation of population activity in early visual cortex during elementary perceptual tasks. These modulations were largely decoupled (in space and/or time) from cortical stimulus responses but closely linked to behaviorally relevant events (Jack et al., 2006; Wilke et al., 2006; Donner et al.,

Table 1. Main effect of MIB disappearance versus baseline

Area	Hemi-sphere	Number of Voxels	Peak Value (Z)	MAX X (mm)	MAX Y (mm)	MAX Z (mm)
Lingual Gyrus	**RH**	**7310.0**	**6.45**	**12.0**	**-86.0**	**-6.0**
Insular Cortex	**RH**	**1692.0**	**5.59**	**32.0**	**24.0**	**-2.0**
Left Putamen	**LH**	**1192.0**	**4.85**	**-24.0**	**-2.0**	**4.0**
Superior Parietal Lobule	**LH**	**374.0**	**3.62**	**-30.0**	**-56.0**	**60.0**
Precentral Gyrus	**LH**	**332.0**	**5.12**	**-38.0**	**-14.0**	**44.0**
Supplementary Motor Cortex	RH	220.0	4.27	4.0	6.0	58.0
Paracingulate Gyrus	RH	218.0	4.14	8.0	26.0	36.0
Precentral Gyrus	LH	182.0	4.01	-20.0	-28.0	68.0
Supramarginal Gyrus	RH	180.0	3.65	38.0	-38.0	38.0
Lateral Occipital Cortex	RH	168.0	3.61	32.0	-58.0	66.0
Insular Cortex	LH	150.0	4.2	-32.0	24.0	4.0
Supramarginal Gyrus	RH	137.0	3.65	60.0	-20.0	28.0
Precentral Gyrus	RH	134.0	2.91	50.0	8.0	22.0
Brain-Stem	RH	108.0	3.65	10.0	-28.0	-14.0
Frontal Pole	RH	93.0	3.28	28.0	36.0	26.0
Left Cerebral White Matter	LH	84.0	3.39	-4.0	-18.0	-12.0
Precentral Gyrus	RH	75.0	3.03	14.0	-24.0	42.0
Precentral Gyrus	RH	69.0	3.39	38.0	-8.0	44.0
Supramarginal Gyrus	RH	62.0	4.4	52.0	-36.0	50.0
Superior Frontal Gyrus	LH	55.0	3.31	-22.0	0.0	52.0
Frontal Pole	LH	54.0	3.06	-38.0	50.0	6.0

Table 2. Main effect of MIB reappearance versus baseline

Area	Hemi-sphere	Number of Voxels	Peak Value (Z)	MAX X (mm)	MAX Y (mm)	MAX Z (mm)
Lingual Gyrus	**RH**	**35746.0**	**7.93**	**4.0**	**-82.0**	**-6.0**
Frontal Pole	**LH**	**490.0**	**4.17**	**-28.0**	**38.0**	**30.0**
Frontal Pole	RH	388.0	5.78	42.0	38.0	34.0
Insular Cortex	LH	96.0	3.97	-30.0	14.0	10.0
Frontal Pole	RH	59.0	2.94	28.0	42.0	4.0
Insular Cortex	RH	54.0	2.81	30.0	16.0	8.0
Insular Cortex	RH	54.0	3.61	38.0	-6.0	-6.0
Cingulate Gyrus	RH	50.0	3.33	8.0	22.0	32.0

Table 3. Main effect Replay disappearance versus baseline

Area	Hemi-sphere	Number of Voxels	Peak Value (Z)	MAX X (mm)	MAX Y (mm)	MAX Z (mm)
Occipital Pole	RH	969.0	5.58	18.0	-96.0	0.0
Occipital Pole	LH	711.0	3.96	-16.0	-94.0	4.0
Superior Parietal Lobule	RH	427.0	3.32	26.0	-52.0	58.0
Inferior Frontal Gyrus	LH	227.0	2.89	-54.0	22.0	-6.0
Frontal Pole	RH	223.0	3.36	52.0	38.0	-2.0
Middle Temporal Gyrus	LH	179.0	3.14	-62.0	-50.0	-10.0
Superior Frontal Gyrus	LH	178.0	3.72	0.0	32.0	44.0
Middle Frontal Gyrus	RH	144.0	2.54	52.0	22.0	42.0
Angular Gyrus	LH	128.0	3.28	-48.0	-52.0	50.0
Lateral Occipital Cortex	RH	124.0	3.08	56.0	-72.0	-14.0
Superior Parietal Lobule	LH	108.0	2.66	-24.0	-48.0	36.0
Inferior Temporal Gyrus	RH	103.0	3.67	58.0	-34.0	-16.0
Paracingulate Gyrus	LH	64.0	3.18	-8.0	40.0	28.0
Lateral Occipital Cortex	RH	63.0	2.92	24.0	-78.0	44.0
Inferior Frontal Gyrus	RH	56.0	2.7	54.0	30.0	18.0

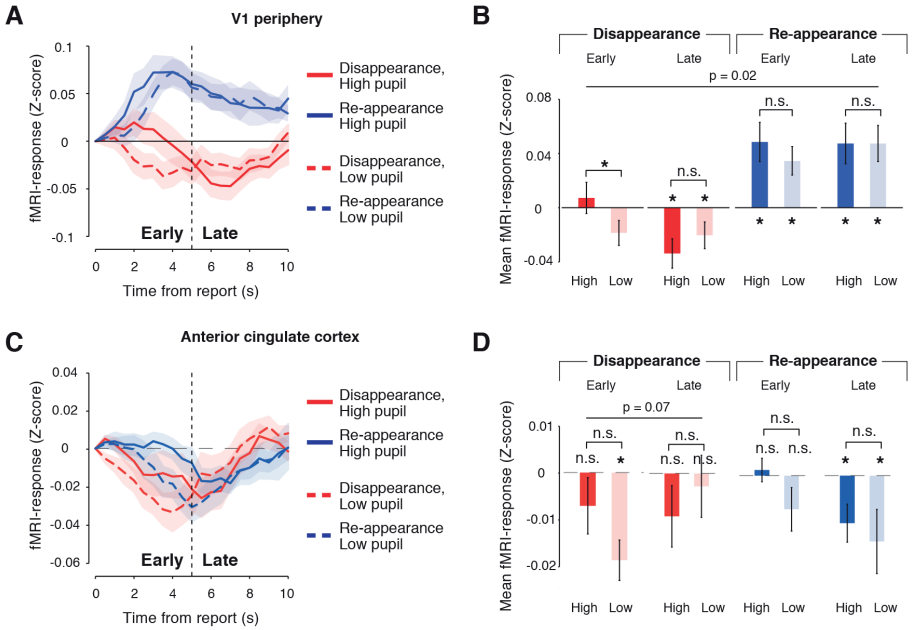

Figure 5 | fMRI activity in V1 periphery and ACC around target disappearance is linked to strength of concomitant pupil amplitude

A. Time courses of modulation of fMRI-activity in V1 periphery following perceptual reports, separately for low and high pupil trials. Conventions as in Figure 3. **B.** Corresponding bar graphs of mean modulation in early and late intervals. Left panels, target disappearance; right panels, re-appearance. **C., D.** Corresponding modulations in anterior cingulate cortex (ACC).

Table 4. Main effect of Replay reappearance versus baseline

Area	Hemi-sphere	Number of Voxels	Peak Value (Z)	MAX X (mm)	MAX Y (mm)	MAX Z (mm)
Precuneous Cortex	**RH**	**5971.0**	**5.16**	**8.0**	**-54.0**	**74.0**
Cuneal Cortex	**LH**	**877.0**	**3.77**	**-18.0**	**-80.0**	**14.0**
Supplementary Motor Cortex	**RH**	**875.0**	**4.71**	**2.0**	**8.0**	**58.0**
Precentral Gyrus	**LH**	**839.0**	**4.24**	**-32.0**	**-6.0**	**64.0**
Occipital Fusiform Gyrus	**RH**	**669.0**	**3.92**	**26.0**	**-70.0**	**-22.0**
Frontal Pole	**RH**	**301.0**	**3.27**	**36.0**	**40.0**	**32.0**
Lateral Occipital Cortex	LH	246.0	3.98	-48.0	-72.0	8.0
Angular Gyrus	LH	228.0	2.94	-50.0	-52.0	16.0
No label found!	RH	227.0	3.82	38.0	-52.0	-28.0
Lingual Gyrus	LH	223.0	3.42	-4.0	-46.0	-4.0
Left Pallidum	LH	148.0	4.52	-18.0	-6.0	-6.0
Supramarginal Gyrus	LH	145.0	3.17	-36.0	-40.0	36.0
Left Thalamus	LH	110.0	3.67	-10.0	-22.0	12.0
Right Putamen	RH	91.0	2.99	26.0	-2.0	-4.0
Right Thalamus	RH	77.0	2.86	6.0	-20.0	8.0
Left Cerebral White Matter	LH	72.0	3.01	-36.0	-34.0	2.0
Postcentral Gyrus	LH	71.0	2.73	-40.0	-20.0	30.0
Precuneous Cortex	LH	69.0	2.93	-14.0	-48.0	20.0
Frontal Pole	LH	65.0	2.64	-38.0	50.0	18.0
Cingulate Gyrus	RH	61.0	2.64	14.0	-22.0	38.0
Precuneous Cortex	RH	54.0	2.34	14.0	-58.0	36.0
Postcentral Gyrus	LH	51.0	3.37	-60.0	-20.0	20.0
Middle Temporal Gyrus	LH	51.0	2.85	-56.0	-20.0	-14.0

2008; Hsieh and Tse, 2009; Sirotin and Das, 2009; Cardoso et al., 2012; de-Wit et al., 2012; Swallow et al., 2012; Donner et al., 2013; Choe et al., 2014). Specifically, previous studies have discovered a widespread, decision-related suppression of fMRI-activity and beta-band power in human V1 during report of the (illusory or veridical) disappearance of a salient visual target (Donner et al., 2008; Siegel et al., 2011; Donner et al., 2013; Kloosterman et al., 2014). Here, we replicate this finding for the MIB condition and map out the spatial distribution of this modulation across occipital cortex as well as in other brain regions, in particular frontal midline structures. We further show that part of the amplitude and time course of the modulation during disappearance is linked to the amplitude of the associated pupil dilation.

The fMRI-suppression following MIB target disappearance was stronger for low than high pupil trials in the early interval, followed by stronger modulation for high pupil trials in the late interval. This finding suggests that at least two pupil-linked, but functionally distinct, neural processes dominated the modulation in each interval. However, statistical power of our small data set of nine subjects was low, precluding firm conclusions about the strength of a link between fMRI-activity and pupil dilation.

An important aspect of our findings is that the larger part of the negative modulation in V1 periphery remains present in low pupil trials during MIB disappearance, in which only a small phasic pupil response occurs. Moreover, the positive modulation around re-appearance is identical for low and high pupil trials (Figures 5A and 5B). These findings indicate that other factors not linked to pupil dilation also affect fMRI-activity around the switches. At least two such factors could be at play. First, slow fluctuations in attention level that presumably occur throughout the continuous presentation of the MIB stimulus might also affect the trial-to-trial modulation of fMRI-activity. Second, fMRI-activity in the central, stimulated parts of V1 showed strong positive modulations around the perceptual switches in our study, which possibly resulted in suppression of fMRI-activity in the periphery of V1 due to reduced blood flow to this region (Woolsey et al., 1996). Taken together, our results suggest that a portion of the modulation during disappearance is linked to pupil dilation, but it remains to be seen which other, non-pupil-linked factors underlie the modulation.

One process underlying the stronger late suppression for high pupil trials around target disappearance could be the hypothesized transient release of modulatory

neurotransmitters in the cortex around perceptual switches, which is tracked by phasic pupil dilation and which change the internal state of the visual cortex. The LC-NA system is one candidate system (Aston-Jones and Cohen, 2005; Murphy et al., 2014), but other pupil-linked neuromodulatory systems (e.g. the cholinergic system) might be at play as well. The involvement of the LC-NA system predicts a phasic activation around the switches of the LC, which is a small nucleus in the brainstem. Investigating this region's activity is hampered by physiological noise due to heart rate and respiration. We corrected for these artifacts in our data by using the RETROICOR method in our preprocessing (Glover et al., 2000) (see *Materials and Methods*). We next plan to examine the activity in the brainstem on non-smoothed data to further investigate the role of the LC-NA system in the decision-related modulation.

Several factors other than pupil-linked neuromodulation might contribute to the observed relationship between pupil dilation and fMRI-activity. One process that could enhance modulation of fMRI-activity around both target disappearance and re-appearance is the transient increase in the amount of light hitting the visual cortex due to the concomitant dilation of the pupil around the switches (Figure 2) (Haynes et al., 2004; Kloosterman et al., 2015b). Specifically, this effect might underlie the stronger positive modulation in V1 periphery for high than low pupil trials in the early interval for both types of switches (Figure 5A). In line with this idea, the positive modulation in the early interval was more pronounced in the physically stimulated parts of V1 (data not shown). The lack of initial positive modulation in the ACC also speaks for this possibility, since it seems unlikely that this non-visual region would respond to a transient light increase. Another process possibly enhancing pupil-linked modulations in visual cortex could be a transient arousal around the switches due to the occurrence of a task-relevant event (Jack et al., 2006). Future work should address the relative contributions of these factors to modulation of fMRI-activity and pupil dilation.

The decision-related top-down modulation of fMRI-activity during MIB reflected the content of the perceptual report, with positive sign for re-appearance and negative sign for disappearance. This finding has been reported previously for both fMRI-activity (Donner et al., 2008) and neurophysiological activity (Kloosterman et al., 2014). The previous fMRI-study by Donner et al. (2008), however, found this perceptual content effect also in the Replay condition, whereas we currently only observe the negative modulation after Replay disappearance, but virtually no modulation around re-appearance. This suggests

that the modulation is related to a process that terminates illusory invisibility of the target. The difference might also be due to the increased size and flicker of the target during Replay.

The present study shows suppression of activity around target disappearance in the thalamus, in which similar perceptual modulations have been observed in monkeys (Wilke et al., 2009). Critically, we also show that the perceptual content effect is evident (and largely homogenous) across the visual field map of V1, reaching into the far periphery representation. Further, our current whole-brain analysis reveals that disappearance and re-appearance are also associated with considerably different activations beyond visual and motor cortex (the latter obviously being recruited for behavioral report in both conditions): Only re-appearance (not disappearance) exhibits the robust activation of posterior parietal and lateral prefrontal cortex that is commonly observed during perceptual switches in other bistable perceptual illusions (Knapen et al., 2011; Weilnhammer et al., 2013; Frassle et al., 2014). Notably, however, we find a transient suppression of activity in frontal midline structures, which is largely overlapping between target disappearance and re-appearance reports, and which has so far, not been reported.

Taken together, our study adds initial support to the idea that fast and widespread changes in the internal state of the cortex occur around perceptual decisions, possibly mediated by pupil-linked neuromodulatory systems (Aston-Jones and Cohen, 2005; Gilbert and Sigman, 2007; Parikh et al., 2007). These state changes likely alter the processing of subsequent sensory information, for example by stabilizing the newly selected interpretation of ambiguous input (Kloosterman et al., 2014). However, significant modulation remains present in trials with only small pupil dilation, indicating that non-pupil-linked processes underlie the larger part of the modulation of fMRI-activity. Future work should further investigate the role of the LC-NA and the Ach systems in these state changes, for example by examining LC activity around perceptual decisions (Murphy et al., 2014). Moreover, it remains to be seen which other factors that are not linked to pupil dilation could explain the modulation of fMRI activity.

ACKNOWLEDGEMENTS

fMRI-scanning costs were in part funded by the Amsterdam Brain Imaging Platform (ABIP), Amsterdam, The Netherlands. V.A.F.L. was supported by an advanced investigator grant from the ERC. The authors declare no conflict of interest.

Chapter 7

Summary and Discussion

The internal state of our brain changes constantly, affecting the way in which the cerebral cortex processes information. Changes of cortical state have traditionally been associated with slow and largely automatic fluctuations of wakefulness and arousal, but they can also occur on a rapid (sub-second to second) time scale and be triggered in a top-down fashion by cognitive acts – for example, detecting perceptual changes in a visual stimulus. In this thesis, I aimed to detail the neurophysiological properties of fast changes in cortical state and their consequences for perception.

Chapter 2 reports an MEG study investigating modulations in cortical population activity during perceptual changes in the MIB bistable visual illusion and their consequences for perception. My colleagues and I observed a transient, retinotopically widespread modulation of beta (12-30 Hz) frequency power over visual cortex that is closely linked to the time of subjects' behavioral report of the target disappearance. We show that this beta-modulation is a top-down signal, in the sense that it is decoupled from both the physical stimulus properties and the motor response, but contingent on cognitive factors such as behavioral relevance of perceptual changes. Critically, the modulation amplitude predicts the duration of the subsequent illusory target disappearance. Taken together, these findings suggest that the transformation of the perceptual change into a report triggers a top-down mechanism that stabilizes the newly selected perceptual interpretation.

Chapter 3 further pinpoints the factors driving the beta-band modulation by demonstrating that the beta suppression over visual cortex occurs not only when subjects promptly report the target disappearances by button press, but also when they silently count them. This finding establishes behavioral relevance as a key factor underlying the top-down signal and indicates that the beta modulation is not due to the motor act used to report switches. **Chapter 4** provides further psychophysical support for a stabilization mechanism in bistable perception that prevents immediate return transitions by showing that the typically observed lack of very brief percepts in bistable perception is not due to an inability to report these short-lived percepts.

Due to their abundant projections to the cerebral cortex, neuromodulatory centers in the brainstem are able to control the global brain state. The activity of these brainstem centers can be measured non-invasively in the phasic dilation of the pupil. We reasoned that if these systems exert such an influence around the time of perceptual decisions,

then there should be pupil dilation during the perceptual switches. The pupillometry study reported in **Chapter 5** shows that the pupil indeed transiently dilates during perceptual switches, even in the absence of immediate motor reports. Importantly, we report that the pupil responds differently depending on the type of perceptual switch that is reported during MIB, with stronger dilation following target disappearance than re-appearance report. This finding is consistent with the modulation of fMRI- and MEG-activity around perceptual reports that also reflects perceptual content during MIB and Replay, suggesting that pupil dilation indeed provides an index of fast changes in brain state. In addition, this pupil response scales with the level of surprise about perceptual switches, suggesting that surprise about the timing of perceptual events also affects the internal state of the brain.

Finally, in **Chapter 6** we directly correlate this index of brain state to modulations of neural population activity during the perceptual switches. The chapter reports concurrent pupillometry and whole-brain fMRI to characterize the complete cortical and subcortical distribution of activity modulations during perceptual switches in MIB separately for trials associated with large and small pupil dilation. We find modulations of fMRI activity throughout early visual, parietal and anterior cingulate cortices (ACC) around the perceptual events. While visual and parietal cortex are key players in the MIB illusion, ACC is known to send top-down inputs to neuromodulatory brainstem centers such as the locus coeruleus (LC). The stronger suppression of fMRI-activity in visual cortex during MIB disappearance trials with larger phasic pupil dilation provides a new clue for a link between neuromodulatory systems controlling pupil diameter and top-down signals in the brain.

Despite this finding, this study also highlights that the majority of the fMRI-activity modulation in our peripheral region of V1 shows no relationship with the concomitant phasic dilation of the pupil. At least two factors other than pupil-linked neuromodulation could be at play. First, slow fluctuations in attention level that presumably occur throughout the continuous presentation of the MIB stimulus might also affect the trial-to-trial modulation of fMRI-activity. Second, fMRI-activity in the central, stimulated parts of V1 showed strong positive modulations around the perceptual switches in our study, which possibly resulted in suppression of fMRI-activity in the periphery of V1 due to reduced blood flow to this region (Woolsey et al., 1996).

Taken together, the work presented in this thesis establishes the existence of a novel type of top-down signal in visual cortex around perceptual decisions, which has a profound influence on neural activity and the dynamics of perception. In this last chapter, I will elaborate on the possible sources of the top-down signal, focusing on phasic neuromodulation. To accommodate this set of results within a currently prevalent theoretical framework, I will provide an extension of the standard class of models of bistable perception (see Chapter 1) that modulates the activity of stimulus-specific populations of neurons following the commitment to a new percept. Further, I will review existing evidence for top-down signals during other perceptual tasks, speculate about their role in higher-level cognitive tasks and psychopathology and posit research questions to be addressed in future studies.

The origin of fast changes in brain state

What is the source of the top-down signals observed in visual cortex? The signal might originate from higher cortical areas (Nienborg and Cumming, 2009; Siegel et al., 2012), the thalamus (Wilke et al., 2009), neuromodulatory brainstem centers (Aston-Jones and Cohen, 2005; Parikh et al., 2007; Einhauser et al., 2008; Hupe et al., 2009; de Gee et al., 2014), or from a combination of cortical feedback and neuromodulation (Noudoost and Moore, 2011).

A number of characteristics of the top-down signal reported in this thesis suggest that phasic neuromodulation might be the key underlying mechanism. Neuromodulatory brainstem systems, such as the noradrenergic (NA) locus coeruleus (LC) and the cholinergic (Ach) basal forebrain systems, also exhibit transient activity during perceptual reports, which can reflect the content of the report, both during bistable perceptual tasks (Einhauser et al., 2008; Hupe et al., 2009) and detection tasks (Aston-Jones and Cohen, 2005; Parikh et al., 2007; de Gee et al., 2014). In addition, these brainstem systems have strong anatomical connections with the cerebral cortex (Aston-Jones and Cohen, 2005) (Figure 1). Further, beta-band oscillations, as observed in the MEG around perceptual switches in Chapters 2 and 3, are often associated with attentional demands and cognitive tasks (Engel and Fries, 2010; Donner and Siegel, 2011). Moreover, modulations of beta-band power in visual cortex during visual stimulation have been suggested to index changes in neuromodulatory state (Belitski et al., 2008; Donner and Siegel, 2011). Neuromodulatory brainstem systems might be in an ideal position to stabilize bistable

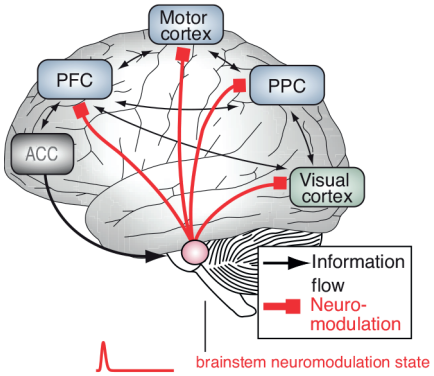

Figure 1 | Neuromodulatory brain stem systems affect cortical decision processes

A perceptual decision, for example to report a switch in perception during MIB, involves a long-range network of brain regions. Following the decision, neuromodulatory systems in the brain stem activate transiently due to signals sent from ACC (shown here on the outside of the brain for illustration purposes). These brainstem systems, in turn, send diffuse projections of neuromodulator to the cerebral cortex, thereby changing the global, internal state of the brain. ACC, anterior cingulate cortex; PFC, prefrontal cortex; PPC, posterior parietal cortex.

perceptual dynamics, because they can dynamically alter key cortical circuit parameters in profound ways. In particular, neuromodulators suppress cortical variability (Polack et al., 2013) and may amplify inhibitory interactions in cortical circuits (Haider et al., 2012). Finally, given that the anterior cingulate cortex (ACC) is the hypothesized source of decision-related signals in the LC (Aston-Jones and Cohen, 2005), the finding of fMRI-activation in ACC around perceptual reports during MIB (Chapter 6) also fits well with this explanation.

In spite of this indirect evidence, more research is needed to directly test the role of neuromodulatory systems in the top-down modulation. One fruitful approach could be to manipulate central NA or Ach levels pharmacologically in humans during bistability or other perceptual decision making tasks while measuring neural activity with MEG. If these systems play such a role, then amplifying their level of activity would result in both larger pupil dilation as well as stronger decision-related beta-band modulation in visual cortex. Additionally, by comparing the variability of neural activity during drug and placebo conditions (for instance by computing the trial-to-trial variance), this approach could reveal whether increased neuromodulator levels are related to suppression of cortical variability.

A simple computational model of bistable perceptual stabilization

How can a transient top-down signal in visual cortex stabilize a perceptual illusion? As explained in Chapter 2, the movement of a “percept variable” (green ball in Figure 2A) (Moreno-Bote et al., 2007; Braun and Mattia, 2010) across an energy landscape with

two valleys (basins of attraction; in the case of MIB corresponding to target visible and invisible) provides a useful metaphor for understanding this effect (Deco and Romo, 2008). In this scheme, the stabilizing state change can be conceived as an active force (red arrow) transiently deepening the valleys. Only if the sensory input is ambiguous and, consequently, the perceptual interpretation meta-stable (i.e., during MIB), does this transient state change culminate in a perceptual stabilization: the stronger the state change (i.e., the longer the red arrow) during a perceptual transition, the longer the subsequent perceptual illusion. During Replay, the physical removal of the target stimulus instantaneously alters the energy landscape, thus overriding the effect of the internal state change and precluding a link to percept duration.

By simulating an extension of one version of the current neural models of bistable perception (Noest et al., 2007) we established that this stabilization scheme during MIB could be implemented by transiently boosting, via feedback, the strength of mutual inhibition between stimulus-selective neural populations in visual cortex (Figure 2B, C). As explained in the Introduction, the standard model consists of two populations of neurons driven by distinct stimulus components (e.g. static target and moving mask). These populations are subject to slow decay in activity due to adaptation and compete with each other by mutual inhibition. The interaction between adaptation, noise, and mutual inhibition gives rise to spontaneous dominance transitions between the two populations. The dominance transitions are thought to underlie the perceptual switches.

We[1] extended this model by adding a third, modulatory neural population, which was driven by the dominance transitions in the two competing populations and, in turn, sent feedback to both competing populations (Figure 2B). The feedback was not selective for one of the competing visual populations (as would, for instance, be expected for top-down selective attention (Desimone and Duncan, 1995; Harris and Thiele, 2011), but equally impinged on both visual populations. Importantly, however, the feedback was temporally specific, peaking precisely at the time of the dominance transition (inset in Figure 2B). The feedback influence modulated the gain of the mutual inhibition between the two cortical populations, which, in turn, deepens the valleys in the energy landscape in Figure 2A. The phasic release of modulatory neurotransmitters such as noradrenaline (NA) or acetylcholine (Ach), could mediate such an effect (Aston-Jones and Cohen, 2005;

[1] The model extension was conceived and implemented by Tobias Donner and Tomas Knapen.

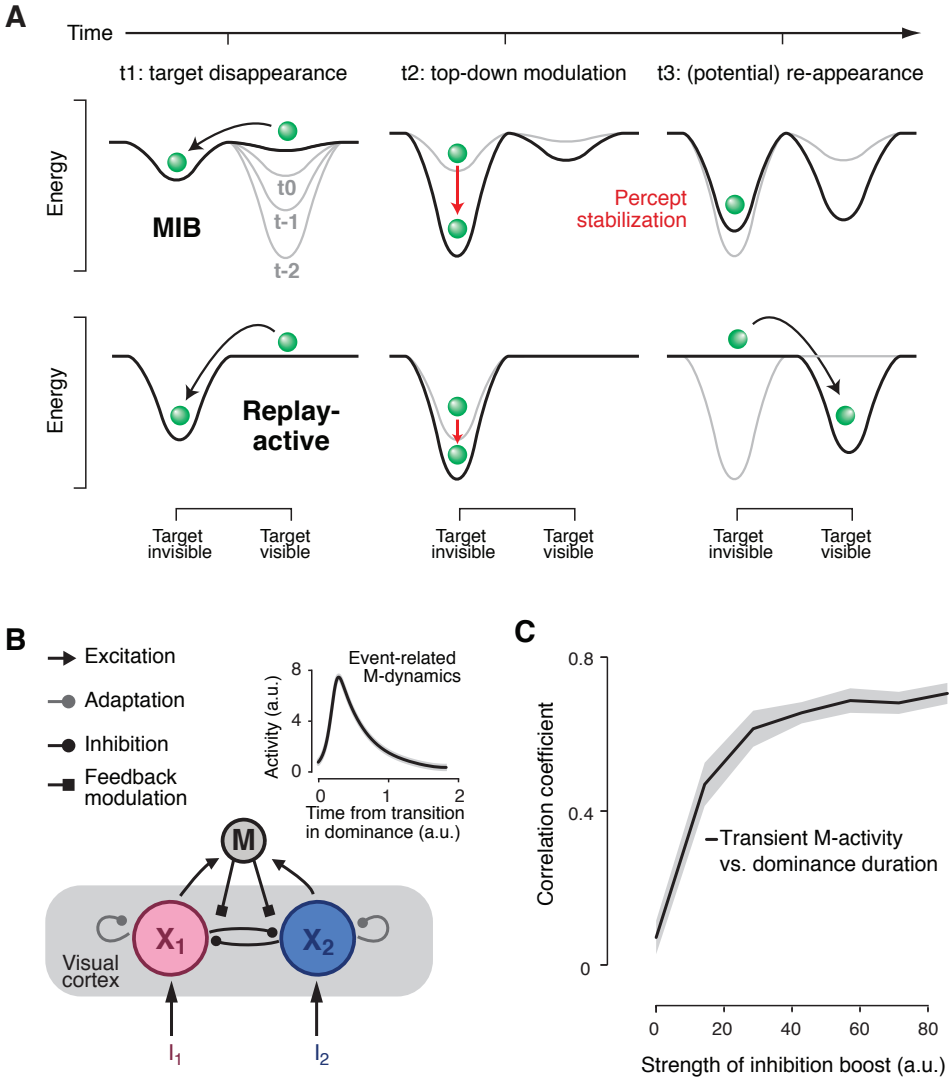

Figure 2 | Conceptual model of beta-power transient

A. Schematic of dynamical algorithm for cortical state change and perceptual stabilization. In both MIB (top) and Replay-active (bottom), the percept (green ball) is in the "target visible" valley. Adaption gradually flattens this valley before target disappearance (sequence: t_{-2}, t_{-1}, t_0). The ball then hops into the "target invisible" valley (perceptual switch, t_1). Behavioral report of this perceptual event induces a state change that deepens the target invisible valley (t_2, red arrows). This, in turn, stabilizes perception during MIB (t_3: top right): When the state change is strong, the percept variable is less likely to move back to the visible valley some time after the switch (t_3). By contrast, during Replay (t_3: bottom right), the physical target re-appearance alters the energy landscape (i.e., eliminates the target invisible valley), and thereby prevents the state change at t_2 from affecting the percept duration. **B.** Extension of the bistability model. Two neural populations (X_1 and X_2) are driven by distinct inputs (I_1, I_2), subject to slow adaptation dynamics, and compete via mutual inhibition. In our extension of this class of models, transients of X_1 and X_2 drive a third population (M), which sends non-specific modulatory feedback to the competing populations, boosting their mutual inhibition. Inset: Average time course of M-output, time-locked to switches in dominance between X_1 and X_2. **C.** Correlation between M-response during dominance transition and duration of subsequent dominance state across different strengths of the inhibition boost.

Einhauser et al., 2008; Sarter et al., 2009). Specifically, Polack et al. (2013) recently found that NA depolarized membrane potentials of neurons in mouse visual cortex during locomotion, thereby enhancing the gain (multiplicative transformation) of the V1 neurons.

Our simulation confirmed that the stronger the transient response of the "modulatory" (M) population during perceptual switches, the longer the subsequent dominance duration lasted. There was a robust, positive correlation between the strength of the transient M-response around the switch and the subsequent dominance duration (Figure 2C). The magnitude of this correlation increased monotonically with the strength of the relative contribution of the inhibition boosting effect to the overall mutual inhibition (see Supplement 1 for model details). Note that the activity of the modulatory population was positively correlated to the percept duration, whereas the report-related beta-band modulation in visual cortex observed in our MEG measurements in Chapter 1 was negatively correlated to the percept duration. One explanation for the opposite sign could be that the beta-band modulation in visual cortex did not reflect the modulatory population *per se* (which we assume is located in a brain region outside of visual cortex and shows an increase in activity, see *The origin of fast changes in brain state*), but rather its modulatory feedback effect on neural (dendritic) population activity in visual cortex (i.e., state change), as measured by MEG. Future work could investigate whether the possible brain regions containing modulatory populations, such as the LC or basal forebrain, indeed increase their activity around the decisions.

Although this model is consistent with an active role of phasic neuromodulation around perceptual switches, there are other possibilities. First, by simulating an alternative feedback model, we found that a global suppression of the input gain in visual cortex yielded similar results as the inhibition boost (data not shown). However, if reflecting global input suppression, the MEG power modulations during MIB disappearance should have been the converse of the stimulus-induced MEG response shown in Chapter 2 (Figure 1C) and Chapter 3 (Figure 1C). This would predict high-frequency suppression and low-frequency enhancement, in sharp contrast with the data (see e.g. Chapter 2, Figure 2D and Chapter 3, Figure 2A). Second, passive adaptation of the neurons representing the target stimulus could also have a stabilizing effect due to a prolonged suppression of this weakened population's activity by the competing pool of sensory neurons. Future studies could investigate whether adaptation alone could account for a perceptual stabilization

mechanism, for instance by testing whether subjects with stronger adaptation dynamics also show longer median bistable percept durations.

Concluding remarks

In this thesis, I have explored how a new and unexpected class of top-down signals shapes neural activity and perception in the human brain. These signals occur around perceptual decisions about the disappearance of a salient stimulus and seem to reflect the transformation of a perceptual change into a behavioral report. One possible underlying mechanism of these signals is a phasic activation of brainstem systems, which diffusely release neuromodulator across the brain around decisions about task-relevant perceptual changes, thereby changing its internal state.

The global (i.e. retinotopically non-specific) state change in visual cortex is likely a general phenomenon. Besides during MIB, functionally analogous modulations of fMRI activity have been observed in human early visual cortex around perceptual reports in various other bistable phenomena: bistable motion binding (de-Wit et al., 2012), plaids (N. Rubin, personal communication), 3D structure from motion, apparent motion, and binocular rivalry (unpublished observations from our lab), as well as during visual detection tasks (Nienborg and Cumming, 2009; Choe et al., 2014).

It has remained unknown which (if any (Sirotin and Das, 2009)) component of electrophysiological activity these global hemodynamic responses reflect, and how the underlying cortical state change affects perception. By characterizing the underlying patterns of electrophysiological population activity in visual cortex, this thesis reveals beta-band modulation as an index of internal state changes, in line with results from LFP recordings in monkey (Wilke et al., 2006; Belitski et al., 2008). Further, the work presented here establishes that the global state change around perceptual reports shapes the stability of bistable perceptual interpretations. Taken together, the thesis provides an initial understanding of this previously neglected class of signals in visual cortex. Future studies could test the scope of these top-down signals across other bistable illusions, such as binocular rivalry (Knapen et al., 2011), 3D structure-from-motion (Klink et al., 2012), or the Necker cube, as well as during non-perceptual decision tasks, such as economic or value-based decision-making.

The findings presented in this thesis have implications for the putative link between the fMRI-signal and neural oscillations, as measured here with MEG. During visual stimulation, both the fMRI-signal and oscillations in the high frequency (gamma) band increase (Niessing et al., 2005; Donner and Siegel, 2011). In contrast, around the perceptual reports in MIB and its replay we observed no modulation in the gamma band but strong modulation in both the low-frequency band and the fMRI signal. This suggests that the coupling between band-limited oscillatory activity and the fMRI-signal is process-dependent, with no fixed mapping between these signals (Kopell et al., 2000; Maier et al., 2008; Donner and Siegel, 2011). Moreover, it suggests that the fMRI-response reflects a mixture of stimulus-related signals and neuromodulatory signals related to top-down factors, such as task instructions. Future studies could employ simultaneous fMRI and EEG during perceptual tasks to study the relative contributions of these stimulus-related and top-down signals to the fMRI-signal on a trial-by-trial basis (Philiastides and Sajda, 2007).

It is tempting to speculate that the stabilization mechanism introduced in this thesis generalizes to psychological phenomena related to decision commitment. Specifically, decision-makers often show a striking tendency to stick to their previous judgments, even in the face of salient counterevidence. For example, a juror could decide whether a defendant is guilty based on preliminary evidence and then fails to reconsider that decision even when strong contradictory evidence is presented at trial – a phenomenon known as confirmation bias (Nickerson, 1998). Confirmation bias can be seen as an excessive stabilization of an initial decision, resulting in extreme commitment to the decision and a bias to confirm it[2]. Relatedly, in the phenomenon of cognitive dissonance an individual is confronted with new information that conflicts with existing beliefs, ideas, or values, leading to psychological discomfort (Festinger, 1957). Similarly, these fixed, incongruent beliefs could be the result of an excessive commitment to a previous decision. It would be interesting to investigate whether similar changes in brain state occur during commitment to decisions in these phenomena and if the strength of top-down signals during decisions scales with the strength of decision commitment (Jazayeri and Movshon, 2007; Stocker and Simoncelli, 2008).

[2] Another example is the neuromodulation hypothesis laid out in this thesis.

Finally, understanding fast brain state changes identified in this thesis can help to understand psychopathological conditions in which the dynamics of thought and brain state are disturbed. For instance, depressive patients tend to dwell on the same negative thoughts for a long time, without being able to change their mind. It is possible that these symptoms result from an altered functioning of the stabilization mechanism, possibly mediated by the disturbance of neuromodulatory systems in these patients. Another condition that could possibly involve altered brain state dynamics is schizophrenia. One unresolved question is why delusions (for instance, paranoid convictions) are so persistent in these patients, despite a lack of supporting sensory evidence (Schmack et al., 2013). Again, this symptom can be seen in terms of commitment to a decision or belief, which in this case is strikingly dissociated from reality. Indeed, schizophrenic patients show altered bistable perceptual dynamics (Sanders et al., 2014), suggesting alterations in the neural mechanism underlying the time course of bistable perception. Using MIB and other bistable phenomena, future studies could investigate whether the bistable dynamics in schizophrenia are affected by an altered functioning of top-down signals associated with brain state (Notredame et al., 2014).

In this thesis, I aimed to establish the existence of fast changes in brain state that occur as a consequence of cognitive processes. These changes in brain state not only affect brain activity, but also shape the contents of our subjective experience over time. The mechanisms described here might explain one of the most striking properties of consciousness: the spontaneous and abrupt changes in our everlasting stream of thought.

SUPPLEMENT 1: SIMULATION METHODS FOR NEURAL MODEL OF VISUAL BISTABILITY WITH FEEDBACK MODULATION

We extended an established model of the neural mass dynamics underlying perceptual bistability in visual cortex (Noest et al., 2007). The "standard model" consists of two populations of neurons (X_1 and X_2), which are driven by two distinct constant stimuli (I_1 and I_2), and inhibit each other, and which are subject to slow adaptation and noise. In our extension, the following pair of differential equations governed the dynamics of these two populations:

$$\begin{aligned}\tau\partial X_1 &= I_1 - (1+A_1)X_1 - (\gamma+\mu S[M])S[X_2] + N(0,\sigma_{X1}) \\ \tau\partial X_2 &= I_2 - (1+A_2)X_2 - (\gamma+\mu S[M])S[X_1] + N(0,\sigma_{X2})\end{aligned} \quad (1),$$

where *S[X$_i$]* corresponds to a Naka-Rushton function of the "local fields" in X_i (Noest et al., 2007), *N* corresponds to normally distributed noise, and A_i describes adaptation. See Table 1 for definitions of the other model parameters, and their selected values. The "standard model" does not contain *M* ($\mu = 0$, i.e. no effect of *M*). The adaptation dynamics is given by:

$$\begin{aligned}&\tau_A\partial A_i = -A_i + \alpha S[X_i], \\ &i,j \in \{1,2\}\end{aligned} \quad (2)$$

Simulating this model with continuous inputs X_1 and X_2 yielded spontaneous fluctuations in the activity of X_1 and X_2, which, in turn, produced spontaneous alternations between dominance of the two populations of visual cortical neurons.

We extended this standard model by means of a "modulatory population" *M*, which was driven by the two cortical populations:

$$\tau_M\partial M = -A_i + \nu S[X_1] + \nu S[X_2] + N(0,\sigma_M) \quad (3)$$

M fed back to the two cortical populations X_i and modulated the strength of their mutual inhibition in an additive fashion, governed by parameter μ in eq. 1, which controls the effect of *S[M]* on the two cortical populations. See Table 1 for a complete list of parameters used in the simulations.

Table 1, related to Figure 2 | Model parameters used for simulations

Model parameters, their meanings, and values used in simulations		
τ	Timescale of X population activities	1.0
τ_A	Timescale of adaptation	125.0
τ_M	Timescale of M population activity	15
α	Gain of Adaptation	4.0
ν	Gain of M-population	120
γ	Inhibition Gain	3.0
μ	Gain of influence of M on X-populations	40 [0.1,100] (on inhibition) 3 [0.1, 4.0] (on inputs)
σ_{X1}, σ_{X2}	Standard deviation of noise in X-populations	0.003, [0.0, 0.015]
σ_M	Standard deviation of noise in M-population	0.03, [0.0, 0.05]

Numbers are (means of) the parameters used for simulations reported in this paper. Numbers in parentheses indicate the range of parameters used. Only the gain of the modulatory M-influence on the X populations in the noise level in all three populations was varied across the range indicated.

Analyses of model dynamics and perceptual stabilization

We systematically varied the strength of the parameter controlling the relative contribution of the *M*-influence on the mutual inhibition between X_1 and X_2 across a wide range of values, simulated several hundreds of dominance transitions (minimum: 200) for each of these parameter values, and finally computed Spearman correlations between transient *M*-activity and dominance duration for each of these parameter values (Figure 2C). To this end, we extracted the durations of individual dominance intervals from the simulated dynamics of X_1 and X_2 as follows. We computed the time course of the difference between $S[X_1]$ and $S[X_2]$ and temporally smoothed this difference time course using a Gaussian kernel (σ: 25 time steps). Any transgression of 0 was counted as a switch in dominance. Dominance durations were then computed as the intervals between two switches. We averaged the activity of *M* in the interval of [-50,150] time steps around each transition, to correlate this with the dominance durations. We computed the *M*-activity based on

the local fields (i.e., before output non-linearity), because these provide a closer proxy of MEG measurements than neural outputs (Donner and Siegel, 2011).

Chapter 8

Nederlandse samenvatting

Ons brein staat nooit ‘uit’. Wel kent het brein verschillende interne toestanden, die elk gekenmerkt worden door een specifiek patroon van neurale activiteit. De interne toestand van het brein bepaalt in hoge mate hoe binnenkomende informatie wordt verwerkt. Van oudsher wordt gedacht dat veranderingen in de toestand van het brein samengaan met langzame, geleidelijke transities in de mate van fysieke opwinding, zoals overgangen van slaap naar waken. Recent onderzoek laat echter zien dat toestandsveranderingen ook kunnen plaatsvinden op een veel kortere tijdsschaal; in slechts luttele seconden of zelfs sneller. Deze snelle toestandsveranderingen lijken nauw samen te hangen met cognitieve processen, zoals het actief detecteren van perceptuele veranderingen in je omgeving.

Bekijk bijvoorbeeld eens het plaatje in Figuur 1 om zelf zo’n snelle verandering in brein-toestand te ervaren. Als je dit plaatje nog nooit eerder gezien hebt, zie je waarschijnlijk niets bijzonders, zelfs als je er langere tijd naar kijkt. Maar blader nu eens verder naar Figuur 2 op de volgende bladzijde en keer dan terug naar Figuur 1. Het blijkt dat een typisch Nederlands dier je al die tijd stond aan te kijken. Wat is hier aan de hand? Op het moment dat je Figuur 1 opnieuw bekeek veroorzaakte de nieuwe kennis een plotselinge verandering in de verwerking van het plaatje in je visuele cortex, een gebied achter in het brein. Daardoor zag je ineens het dier verschijnen. Maar dit is nog niet alles; deze ‘Aha-erlebnis’ veranderde op zijn beurt de toestand van je brein (Figuur 3). Hierdoor werd de veranderde verwerking van het plaatje in het brein blijvend; je kunt immers niet meer terug naar het niet zien van het dier.

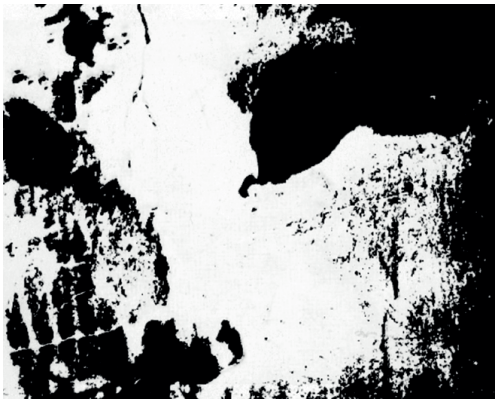

Figuur 1 | Verandering in de toestand van het brein beïnvloedt onze waarneming

Zie je welk dier hier afgebeeld staat? De meeste mensen zien op het eerste gezicht niets bijzonders. Maar het kennen van de oplossing veroorzaakt een drastische verandering van je waarneming, die op zijn beurt een toestandsverandering van je brein tot gevolg heeft. Zie Figuur 2 voor de oplossing en Figuur 3 voor een overzicht van de veronderstelde processen die rond de perceptuele overgang optreden.

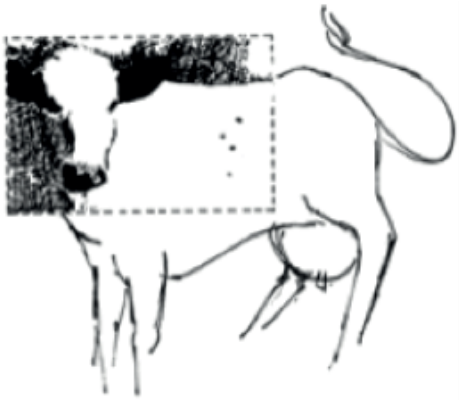

Figuur 2 | Oplossing van het plaatje afgebeeld in Figuur 1

De gestippelde lijn toont het kader van Figuur 1. Als je nu terugbladert naar Figuur 1 zal je waarneming van deze afbeelding waarschijnlijk drastisch veranderen.

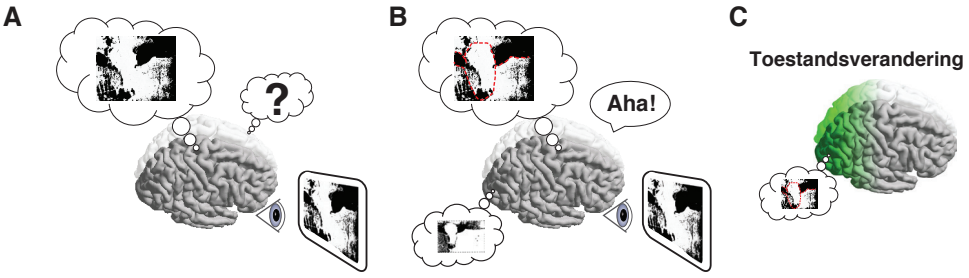

Figuur 3 | Toestandsverandering in het brein na een perceptuele overgang

Overzicht van de processen rond het ontdekken van het dier in de afbeelding. **A.** Voordat je de oplossing kent, neem je niets anders waar dan een verzameling vlekken. **B.** Het kennen van de oplossing (zie Figuur 2) leidt vervolgens tot de ontdekking van het dier in de originele afbeelding. De rode gestippelde lijn in de gedachtenballon illustreert de ontdekking van het dier in de originele afbeelding. **C.** De perceptuele overgang zet op zijn beurt een, in dit geval blijvende, verandering in de toestand van het brein in gang.

Dit proefschrift gaat over dit soort toestandsveranderingen van het brein. Wat zijn de cognitieve en neurale factoren die zulke snelle veranderingen in de toestand van het brein veroorzaken? Kunnen we ze meten in het menselijke brein? En wat zijn de precieze effecten van toestandsveranderingen op latere perceptie?

Bi-stabiele visuele illusies als een instrument om toestandsveranderingen te bestuderen.

Afbeeldingen zoals die in Figuur 1 leveren maar één perceptuele overgang per proefpersoon op; je kunt immers nooit terug naar het niet zien van het dier. Dit maakt deze plaatjes onpraktisch voor zorgvuldig onderzoek naar de daarbij optredende

toestandsveranderingen in het brein, omdat je dan massa's proefpersonen nodig zou hebben. In mijn onderzoek maakten mijn collega's en ik daarom gebruik van een ander type stimulus om de toestandsveranderingen te bestuderen; zogenaamde bi-stabiele visuele illusies. In deze illusies vinden aan de lopende band perceptuele overgangen tussen twee of meer alternatieven plaats, terwijl de stimulus steeds dezelfde blijft. Tijdens het bekijken van een dergelijke illusie lijkt het dus alsof het brein voortdurend 'van gedachten verandert'. Bi-stabiele illusies bieden een efficiënte en gecontroleerde manier om de toestandsveranderingen rond perceptuele overgangen te onderzoeken.

Een beroemd voorbeeld van een bi-stabiele stimulus is de Neckerkubus, waarin de subjectieve waarneming van een kubus voortdurend wisselt tussen twee perspectieven (Figuur 4A). Een andere, bijzonder sterke visuele illusie is motion-induced blindness (MIB), waarin een kleine, gele stip af en toe compleet uit de waarneming verdwijnt als deze wordt omgeven door een langzaam draaiend 'masker' (Figuur 4B). In werkelijkheid blijft de stip echter altijd op het scherm aanwezig. In de studies beschreven in dit proefschrift gebruikten we MIB om de toestandsveranderingen te onderzoeken. We vroegen proefpersonen om de verdwijningen en verschijningen van de stip te rapporteren door middel van het drukken op een knop, terwijl we hun hersenactiviteit en andere fysiologische activiteit maten.

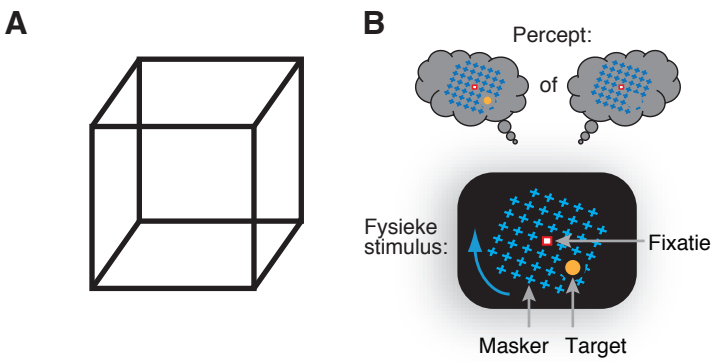

Figuur 4 | Bi-stabiele visuele illusies

A. Neckerkubus. Als je voor langere tijd naar dit plaatje kijkt, gaat je waarneming heen en weer tussen het zien van de kubus van bovenaf en vanaf beneden **B.** Motion-induced blindness (MIB). Onder: fysieke stimulus. Een heldere stip (gele stip) wordt omgeven door een langzaam draaiend patroon van kruizen (masker). Boven: afwisselende waarneming van de stip door MIB. De constant aanwezige stip verdwijnt af en toe compleet uit de waarneming, om na een tijdje weer terug te keren. Zie Bonneh and Donner (2011) voor een demo.

Dit proefschrift

Dit proefschrift begint met een algemene introductie van de snelle toestandsveranderingen en bi-stabiele visuele illusies (**Hoofdstuk 1**). Daarna volgen vijf hoofdstukken met empirische studies naar de toestandsveranderingen, gevolgd door een Engelstalige samenvatting en discussie.

Het voorbeeld van de koe in Figuur 1 laat zien dat de snelle toestandsveranderingen in het brein het gevolg zijn van cognitieve processen, in dit geval een plotselinge perceptuele verandering. Maar het is onduidelijk of de toestandsveranderingen op hun beurt ook weer de daaropvolgende subjectieve waarneming beïnvloeden. De eerste centrale vraag in dit proefschrift was dan ook of de toestandsveranderingen het verloop van onze subjectieve waarneming in de tijd bepalen. Eén manier waarop dit zou kunnen gebeuren is door de subjectieve waarneming voor bepaalde tijd te *stabiliseren*. Bi-stabiele waarnemingen variëren enorm in duur. Kijk bijvoorbeeld nog eens een tijdje naar de kubus in Figuur 4A; je zult merken dat korte en langere waarnemingen elkaar willekeurig afwisselen. De grote variatie in waarnemingsduren in bi-stabiele visuele illusies stelt ons in staat om het verband tussen toestandsveranderingen en perceptuele stabiliteit te onderzoeken door te testen of sterkere toestandsveranderingen gepaard gaan met langere daaropvolgende waarnemingen.

Voordat deze hypothese getest kan worden, is het echter nodig om nauwkeurig de neurale activiteit in kaart te brengen die optreedt rond de perceptuele veranderingen. **Hoofdstuk 2** beschrijft de hersenactiviteit die optreedt tijdens de snelle toestandsveranderingen in MIB. In deze studie maten we de hersenactiviteit van onze proefpersonen met magneto-encefalografie (MEG) terwijl zij op knoppen drukten om hun perceptuele overgangen te rapporteren. MEG vangt de geringe magnetische velden op die optreden door de elektrische activiteit in de hersenschors. De studie liet zien dat op het moment van rapportage van een stipverdwijning een tijdelijke modulatie (verandering) van MEG-activiteit optrad in de visuele cortex. Deze zogenaamde ‘beta’-modulatie (met een frequentiebereik van 12 tot 30 Hz) weerspiegelde niet de stimulus (stip en masker) op het scherm of het drukken op de knop, maar hing wel nauw samen met de *relevantie* van de perceptuele overgangen voor de proefpersoon: de modulatie verdween namelijk volledig wanneer niet gedrukt hoefde te worden na een overgang. Deze eigenschappen suggereren dat de modulatie een snelle toestandsverandering van het brein weerspiegelt:

de modulatie was namelijk niet direct gerelateerd aan ofwel de stip, het masker of het drukken op de knop, maar weerspiegelde een cognitief proces, namelijk het waarnemen en rapporteren van de perceptuele veranderingen over de tijd.

Nadat we zo vaststelden dat de toestandsveranderingen inderdaad meetbaar zijn in het brein, testten we onze hypothese dat de toestandsveranderingen betrokken zijn bij stabilisatie van percepten. En inderdaad, we vonden dat de gele stip inderdaad langer onzichtbaar was als de beta-modulatie rond het rapporteren van de stip-verdwijning sterker was. Deze resultaten suggereren dat het actieve waarnemen en rapporteren van een perceptuele overgang een verandering in de toestand van het brein in gang zet die de nieuwe perceptuele interpretatie stabiliseert.

In **Hoofdstuk 3** karakteriseerden we vervolgens de beta-modulatie verder in een nieuwe groep proefpersonen met een andere MEG-scanner. We toonden aan dat de modulatie niet alleen optrad als proefpersonen de perceptuele verdwijningen direct rapporteren met een druk op de knop, maar ook als ze de verdwijningen alleen in zichzelf telden, zonder te drukken. Deze bevinding levert belangrijk aanvullend bewijs dat relevantie van de perceptuele overgangen een sleutelrol speelt in de modulatie. Er hoeft dus met andere woorden niet per se direct een actie (druk op de knop) aan de stip-verdwijningen vast te zitten: de 'Aha-Erlebnis' is voldoende, net als bij het voorbeeld van de koe (Figuur 3) .

Individuele proefpersonen variëren aanzienlijk in de typische duur van hun bi-stabiele waarnemingen, maar hebben gemeen dat ze nauwelijks waarnemingen rapporteren die korter zijn dan hun typische waarnemingsduur. Enerzijds zou het ontbreken van deze kortdurende waarnemingen kunnen komen door een mechanisme in het brein dat de waarneming stabiliseert en daarmee korte waarnemingen voorkomt, zoals Hoofdstuk 2 suggereert. Anderzijds kan deze eigenschap echter ook wellicht verklaard worden doordat proefpersonen simpelweg niet in staat zijn snel genoeg op de knop drukken om kortdurende waarnemingen te rapporteren. **Hoofdstuk 4** beschrijft een gedragsstudie naar de mogelijke oorzaak van het ontbreken van zeer kortdurende waarnemingen in bi-stabiele visuele illusies. De studie liet zien dat een grote groep proefpersonen goed in staat was om zeer korte waarnemingen te rapporteren, zelfs als die structureel veel korter waren dan hun eigen typische waarnemingsduur. Dit gold voor zowel MIB als een andere visuele illusie. Het ontbreken van kortdurende waarnemingen wordt dus niet verklaard

doordat individuen de snelle overgangen niet kunnen bijhouden met een druk op de knop en wijst dus op een mechanisme in het brein dat bi-stabiele waarnemingen stabiliseert.

De tweede centrale vraag in dit proefschrift was hoe en waar de veranderingen in de toestand van het brein ontstaan. Een mogelijk mechanisme is de kortdurende activatie van zogenaamde neuromodulatie-systemen in dieper gelegen delen van het brein. Deze systemen hebben een wijd verbreid netwerk van verbindingen met de hersenschors, wat ze in staat stelt de globale toestand van het brein te beïnvloeden. Het is al langer bekend dat neuromodulatie-systemen de algemene mate van fysieke opwindingen beïnvloeden (denk maar aan de partydrug xtc, waarbij grotere hoeveelheden van onder andere de neuromodulator noradrenaline in het brein vrijkomt). Deze systemen kunnen echter ook kortdurend neuromodulators verspreiden ten tijde van snelle cognitieve processen, zoals bij beslissingen. Onderzoek laat zien dat de grootte van de pupil in het oog niet alleen reageert op veranderingen in lichtomstandigheden, maar ook de activiteit van deze neuromodulatie-systemen volgt.

De studies in hoofdstukken 5 en 6 gaan nader in op de rol van neuromodulatie in de snelle toestandsveranderingen. We deden dit door de grootte van de pupil te meten tijdens de perceptuele overgangen in MIB. We redeneerden dat als deze systemen inderdaad een actieve rol spelen in de snelle toestandsveranderingen, dan zou er rond de perceptuele overgangen in MIB (waarbij lichtomstandigheden immers gelijk blijven) ook een tijdelijke dilatatie van de pupil moeten plaatsvinden. **Hoofdstuk 5** laat niet alleen zien dat inderdaad pupildilatatie plaatsvindt tijdens de overgangen, maar dat zelfs het *soort* perceptuele overgang (verdwijning of verschijning van de stip) af te leiden is uit de pupildilatatie ten tijde van de overgang. De dilatatie bleek namelijk groter bij het verdwijnen van de stip dan bij het weer verschijnen. Deze bevinding suggereert dat pupil-gelinkte neuromodulatie-systemen verschillend actief worden tijdens de twee soorten overgangen. Neuromodulatie-systemen bepalen dus niet alleen de algemene mate van opwinding, maar hun activatie hangt ook specifiek samen met de inhoud van snelle cognitieve processen.

Tenslotte onderzochten we in **Hoofdstuk 6** de relatie tussen pupildilatatie en hersenactiviteit door gelijktijdig pupilgrootte en hersenactiviteit te meten met functional magnetic resonance imaging (fMRI) terwijl proefpersonen de perceptuele overgangen rapporteerden. fMRI meet elke twee seconden hersenactiviteit in het hele brein in kleine

drie-dimensionale pixels. Deze studie liet zien dat een verminderde fMRI activiteit in de visuele cortex rond stipverdwijningen sterker was wanneer dit vergezeld ging van grotere pupildilatatie. Ook zagen we activiteit rond de overgangen in de anterior cingulate cortex, een gebied aan de voorkant van het brein waarvan wordt aangenomen dat het neuromodulatie-systemen in de hersenstam aanstuurt. De studie levert dus een nieuwe aanwijzing dat deze neuromodulatie-systemen een actieve rol spelen bij de toestandsveranderingen in het brein. Tegelijkertijd was er ook aanzienlijke fMRI-activiteit rond overgangen waarbij bijna geen pupildilatatie is. Dit lijkt er op te duiden dat andere processen die los staan van pupildilatatie eveneens een grote rol spelen in de snelle toestandsveranderingen.

Onze onderzoeken hebben laten zien dat toestandsveranderingen een belangrijke rol spelen in bi-stabiele illusies. In **Hoofdstuk 7** beschrijf ik gedetailleerd de mogelijke onderliggende mechanismen en plaats ik de snelle toestandsveranderingen in een bestaand computermodel van bi-stabiele perceptie, dat de neurale processen tijdens bi-stabiele perceptie simuleert. Tot slot speculeer ik wat de rol van snelle toestandsveranderingen zou kunnen zijn in bekende psychologische fenomenen zoals cognitieve dissonantie en in psychische stoornissen zoals schizofrenie.

In dit proefschrift heb ik het bestaan willen aantonen van snelle toestands-veranderingen in het brein die het gevolg zijn van cognitieve processen. Deze toestandsveranderingen bepalen niet alleen het patroon van hersenactiviteit, maar ook hoe onze subjectieve ervaring van de wereld verloopt over de tijd. De hier beschreven mechanismen verklaren mogelijk één van de opvallendste kenmerken van ons bewustzijn: de spontane en abrupte veranderingen in onze voortdurende stroom van gedachten.

Appendix

References
List of publications
Dankwoord

REFERENCES

Alais D, Blake R (1999) Neural strength of visual attention gauged by motion adaptation. Nat Neurosci 2:1015-1018.

Alais D, Blake R (2005) Binocular rivalry: MIT press.

Aston-Jones G, Cohen JD (2005) An integrative theory of locus coeruleus-norepinephrine function: adaptive gain and optimal performance. Annu Rev Neurosci 28:403-450.

Aston-Jones G, Rajkowski J, Kubiak P, Alexinsky T (1994) Locus coeruleus neurons in monkey are selectively activated by attended cues in a vigilance task. J Neurosci 14:4467-4480.

Bárány EH, Halldén U (1948) Phasic inhibition of the light reflex of the pupil during retinal rivalry: Am Physiological Soc.

Beatty J (1982) Task-evoked pupillary responses, processing load, and the structure of processing resources. Psychological bulletin 91:276-292.

Belitski A, Gretton A, Magri C, Murayama Y, Montemurro MA, Logothetis NK, Panzeri S (2008) Low-frequency local field potentials and spikes in primary visual cortex convey independent visual information. J Neurosci 28:5696-5709.

Blake R, Logothetis NK (2002) Visual competition. Nat Rev Neurosci 3:13-21.

Blake R, Sobel KV, Gilroy LA (2003) Visual motion retards alternations between conflicting perceptual interpretations. Neuron 39:869-878.

Bonneh YS, Donner TH (2011) Motion induced blindness. Scholarpedia 6:3321.

Bonneh YS, Cooperman A, Sagi D (2001) Motion-induced blindness in normal observers. Nature 411:798-801.

Bonneh YS, Donner TH, Cooperman A, Heeger DJ, Sagi D (2014) Motion-induced blindness and troxler fading: common and different mechanisms. PLoS One 9:e92894.

Bonneh YS, Donner TH, Sagi D, Fried M, Cooperman A, Heeger DJ, Arieli A (2010) Motion-induced blindness and microsaccades: cause and effect. J Vis 10:22.

Bosman CA, Womelsdorf T, Desimone R, Fries P (2009) A microsaccadic rhythm modulates gamma-band synchronization and behavior. J Neurosci 29:9471-9480.

Bouret S, Sara SJ (2005) Network reset: a simplified overarching theory of locus coeruleus noradrenaline function. Trends Neurosci 28:574-582.

Brascamp JW, van Ee R, Noest AJ, Jacobs RH, van den Berg AV (2006) The time course of binocular rivalry reveals a fundamental role of noise. J Vis 6:1244-1256.

Braun J, Mattia M (2010) Attractors and noise: twin drivers of decisions and multistability. Neuroimage 52:740-751.

Britz J, Landis T, Michel CM (2008) Right Parietal Brain Activity Precedes Perceptual Alternation of Bistable Stimuli. Cereb Cortex.

Britz J, Pitts MA, Michel CM (2011) Right parietal brain activity precedes perceptual alternation during binocular rivalry. Human Brain Mapping 32:1432-1442.

Cardoso MM, Sirotin YB, Lima B, Glushenkova E, Das A (2012) The neuroimaging signal is a linear sum of neurally distinct stimulus- and task-related components. Nature neuroscience 15:1298-1306.

Carter OL, Pettigrew JD (2003) A common oscillator for perceptual rivalries? Perception 32:295-305.

Choe KW, Blake R, Lee SH (2014) Dissociation between Neural Signatures of Stimulus and Choice in Population Activity of Human V1 during Perceptual Decision-Making. J Neurosci 34:2725-2743.

Crain K (1961) Binocular rivalry: its relation to intelligence, and general theory of its nature and physiological correlates. The Journal of General Psychology 64:259-283.

Dale AM (1999) Optimal experimental design for event-related fMRI. Hum Brain Mapp 8:109-114.

de Gee JW, Knapen T, Donner TH (2014) Decision-related pupil dilation reflects upcoming choice and individual bias. Proc Natl Acad Sci U S A 111:E618-625.

de-Wit LH, Kubilius J, Wagemans J, Op de Beeck HP (2012) Bistable Gestalts reduce activity in the whole of V1, not just the retinotopically predicted parts. Journal of vision 12.

Deco G, Romo R (2008) The role of fluctuations in perception. Trends Neurosci 31:591-598.

Desimone R, Duncan J (1995) Neural mechanisms of selective visual attention. Annu Rev Neurosci 18:193-222.

Donner TH, Siegel M (2011) A framework for local cortical oscillation patterns. Trends Cogn Sci 15:191-199.

Donner TH, Sagi D, Bonneh YS, Heeger DJ (2008) Opposite neural signatures of motion-induced blindness in human dorsal and ventral visual cortex. J Neurosci 28:10298-10310.

Donner TH, Siegel M, Fries P, Engel AK (2009) Buildup of choice-predictive activity in human motor cortex during perceptual decision making. Curr Biol 19:1581-1585.

Donner TH, Sagi D, Bonneh YS, Heeger DJ (2013) Retinotopic patterns of correlated fluctuations in visual cortex reflect the dynamics of spontaneous perceptual suppression. J Neurosci 33:2188-2198.

Dumoulin SO, Wandell BA (2008) Population receptive field estimates in human visual cortex. Neuroimage 39:647-660.

Efron B, Tibshirani R (1998) An introduction to the bootstrap, 1st CRC Press reprint. Edition. Boca Raton, Fla.: Chapman & Hall/CRC.

Einhauser W, Koch C, Carter OL (2010) Pupil dilation betrays the timing of decisions. Frontiers in human neuroscience 4:18.

Einhauser W, Stout J, Koch C, Carter O (2008) Pupil dilation reflects perceptual selection and predicts subsequent stability in perceptual rivalry. Proc Natl Acad Sci U S A 105:1704-1709.

Eldar E, Cohen JD, Niv Y (2013) The effects of neural gain on attention and learning. Nat Neurosci.

Engbert R, Mergenthaler K (2006) Microsaccades are triggered by low retinal image slip. Proceedings of the National Academy of Sciences 103:7192-7197.

Engel AK, Fries P (2010) Beta-band oscillations--signalling the status quo? Curr Opin Neurobiol 20:156-165.

Fahle MW, Stemmler T, Spang KM (2011) How much of the "unconscious" is just pre–threshold? Frontiers in human neuroscience 5.

Festinger LA (1957) A theory of cognitive dissonance: Stanford University Press.

Fiedler S, Glockner A (2012) The dynamics of decision making in risky choice: an eye-tracking analysis. Front Psychol 3:335.

Fischer J, Whitney D (2014) Serial dependence in visual perception. Nature neuroscience.

Fischl B, Sereno MI, Dale AM (1999) Cortical surface-based analysis: II: Inflation, flattening, and a surface-based coordinate system. Neuroimage 9:195-207.

Fischl B, van der Kouwe A, Destrieux C, Halgren E, Ségonne F, Salat DH, Busa E, Seidman LJ, Goldstein J, Kennedy D (2004) Automatically parcellating the human cerebral cortex. Cerebral cortex 14:11-22.

Frassle S, Sommer J, Jansen A, Naber M, Einhauser W (2014) Binocular rivalry: frontal activity relates to introspection and action but not to perception. J Neurosci 34:1738-1747.

Freeman AW (2005) Multistage model for binocular rivalry. J Neurophysiol 94:4412-4420.

Fries P (2009) Neuronal gamma-band synchronization as a fundamental process in cortical computation. Annu Rev Neurosci 32:209-224.

Friston K (2010) The free-energy principle: a unified brain theory? Nature Reviews Neuroscience 11:127-138.

Gail A, Brinksmeyer HJ, Eckhorn R (2004) Perception-related modulations of local field potential power and coherence in primary visual cortex of awake monkey during binocular rivalry. Cerebral cortex 14:300-313.

Gigante G, Mattia M, Braun J, Del Giudice P (2009) Bistable perception modeled as competing stochastic integrations at two levels. PLoS Comput Biol 5:e1000430.

Gilbert CD, Sigman M (2007) Brain states: top-down influences in sensory processing. Neuron 54:677-696.

Gilzenrat MS, Nieuwenhuis S, Jepma M, Cohen JD (2010) Pupil diameter tracks changes in control state predicted by the adaptive gain theory of locus coeruleus function. Cogn Affect Behav Neurosci.

Glover GH, Li TQ, Ress D (2000) Image-based method for retrospective correction of physiological motion effects in fMRI: RETROICOR. Magnetic resonance in medicine 44:162-167.

Green DM, Swets JA (1966) Signal detection theory and psychophysics. New York: Wiley.

Grill-Spector K, Malach R (2004) The human visual cortex. Annu Rev Neurosci 27:649-677.

Haider B, Hausser M, Carandini M (2012) Inhibition dominates sensory responses in the awake cortex. Nature.

Hamalainen M, Hari R, Ilmoniemi RJ, Knuutila J, Lounasmaa OV (1993) Magnetoencephalography - Theory, Instrumentation, and Applications to Noninvasive Studies of the Working Human Brain. Reviews of Modern Physics 65:413-497.

Händel BF, Jensen O (2014) Spontaneous local alpha oscillations predict motion-induced blindness. European Journal of Neuroscience.

Harris CM, Hainline L, Abramov I, Lemerise E, Camenzuli C (1988) The distribution of fixation durations in infants and naive adults. Vision Research 28:419-432.

Harris KD, Thiele A (2011) Cortical state and attention. Nat Rev Neurosci 12:509-523.

Haynes JD, Rees G (2005) Predicting the orientation of invisible stimuli from activity in human primary visual cortex. Nat Neurosci 8:686-691.

Haynes JD, Lotto RB, Rees G (2004) Responses of human visual cortex to uniform surfaces. Proc Natl Acad Sci U S A 101:4286-4291.

Hess EH, Polt JM (1964) Pupil Size in Relation to Mental Activity during Simple Problem-Solving. Science 143:1190-1192.

Hoeks B, Levelt WJM (1993) Pupillary dilation as a measure of attention: a quantitative systems analysis. Behav Res Meth, Instr, & Computers 25 16-26.

Hsieh PJ, Tse PU (2009) Microsaccade rate varies with subjective visibility during motion-induced blindness. PLoS ONE 4:e5163.

Hunt J, Guilford J (1933) Fluctuation of an ambiguous figure in dementia praecox and in manic-depressive patients. The Journal of Abnormal and Social Psychology 27:443.

Hupe JM, Lamirel C, Lorenceau J (2009) Pupil dynamics during bistable motion perception. J Vis 9:10.

Jack AI, Shulman GL, Snyder AZ, McAvoy M, Corbetta M (2006) Separate modulations of human V1 associated with spatial attention and task structure. Neuron 51:135-147.

Jazayeri M, Movshon JA (2007) A new perceptual illusion reveals mechanisms of sensory decoding. Nature 446:912-915.

Jenkinson M, Bannister P, Brady M, Smith S (2002) Improved optimization for the robust and accurate linear registration and motion correction of brain images. Neuroimage 17:825-841.

Jenkinson M, Beckmann CF, Behrens TE, Woolrich MW, Smith SM (2012) Fsl. Neuroimage 62:782-790.

Jensen O, Mazaheri A (2011) Shaping functional architecture by oscillatory alpha activity: gating by inhibition. Front Hum Neurosci 4:186.

Kahneman D, Beatty J (1966) Pupil diameter and load on memory. Science 154:1583-1585.

Kastner S, Ungerleider LG (2000) Mechanisms of visual attention in the human cortex. Annu Rev Neurosci 23:315-341.

Kim CY, Blake R (2005) Psychophysical magic: rendering the visible 'invisible'. Trends Cogn Sci 9:381-388.

Kim YJ, Grabowecky M, Suzuki S (2006) Stochastic resonance in binocular rivalry. Vision research 46:392-406.

Klink PC, van Ee R, van Wezel RJ (2008) General validity of Levelt's propositions reveals common computational mechanisms for visual rivalry. PLoS ONE 3:e3473.

Klink PC, Oleksiak A, Lankheet MJ, van Wezel RJ (2012) Intermittent stimulus presentation stabilizes neuronal responses in macaque area MT. Journal of neurophysiology 108:2101-2114.

Kloosterman NA, Lamme VAF, Donner TH (2015a) Short-term Stabilization in Bistable Visual Perception. In preparation.

Kloosterman, NA, Meindertsma, T, Hillebrand, A, van Dijk, BW, Lamme, VA, & Donner, TH (2015) Top-Down Modulation in Human Visual Cortex Predicts the Stability of a Perceptual Illusion. Journal of neurophysiology, 113(4), 1063-1076.

Kloosterman, NA, Meindertsma, T, Loon, AM, Lamme, VA, Bonneh, YS, & Donner, TH (2015b) Pupil Size Tracks Perceptual Content and Surprise. European Journal of Neuroscience, 41(8), 1068-1078.

Kloosterman NA, Lindh D, de Gee JW, Knapen T, Lamme VAF, Donner TH (2015c) Pupil-linked Modulation of Decision-Related Signals in Human Primary Visual Cortex. In preparation.

Kloosterman NA, Filimon F, Philiastides MG, van Zuijen TL, Werner A, Lindenberger U, Heekeren HR (2015d) Human Prefrontal Cortex Represents Task-Relevant Auditory Sensory Evidence During Perceptual Decision Making. In preparation.

Knapen T, Brascamp J, Pearson J, van Ee R, Blake R (2011) The role of frontal and parietal brain areas in bistable perception. J Neurosci 31:10293-10301.

Kohn A (2007) Visual adaptation: physiology, mechanisms, and functional benefits. J Neurophysiol 97:3155-3164.

Kopell N, Ermentrout GB, Whittington MA, Traub RD (2000) Gamma rhythms and beta rhythms have different synchronization properties. Proc Natl Acad Sci U S A 97:1867-1872.

Laeng B, Endestad T (2012) Bright illusions reduce the eye's pupil. Proceedings of the National Academy of Sciences 109:2162-2167.

Laeng B, Sulutvedt U (2014) The eye pupil adjusts to imaginary light. Psychological science 25:188-197.

Laing CR, Chow CC (2002) A spiking neuron model for binocular rivalry. Journal of computational neuroscience 12:39-53.

Lee S, Papanikolaou A, Logothetis NK, Smirnakis SM, Keliris GA (2013) A new method for estimating population receptive field topography in visual cortex. Neuroimage 81:144-157.

Lee SH, Dan Y (2012) Neuromodulation of brain states. Neuron 76:209-222.

Lee SH, Blake R, Heeger DJ (2007) Hierarchy of cortical responses underlying binocular rivalry. Nat Neurosci 10:1048-1054.

Leopold DA, Logothetis NK (1996) Activity changes in early visual cortex reflect monkeys' percepts during binocular rivalry. Nature 379:549-553.

Leopold DA, Logothetis NK (1999) Multistable phenomena: changing views in perception. Trends Cogn Sci 3:254-264.

Leopold DA, Murayama Y, Logothetis NK (2003) Very slow activity fluctuations in monkey visual cortex: implications for functional brain imaging. Cereb Cortex 13:422-433.

Leopold DA, Wilke M, Maier A, Logothetis NK (2002) Stable perception of visually ambiguous patterns. Nat Neurosci 5:605-609.

Linkenkaer-Hansen K, Nikulin VV, Palva S, Ilmoniemi RJ, Palva JM (2004) Prestimulus oscillations enhance psychophysical performance in humans. J Neurosci 24:10186-10190.

Loewenfeld IE, Lowenstein O (1993) The pupil: Anatomy, physiology, and clinical applications: Iowa State University Press Ames.

Logothetis NK, Schall JD (1989) Neuronal correlates of subjective visual perception. Science 245:761-763.

Logothetis NK, Schall JD (1990) Binocular motion rivalry in macaque monkeys: eye dominance and tracking eye movements. Vision Res 30:1409-1419.

Logothetis NK, Leopold DA, Sheinberg DL (1996) What is rivalling during binocular rivalry? Nature 380:621-624.

Lowe SW, Ogle KN (1966) Dynamics of the pupil during binocular rivalry. Archives of ophthalmology 75:395-403.

Luce RD (1986) Response Time: Their Role in Inferring Elementary Mental Organization. New York: Oxford University Press.

Lumer ED, Friston KJ, Rees G (1998) Neural correlates of perceptual rivalry in the human brain. Science 280:1930-1934.

Maier A, Wilke M, Aura C, Zhu C, Ye FQ, Leopold DA (2008) Divergence of fMRI and neural signals in V1 during perceptual suppression in the awake monkey. Nat Neurosci 11:1193-1200.

Maris E, Oostenveld R (2007) Nonparametric statistical testing of EEG- and MEG-data. Journal of neuroscience methods 164:177-190.

Martinez-Conde S, Macknik SL, Hubel DH (2004) The role of fixational eye movements in visual perception. Nat Rev Neurosci 5:229-240.

Mathot S, van der Linden L, Grainger J, Vitu F (2013) The pupillary light response reveals the focus of covert visual attention. PLoS One 8:e78168.

Meindertsma T, Kloosterman NA, Nolte G, Engel AK, Donner TH (2014) Modulation of Beta-Band Activity in Human Visual Cortex by Covert Perceptual Decisions. In preparation.

Meredith GM (1967) Some attributive dimensions of reversibility phenomena and their relationship to rigidity and anxiety. Perceptual and motor skills 24:843-849.

Mitra P, Bokil H (2008) Observed Brain Dynamics. In: New York NY Oxford University Press.

Mitra PP, Pesaran B (1999) Analysis of dynamic brain imaging data. Biophys J 76:691-708.

Moradi F, Hipp C, Koch C (2007) Activity in the visual cortex is modulated by top-down attention locked to reaction time. J Cogn Neurosci 19:331-340.

Moreno-Bote R, Rinzel J, Rubin N (2007) Noise-induced alternations in an attractor network model of perceptual bistability. J Neurophysiol 98:1125-1139.

Murphy PR, Robertson IH, Balsters JH, O'Connell R G (2011) Pupillometry and P3 index the locus coeruleus-noradrenergic arousal function in humans. Psychophysiology 48:1532-1543.

Murphy PR, O'Connell RG, O'Sullivan M, Robertson IH, Balsters JH (2014) Pupil diameter covaries with BOLD activity in human locus coeruleus. Hum Brain Mapp 35:4140-4154.

Naber M, Frassle S, Einhauser W (2011) Perceptual rivalry: reflexes reveal the gradual nature of visual awareness. PLoS ONE 6:e20910.

Naber M, Frassle S, Rutishauser U, Einhauser W (2013) Pupil size signals novelty and predicts later retrieval success for declarative memories of natural scenes. Journal of vision 13:11.

Nassar MR, Rumsey KM, Wilson RC, Parikh K, Heasly B, Gold JI (2012) Rational regulation of learning dynamics by pupil-linked arousal systems. Nature neuroscience 15:1040-1046.

Necker LA (1832) LXI. Observations on some remarkable optical phænomena seen in Switzerland; and on an optical phænomenon which occurs on viewing a figure of a crystal or geometrical solid.

Nickerson RS (1998) Confirmation bias: A ubiquitous phenomenon in many guises. Review of general psychology 2:175.

Nienborg H, Cumming BG (2009) Decision-related activity in sensory neurons reflects more than a neuron's causal effect. Nature 459:89-92.

Niessing J, Ebisch B, Schmidt KE, Niessing M, Singer W, Galuske RA (2005) Hemodynamic signals correlate tightly with synchronized gamma oscillations. Science 309:948-951.

Nieuwenhuis S, Donner TH (2011) The visual attention network untangled. Nat Neurosci 14:542-543.

Noest AJ, van Ee R, Nijs MM, van Wezel RJ (2007) Percept-choice sequences driven by interrupted ambiguous stimuli: a low-level neural model. J Vis 7:10.

Notredame C-E, Pins D, Deneve S, Jardri R (2014) What visual illusions teach us about schizophrenia. Front Integr Neurosci 8.

Noudoost B, Moore T (2011) Control of visual cortical signals by prefrontal dopamine. Nature 474:372-375.

O'Connell RG, Dockree PM, Kelly SP (2012) A supramodal accumulation-to-bound signal that determines perceptual decisions in humans. Nature neuroscience 15:1729-1735.

Oostenveld R, Fries P, Maris E, Schoffelen JM (2011) FieldTrip: Open source software for advanced analysis of MEG, EEG, and invasive electrophysiological data. Computational intelligence and neuroscience 2011:156869.

Parikh V, Kozak R, Martinez V, Sarter M (2007) Prefrontal acetylcholine release controls cue detection on multiple timescales. Neuron 56:141-154.

Pastukhov A, Braun J (2007) Perceptual reversals need no prompting by attention. J Vis 7:5 1-17.

Pastukhov A, Garcia-Rodriguez PE, Haenicke J, Guillamon A, Deco G, Braun J (2013) Multi-stable perception balances stability and sensitivity. Frontiers in computational neuroscience 7:17.

Pettigrew JD (2001) Searching for the switch: neural bases for perceptual rivalry alternations. Brain and Mind 2:85–118.

Pettigrew JD, Miller SM (1998) A 'sticky' interhemispheric switch in bipolar disorder? Proc Biol Sci 265:2141-2148.

Pfurtscheller G, Lopes da Silva FH (1999) Event-related EEG/MEG synchronization and desynchronization: basic principles. Clin Neurophysiol 110:1842-1857.

Philiastides MG, Sajda P (2007) EEG-informed fMRI reveals spatiotemporal characteristics of perceptual decision making. J Neurosci 27:13082-13091.

Pinto L, Goard MJ, Estandian D, Xu M, Kwan AC, Lee S-H, Harrison TC, Feng G, Dan Y (2013) Fast modulation of visual perception by basal forebrain cholinergic neurons. Nature neuroscience.

Polack PO, Friedman J, Golshani P (2013) Cellular mechanisms of brain state-dependent gain modulation in visual cortex. Nature neuroscience 16:1331-1339.

Polonsky A, Blake R, Braun J, Heeger DJ (2000) Neuronal activity in human primary visual cortex correlates with perception during binocular rivalry. Nat Neurosci 3:1153-1159.

Preuschoff K, t Hart BM, Einhauser W (2011) Pupil Dilation Signals Surprise: Evidence for Noradrenaline's Role in Decision Making. Frontiers in neuroscience 5:115.

Reimer J, Froudarakis E, Cadwell CR, Yatsenko D, Denfield GH, Tolias AS (2014) Pupil Fluctuations Track Fast Switching of Cortical States during Quiet Wakefulness. Neuron 84:355-362.

Ress D, Heeger DJ (2003) Neuronal correlates of perception in early visual cortex. Nat Neurosci 6:414-420.

Ress D, Backus BT, Heeger DJ (2000) Activity in primary visual cortex predicts performance in a visual detection task. Nat Neurosci 3:940-945.

Robertson CE, Kravitz DJ, Freyberg J, Baron-Cohen S, Baker CI (2013) Slower rate of binocular rivalry in autism. The Journal of Neuroscience 33:16983-16991.

Rubin E (1958) Figure and ground. Readings in perception:194-203.

Sanders LLO, Auksztulewicz R, Hohlefeld FU, Busch NA, Sterzer P (2014) The influence of spontaneous brain oscillations on apparent motion perception. NeuroImage 102:241-248.

Sarter M, Parikh V, Howe WM (2009) Phasic acetylcholine release and the volume transmission hypothesis: time to move on. Nat Rev Neurosci 10:383-390.

Schmack K, de Castro AG-C, Rothkirch M, Sekutowicz M, Rössler H, Haynes J-D, Heinz A, Petrovic P, Sterzer P (2013) Delusions and the Role of Beliefs in Perceptual Inference. The Journal of Neuroscience 33:13701-13712.

Shalom DE, de Sousa Serro MG, Giaconia M, Martinez LM, Rieznik A, Sigman M (2013) Choosing in freedom or forced to choose? Introspective blindness to psychological forcing in stage-magic. PLoS One 8:e58254.

Siegel M, Engel AK, Donner TH (2011) Cortical network dynamics of perceptual decision-making in the human brain. Front Hum Neurosci 5:21.

Siegel M, Donner TH, Engel AK (2012) Spectral fingerprints of large-scale neuronal interactions. Nature reviews Neuroscience 13:121-134.

Siegel M, Donner TH, Oostenveld R, Fries P, Engel AK (2008) Neuronal synchronization along the dorsal visual pathway reflects the focus of spatial attention. Neuron 60:709-719.

Sirotin YB, Das A (2009) Anticipatory haemodynamic signals in sensory cortex not predicted by local neuronal activity. Nature 457:475-479.

Sirotin YB, Hillman EM, Bordier C, Das A (2009) Spatiotemporal precision and hemodynamic mechanism of optical point spreads in alert primates. Proceedings of the National Academy of Sciences of the United States of America 106:18390-18395.

Smith SM, Jenkinson M, Woolrich MW, Beckmann CF, Behrens TE, Johansen-Berg H, Bannister PR, De Luca M, Drobnjak I, Flitney DE (2004) Advances in functional and structural MR image analysis and implementation as FSL. Neuroimage 23:S208-S219.

Steriade M (2000) Corticothalamic resonance, states of vigilance and mentation. Neuroscience 101:243-276.

Steriade M (2006) Grouping of brain rhythms in corticothalamic systems. Neuroscience 137:1087-1106.

Sterzer P, Kleinschmidt A (2007) A neural basis for inference in perceptual ambiguity. Proceedings of the National Academy of Sciences of the United States of America 104:323-328.

Sterzer P, Kleinschmidt A, Rees G (2009) The neural bases of multistable perception. Trends Cogn Sci 13:310-318.

Stocker AA, Simoncelli EP (2008) A bayesian model of conditioned perception. Adv Neural Inf Proc Sys 20:1409-1416.

Suppes P, Cohen M, Laddaga R, Anliker J, Floyd R (1983) A procedural theory of eye movements in doing arithmetic. J Math Psychol 27:341-369.

Swallow KM, Makovski T, Jiang YV (2012) Selection of events in time enhances activity throughout early visual cortex. Journal of neurophysiology 108:3239-3252.

Taulu S, Simola J, Kajola M (2004) MEG recordings of DC fields using the signal space separation method (SSS). Neurol Clin Neurophysiol 2004:35.

Tong F, Engel SA (2001) Interocular rivalry revealed in the human cortical blind-spot representation. Nature 411:195-199.

van Ee R (2009) Stochastic variations in sensory awareness are driven by noisy neuronal adaptation: evidence from serial correlations in perceptual bistability. J Opt Soc Am A Opt Image Sci Vis 26:2612-2622.

van Loon AM, Knapen T, Scholte HS, St John-Saaltink E, Donner TH, Lamme VA (2013) GABA shapes the dynamics of bistable perception. Curr Biol 23:823-827.

Wandell BA, Dumoulin SO, Brewer AA (2007) Visual field maps in human cortex. Neuron 56:366-383.

Wang CA, Munoz DP (2014) Modulation of stimulus contrast on the human pupil orienting response. Eur J Neurosci.

Wang CA, Boehnke SE, White BJ, Munoz DP (2012) Microstimulation of the monkey superior colliculus induces pupil dilation without evoking saccades. J Neurosci 32:3629-3636.

Weilnhammer VA, Ludwig K, Hesselmann G, Sterzer P (2013) Frontoparietal cortex mediates perceptual transitions in bistable perception. J Neurosci 33:16009-16015.

Wierda SM, van Rijn H, Taatgen NA, Martens S (2012) Pupil dilation deconvolution reveals the dynamics of attention at high temporal resolution. Proceedings of the National Academy of Sciences of the United States of America 109:8456-8460.

Wilke M, Logothetis NK, Leopold DA (2006) Local field potential reflects perceptual suppression in monkey visual cortex. Proc Natl Acad Sci U S A 103:17507-17512.

Wilke M, Mueller KM, Leopold DA (2009) Neural activity in the visual thalamus reflects perceptual suppression. Proc Natl Acad Sci U S A 106:9465-9470.

Wilson HR (2003) Computational evidence for a rivalry hierarchy in vision. Proc Natl Acad Sci U S A 100:14499-14503.

Woolsey TA, Rovainen CM, Cox SB, Henegar MH, Liang GE, Liu D, Moskalenko YE, Sui J, Wei L (1996) Neuronal units linked to microvascular modules in cerebral cortex: response elements for imaging the brain. Cerebral Cortex 6:647-660.

Wyart V, Tallon-Baudry C (2008) Neural dissociation between visual awareness and spatial attention. J Neurosci 28:2667-2679.

Yu AJ (2012) Change is in the eye of the beholder. Nature neuroscience 15:933-935.

Yuval-Greenberg S, Tomer O, Keren AS, Nelken I, Deouell LY (2008) Transient induced gamma-band response in EEG as a manifestation of miniature saccades. Neuron 58:429-441.

Zagha E, McCormick DA (2014) Neural control of brain state. Current opinion in neurobiology 29:178-186.

Zaretskaya N, Thielscher A, Logothetis NK, Bartels A (2010) Disrupting parietal function prolongs dominance durations in binocular rivalry. Current biology : CB 20:2106-2111.

Zipser K, Lamme VA, Schiller PH (1996) Contextual modulation in primary visual cortex. The Journal of Neuroscience 16:7376-7389.

Zylberberg A, Oliva M, Sigman M (2012) Pupil dilation: a fingerprint of temporal selection during the "attentional blink". Front Psychol 3:316.

LIST OF PUBLICATIONS

Kloosterman, N. A., Meindertsma, T., Loon, A. M., Lamme, V. A., Bonneh, Y. S., & Donner, T. H. (2015). Pupil Size Tracks Perceptual Content and Surprise. *European Journal of Neuroscience, 41*(8), 1068-1078.

Kloosterman, N. A., Meindertsma, T., Hillebrand, A., van Dijk, B. W., Lamme, V. A., & Donner, T. H. (2015). Top-Down Modulation in Human Visual Cortex Predicts the Stability of a Perceptual Illusion. *Journal of neurophysiology, 113*(4), 1063-1076.

Kloosterman, N. A., Lamme, V. A. F., & Donner, T. H. Short-term Stabilization in Bistable Visual Perception. *In preparation.*

Kloosterman N. A., Lindh D., de Gee J. W., Knapen T., Lamme V. A. F., Donner T. H. Pupil-linked Modulation of Decision-Related Signals in Human Primary Visual Cortex. *In preparation.*

Meindertsma, T.*, **Kloosterman, N. A.***, Nolte, G., Engel, A. K., & Donner, T. H. (*=Shared first authorship.) Modulation of Beta-Band Activity in Human Visual Cortex by Covert Perceptual Decisions. *In preparation*.

Filimon, F., Philiastides, M. G., Nelson, J. D., **Kloosterman, N. A.**, & Heekeren, H. R. (2013). How embodied is perceptual decision making? Evidence for separate processing of perceptual and motor decisions. *The Journal of Neuroscience, 33*(5), 2121-2136.

Korjoukov, I., Jeurissen, D., **Kloosterman, N. A.**, Verhoeven, J. E., Scholte, H. S., & Roelfsema, P. R. (2012). The time course of perceptual grouping in natural scenes. *Psychological science, 23*(12), 1482-1489.

Kloosterman, N. A., Filimon, F., Philiastides, M. G., van Zuijen, T. L., Werner, A., Lindenberger, U., & Heekeren, H. R. (2014). Human Prefrontal Cortex Represents Task-Relevant Auditory Sensory Evidence During Perceptual Decision Making. *In preparation.*

DANKWOORD

Het zit erop, waarvan akte! Ik kijk met genoegen terug op de afgelopen vijf jaar, met name dankzij een grote groep mensen die direct of indirect hebben bijgedragen aan de totstandkoming van mijn proefschrift. First of all, I would like to thank Tobias. Tobi, our meetings were always a source of inspiration and motivation for me. If I was stuck again with some analysis, you always knew how to turn things around and make me curious to try out a new approach. I find your knowledge of the field truly amazing. But more importantly, I have come to know you as a warm and fun guy, who is always happy to go out for a good espresso or a beer in the newest cool place. It was great that I was able to wrap up the postdoc from Berlin. I wish you all the best on your new adventure in Hamburg. Don't let the lab get too big!

Victor, we hebben elkaar niet vaak gezien de afgelopen jaren, maar al sinds de collegebanken ben ik een groot fan van je droge stijl en onafhankelijke denkwijze. Dank ook voor de verlenging. Om in de B&C groep te blijven – Johannes, bedankt voor de waanzinnige EEG stage waarin ik ontdekte hoe leuk onderzoek was. Ik hoop dat we na al die jaren nog wat moois uit die data kunnen halen. Steven en Martijn, mijn student-assistentschap bij jullie heeft mijn passie nog verder aangewakkerd. Bedankt voor alles wat ik daar heb geleerd. Also many thanks to Hauke from Berlin and the old MPIB group, who gave me the first taste of what running a complete experiment is really like.

Ik ben ook veel dank verschuldigd aan de Lammetjes, aan wie ik veel steun heb gehad in de eenzame eerste jaren in Tobi's lab. Anouk, als boegbeeld van deze club, wil ik bedanken voor haar altijd goede ideeën, was het niet over hoe een paper te schrijven, dan wel wanneer het tijd was om een kouwe kletser te halen. Iris, de hardwerkende partygirl, was daar ook een expert in. Tomas, ik ken niemand die zoveel experimenten per minuut bedenkt als jij. Thanks voor je bevlogenheid en aanstekelijke enthousiasme. Verder ook veel dank aan Roy Cox de knopjesdrukker en tafelvoetbalkoning, Yaïr de tafelvoetbalkroonprins, Ilya, Manon, Joram, Marlies, Irene, Lotte, Jasper, Hilde, Annelinde, Julia en Andries voor borrelpraat en het delen van promotie-lief en -leed. Olympia, thanks so much for being paranimph and all these years that we went together through Master, PhD and beyond at the UvA. Simonis, ik mis de schuine praatjes, cheesy muziekjes (10 x hetzelfde liedje) en ommetjes langs Bakhuys nu al. Ik betwijfel of er een Duitse evenknie van je bestaat. Bedankt dat je ook paranimf was.

De laatste jaren is het Donnerlab flink gegroeid. Thomas, bedankt ook voor die laatste analyses waardoor het MEG paper eindelijk gepubliceerd kon worden. Berend, Bart, bedankt voor jullie hulp bij Hoofdstuk 4. Daniel, working with you was/is a pleasure! Both of you (and Yaïr) also thanks for helping out with the move, always welcome to visit in Berlin. Jan Willem, bedankt voor de lange, melige uren bij de scanner in Hamburg. Anne, Tom, Anke, Niklas, thanks for the JC's and labmeetings and all the best in Hamburg.

Zonder mijn vrienden had ik al lang de moed verloren. Vera, Zimbardo, Fons, Jesse, Kun, Base, Topper, Vincent, Frederick, Matthijs, bedankt! Ik zie jullie snel hier of daar. Karl Bendix, Franzi and Sebi, danke das ich bei euch wohnen dürfte während meine Zeit am UKE. Uta and Siegfried, danke das ihr mich so warm aufgenommen habt und das wir die erste Monaten in Berlin in eueren Wohnung wohnen konnten. Flora, Ferdi, Nina, Matthias, danke für das Schaukelpferd und Keyboard und das ihr immer so schön Frenzig seid.

Jan en Truus zijn altijd mijn rots in de branding geweest. Pap, mam, jullie onvoorwaardelijke steun heeft me de stevige basis gegeven waardoor ik al mijn plannen, uitmondend in het volbrengen van mijn promotie en de verhuizing naar Berlijn, tot een goed einde heb kunnen brengen. Ontzettend bedankt dat jullie er altijd voor me zijn! Lieve zussies Petra en Ingrid, bedankt dat jullie altijd voor me klaarstaan, wat ook zo duidelijk werd direct na Oona's geboorte. Hugo en Mats, fijn dat jullie zo lollige ventjes zijn die alles weer in perspectief brengen. Zwagertjes Steven en Kristian, tot op de volgende, immer gezellige, Kloosterman herfst meeting.

Liefste Hannah, ik ben zo blij dat we elkaar ontmoet hebben destijds in Berlijn. Ik vind het zo ontzettend knap en stoer dat je het destijds gewaagd hebt samen met mij naar een vreemd land te vertrekken. Sindsdien hebben we samen iets heel moois opgebouwd, met Oona als kers op de taart. Zonder jou aan mijn zijde was er niets van mijn PhD terechtgekomen. Bedankt dat je me altijd met raad en daad terzijde stond en voor de ruimte die je me na Oona's geboorte gaf om het boekje eindelijk af te maken. Ik verheug me zo op onze toekomst met z'n drieën in Berlijn. Tot slot, lieve kleine Oona, het is nog leuker dat je er bent dan ik had gedacht. Dankzij jou wogen de laatste loodjes helemaal niet zo zwaar!